ABSTRACT

Title of Dissertation: INVESTIGATION OF LAMIN A PROCESSING AND REGULATION

Di Wu, Doctor of Philosophy, 2017

Dissertation directed by: Kan Cao, Associate Professor, Department of Cell Biology and Molecular Genetics

Lamin A is a major component of the lamina, which creates a dynamic network underneath the nuclear envelope. Mutations in the lamin A gene (*LMNA*) cause severe genetic disorders. One of the most striking cases is Hutchinson-Gilford progeria syndrome (HGPS). It is caused by a lamin A mutant protein named progerin. Due to the abnormal retaining of a permanent C-terminal farnesyl tail, progerin gradually accumulates on the nuclear membrane, resulting in abnormal nuclear morphology during interphase and perturbing a diversity of signaling and transcriptional events. To better understand lamin A gene's function and regulation, I studied lamin A from three aspects in my dissertation, including its post-translational processing, post-transcriptional degradation, and transcriptional regulation. For post-translational processing, I examined the potential effects of cytoplasmic progerin based on a previous observation that membrane-associated progerin forms visible cytoplasmic aggregates in mitosis. After removal of the nuclear localization signal, I find that both LAΔNLS and PGΔNLS mutants are farnesylated in the cytosol and

associated with a sub-domain of the ER via their farnesyl tails. While the farnesylation on LAΔNLS can be gradually removed by Zempste24, PGΔNLS remains permanently farnesylated and aggregated in the cytosol. Moreover, both ΔNLS mutants dominantly affect emerin's nuclear localization. Previously, the accumulation of progerin has led to the speculation that progerin is more stable than the wild type lamin A. However, the low solubility of lamin proteins renders traditional immunoprecipitation-dependent methods ineffective for comparing the relative stabilities of mutant and wild type lamins. Therefore, to investigate the post-translational degradation of lamin A, I employed a novel platform based on viral 2A peptide-mediated co-translational cleavage to infer differences in lamin stability. My results support the notion that progerin is more stable than lamin A. In addition, treatment of FTI reduces progerin relative stability to the level of wild type lamin A. Last but not the least, I investigated the function of *LMNA* first intron in order to better understand the transcription regulation of lamin A. My results show that a highly conserved region within *LMNA* first intron is essential for the expression repression of lamin A in HL60 cells. This process is fulfilled by the interaction between this conserved region and transcription factor Sp1. Taken together, my results reveal new insights into biogenesis, protein interaction and transcription regulation of lamin A.

INVESTIGATION OF LAMIN A PROCESSING AND REGULATION

by

Di Wu

Dissertation submitted to the Faculty of the Graduate School of the
University of Maryland, College Park, in partial fulfillment
of the requirements for the degree of
Doctor of Philosophy
2017

Advisory Committee:
Professor Kan Cao, Chair
Professor Sridhar Hannenhalli
Professor Zhongchi Liu
Professor Leslie Pick
Professor Sougata Roy

Dedication

This dissertation is dedicated to my family,

my Mom, my Dad, my husband and my son,

for their unconditional love, understanding, support and encouragement.

Especially to my grandma,

I miss you very much.

Acknowledgements

This dissertation would not have been accomplished without my advisor, Dr. Kan Cao. I would like to thank her for providing me the opportunity to join her lab and start my projects as well as her continuous encouragement, inspiration, patience, understanding and support during my entire dissertation work. Importantly, she set a great example of a strong independent woman that will benefit me for the rest of my life.

I would also like to express my gratitude to my committee members, Dr. Leslie Pick, Dr. Sridhar Hannenhalli, Dr. Zhongchi Liu, Dr. Sougata Roy and recently retired Dr. Stephen Wolniak, for always making time to attend my committee meetings and giving me helpful suggestions and feedbacks on my projects.

I would like to acknowledge our collaborators Dr. Philip Yates and Dr. Andrew Flannery for their contribution of providing essential experimental materials and critical ideas to my research.

In addition I thank the fine technique support of Amy Beaven from the imaging core and Kenneth Class from the flow cytometry core of the Core Laboratory Facilities of the Department of Cell Biology and Molecular Genetics at the University of Maryland.

Last, I am the most grateful to all the members that I have been working with in the Cao Lab. They are Dr. Zhengmei Xiong, Dr. Linlin Sun, Dr. Pratima Bharti, Dr. Haoyue Zhang, Kun Wang, Julie Choi, Xiaojing Mao, Yantenew Gedle Gete, Mason Trappio, Megan Leung, Christina Ladana, Eunae Ko, Mike O'Donovan,

Natasha Ivanina, Helen Cai and Jason Albanese. Thank all of you for your help, suggestion and support, and turning the lab into a second home to me!

Table of Contents

List of Figures

Chapter 3: Comparing lamin proteins post-translational relative stability using a 2A peptide-based system reveals elevated resistance of progerin to cellular degradation

Chapter 4: LMNA first intron mediated transcription suppression of lamin A through Sp1 binding

List of Abbreviations

BAF: barrier- to-autointegration factor

CDK1: cyclin-dependent kinase 1

CSIM: cysteine-serine-isoleucine-methionine

ChIP: chromatin immunoprecipitation

Con1: conserved region 1

CRNSP: Ca+2-regulated nuclear scaffold protease

DHS: DNase I hypersensitive site

DSB: double strand breaks

ER: endoplasmic reticulum

ESC: embryonic stem cell

FMDV: mouth disease virus

FTase: farnesyltransferase

FTI: farnesyltransferase inhibitor

GCL: germ-cell-less

hBM-MSCs: human bone marrow-derived mesenchymal stem cells

hESC: human embryonic stem cell

HDAC2: histone deacetylase 2

HGPS: Hutchinson-Gilford progeria syndrome

HEK293T: Human embryonic kidney cells 293T

HP1α: heterochromatin protein 1 α

HSs: hypersensitive sites

H3K9me3: histone H3 lysine 9 trimethylation

H3K27me3: histone H3 lysine 27 trimethylation

H4K20me3: histone H4 lysine 20 trimethylation

Icmt: isoprenylcysteine carboxyl methyltransferase

IF: intermediate filament

INM: inner nuclear membrane

LA: lamin A

LADs: lamin-A-associated domains

LAP2: lamina-associated polypeptide 2

LBR: Lamin B receptor

LB1: lamin B1

L-RARE: retinoic acid responsive element

MAD: mandibuloacral dysplasia

MEF: mouse embryonic fibroblasts

mTOR: mechanistic target of rapamycin

NAC: N-acetyl cysteine

NE: nuclear envelope

NLS: nuclear localization sequence

ORF: open reading frame

PG: progerin

pol II: RNA polymerase II

P2A: 2A sequence from Porcine teschovirus-1

RAR: retinoid acid receptors

Rb: retinoblastoma

Rce1: Ras-converting enzyme 1

RD: restricted dermopathy

Rluc: Renilla luciferase

ROCK: Rho-associated protein kinase

ROS: reactive oxygen species

RXRβ: retinoic X receptor β

SFFV: spleen focus-forming virus

SREBP1: sterol response element binding protein 1

SSIM: serine-serine-isoleucine-methionine

TFs: transcription factors

TSS: transcription start site

UTR: untranslated region

WS: Werner's syndrome

Zmpste24: Zinc metalloprotease related to Ste24p

ΔNLS: deleted NLS

Publication information

The data from this thesis composed the following publications.

Wu D, Flannery AR, Cai H, Ko E, Cao K. Nuclear localization signal deletion mutants of lamin A and progerin reveal insights into lamin A processing and emerin targeting. Nucleus. 2014 Jan-Feb;5(1):66-74.

Wu D, Yates PA, Zhang H, Cao K. Comparing lamin proteins post-translational relative stability using a 2A peptide-based system reveals elevated resistance of progerin to cellular degradation. Nucleus. 2016Nov;7(6):585-596.

Chapter 1: Introduction

1.1 The nuclear lamina and lamins

1.1.1 Nuclear lamina composition and organization

In eukaryotic cells, there is a dense (~30 to 100 nm thick) fibrillar network structure lying underneath the nuclear envelope (NE), named nuclear lamina. It is composed of intermediate filaments (IF) and membrane associated proteins, and located at the interface between chromatin and the inner nuclear membrane (Fawcett, 1966; Goldman et al., 2002; Rodgers et al., 1995). Besides providing mechanical support to the nucleus in the cell, nuclear lamina participates in important cellular processes including DNA replication, chromatin remodeling and so on (Bridger et al., 2007; Goldman et al., 2002; Gruenbaum and Foisner, 2014; Gruenbaum et al., 2005; Spann et al., 2002).

In metazoan cells, the major components of the nuclear lamina are A and B type lamins, which are type V intermediate filaments and differ in their structural and protein features and expression patterns (Dittmer and Misteli, 2011). There are three different genes responsible for at least seven lamin protein isoforms' expression in mammalian cells (Dittmer and Misteli, 2011). The A type lamins include lamin A, AΔ10, C, and C2 variants. They are generated from the *LMNA* gene on 1q21 by alternative splicing and only expressed upon differentiation (Furukawa et al., 1994; Krohne et al., 2005; Machiels et al., 1996; McKeon et al., 1986). Lamin A and C are the major isoforms. They share the same first 566 amino acids, but lamin C lack 98 amino acids at the carboxyl terminus and the CaaX box which are present in prelamin A before lamin A maturation by post translational modification, and contains a

unique six amino acid carboxyl terminus (Dittmer and Misteli, 2011). B-type lamins are constitutively expressed in both undifferentiated and differentiated cell. Three B type lamins are encoded from two separate genes: lamin B1 is encoded by *LMNB1* on 5q23, while lamin B2 and B3 are isoforms derived from *LMNB2* on 19q13 (Furukawa and Hotta, 1993; Krohne et al., 2005; Pollard et al., 1990). Both lamin C2 and B3 are germ cell specific.

1.1.2 Lamin proteins structural features and assembly

As members of IF family, nuclear lamins possess similar protein structures as cytoplasmic intermediate filaments. They contain a central a-helical rod domain flanked by a globular amino-terminal head domain and a carboxy-terminal tail domain (Fig 1-1) (Burke and Stewart, 2012; Stuurman et al., 1998). The central rod domain comprises four coiled-coil domains separated by flexible linker regions. The

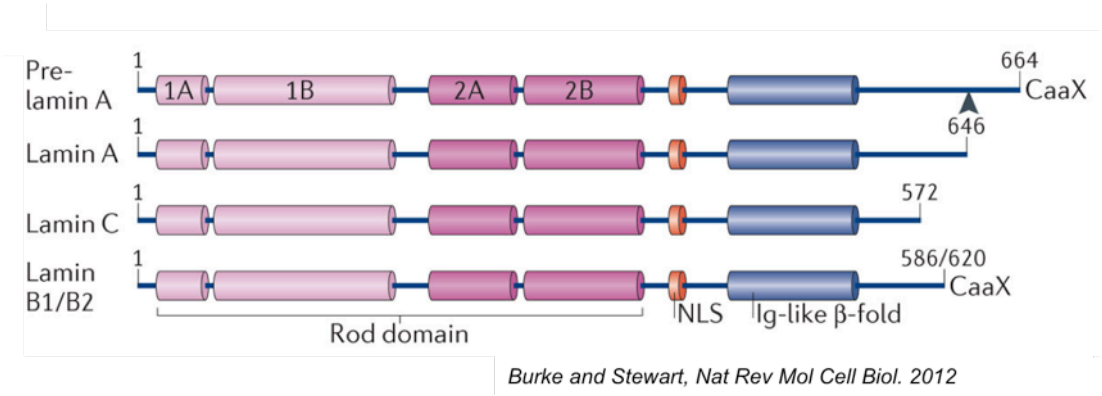

Figure 1-1. The structure of A- and B-type lamins. (A) Each of the lamins features a small (10–20 residues) 'head' domain followed by a central rod domain containing four coiled-coil regions (termed 1A, 1B, 2A and 2B). The large non-helical 'tail' domain is organized around an immunoglobulin (Ig)-like β-fold. A nuclear localization sequence (NLS) lies immediately downstream of the rod domain. Proteolytic cleavage of pre-lamin A (indicated by a black arrowhead) results in the appearance of mature lamin A. Lamin A and each of the B-type lamins contain a carboxy-terminal CaaX motif (where C is Cys, a is an aliphatic residue and X is usually represented by a Met) that defines a site of farnesylation and carboxy methylation (Burke and Stewart, 2012).

high order structure of lamin filaments is initially organized through the dimerization of central rod domains. Two lamin proteins first coil around each other parallelly to forming a lamin dimer. This is the basic building block of lamin assembly. Lamin dimers organize in a head-to-tail manner, generating lamin polymers, which then form protofilaments through anti-parallel association. Lamin filaments are eventually formed between three and four protofilaments in a diameter around 10nm (Fig 1-2) (Eriksson et al., 2009; Ho and Lammerding, 2012). Comparing to cytoplasmic IF, the lamins tend to carry a shorter amino-terminal head domain despite the size variations (Dittmer and Misteli, 2011). The carboxy-terminal tail domain of lamin proteins harbors a nuclear localization signal (NLS), an Ig domain and, in most cases, a CaaX box (Fig 1-1). The Ig domain mediates diverse protein-protein and protein-ligand interactions (Krimm et al., 2002; Shumaker et al., 2005). The CaaX box at the c-terminus is a target for isoprenylation and carboxymethylation. It contains a cysteine (C), followed by two of any aliphatic amino acids (a), and a forth amino acid

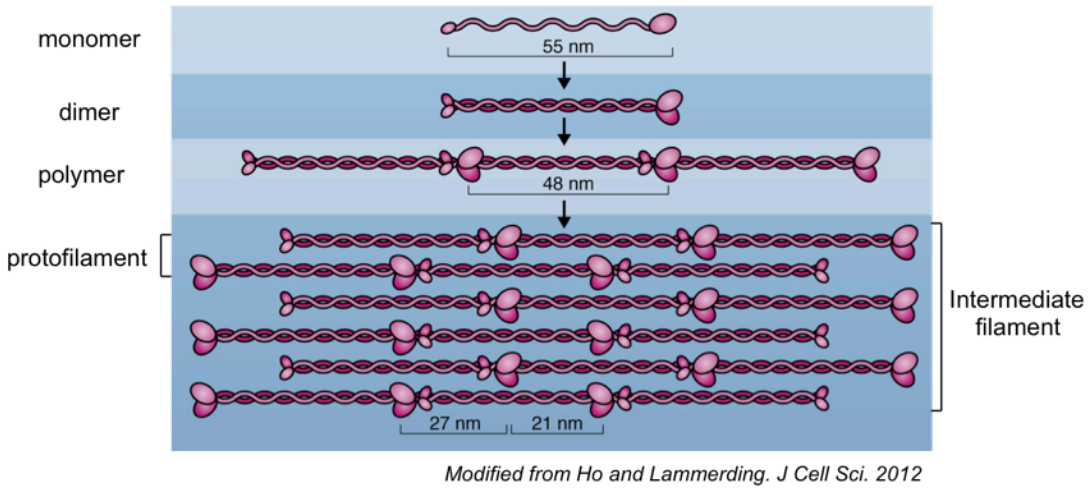

Figure 1-2. Assembly of lamins into intermediate filaments. Dimerization of lamins is driven by the coiled-coil formation of their central rod. Lamin dimers then assemble head to tail into polar polymers, which requires an overlapping interaction between the head and tail domains. These polymers then laterally assemble in an anti-parallel fashion into non-polar filaments (Ho and Lammerding, 2012).

that determines the kind of modification (X) (Fig 1-1). For example, CaaX box for mammalian lamin A and B1 is CSIM and CAIM respectively, therefore farnesyltransferase recognizes the box and mediates farnesylation for these lamin proteins (Dechat et al., 2010; Eriksson et al., 2009; Stuurman et al., 1998).

1.1.3 Lamin proteins processing and maturation

As mentioned earlier, lamin A and B type lamins contain a CaaX box at their C-terminus. Proper processing of the CaaX box is critical for the membrane association, localization and function of lamin proteins (Capell et al., 2005; Gelb et al., 2006; Yang et al., 2005). Lamin precursors undergo extensive post-translational modifications on the CaaX box to become mature lamin proteins (Fig 1-3) (Burke and Stewart, 2012; Rusiñol and Sinensky, 2006; Yang et al., 2005). In the first step, a farnesyl group is attached to the cysteine of the CaaX box by a farnesyltransferase (FTase), followed by the removal of the aaX residues by Rce1 (Ras-converting enzyme 1) and/or Zmpste24 (Zinc metalloprotease related to Ste24p)/FACE 1 (Rusiñol and Sinensky, 2006). Next, the farnesylated cysteine is carboxymethylated by isoprenylcysteine carboxyl methyltransferase (Icmt). At this step, the process of B type lamins maturation is terminated. Therefore, B type lamins such as lamin B1 and B2 permanently retain the farnesylated and carboxymethylated C-terminus (Dechat et al., 2010). Whereas there is one last step to be completed that is crucial for lamin A maturation. In the final step, the last 15 amino acids of prelamin A including the farnesylated C-terminus are further excised by Zmpste24 to allow the release of mature lamin A from the inner nuclear membrane (INM) (CORRIGAN et al., 2005).

It is notable that lamin C (a splice variant of the *LMNA* gene) lacks a CaaX box and is not modified at all.

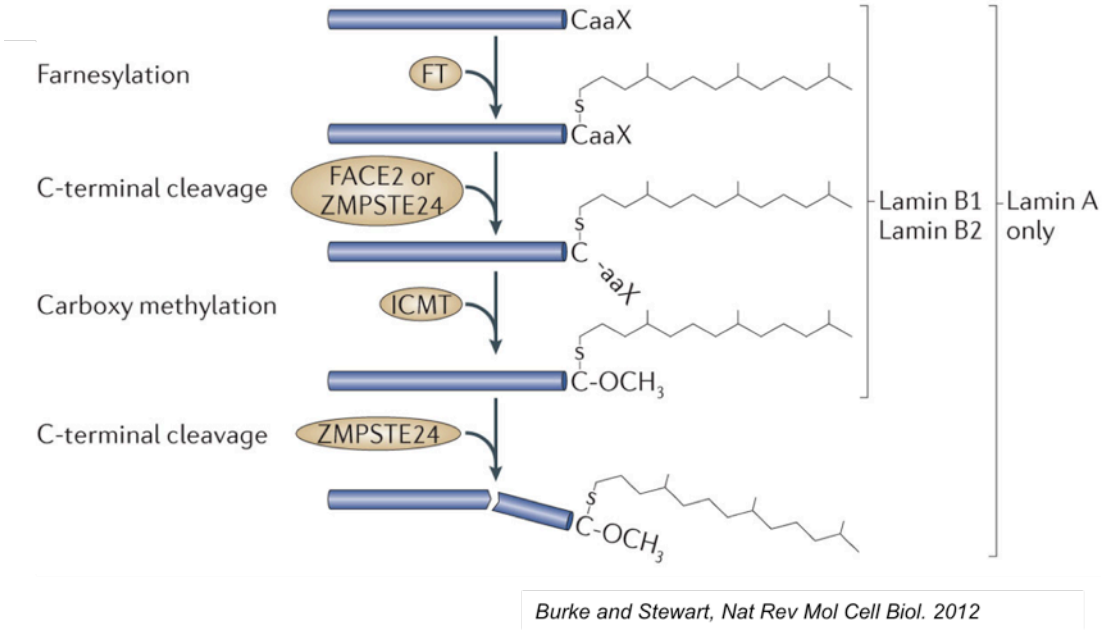

Figure 1-3. Processing of A- and B-type lamins. Farnesylation of lamins on the CaaX Cys residue by a protein farnesyltransferase occurs soon after synthesis. This is followed by proteolysis of the aaX residues by farnesylated proteins-converting enzyme 2 (FACE2; also known as CaaX prenyl protease) in the case of the B-type lamins, and by ZMPSTE24, a zinc metallo-endoprotease, in the case of lamin A. Processing of the CaaX motif is completed by carboxyl methylation by ICMT (isoprenylcysteine carboxymethyltransferase) of the new C terminus. Once incorporated into the nuclear lamina, lamin A, but not the B-type lamins, undergoes an additional ZMPSTE24-mediated cleavage step (in human lamin A this occurs after Tyr646, black arrowhead in a), which removes an additional 15 amino acids, including the farnesylated Cys, leading to the appearance of non-farnesylated mature lamin A (Burke and Stewart, 2012).

1.1.4 Functional roles of nuclear lamins

Grouped into IF superfamily, nuclear lamins were originally thought to be the structural proteins that provide mechanical support to the nucleus, maintaining nuclear morphology and resisting to chromatin deformation (Hutchison, 2002). In support of this idea, depletion of lamins resulted in small and fragile nuclei in *Xenopus* nuclear assembly systems (Ellis et al., 1997; Meier et al., 1991; Newport et

al., 1990; Spann et al., 1997). In addition, fibroblasts from Lmna-/- mice showed that the nuclei are more easily to be deformed and less resistant to physical compression comparing to Lmna+/+ littermates (Lammerding et al., 2004). However, with intensive research carried out on lamins, more of their cellular functions have been revealed. They are not limited to mechanical support but entangled with a wild range of cellular regulations, including chromatin organization, DNA replication, transcription, differentiation and development etc. (Bridger et al., 2007; Goldman et al., 2002; Gruenbaum and Foisner, 2014; Spann et al., 2002).

1.1.4.1 Chromatin organization

Lamins globally regulate chromatin organization. Nuclear lamina tends to associate with transcriptionally silent regions of the genome, such as centromeres, telomeres and the inactive X chromosome (Belmont et al., 1993; Fawcett, 1966; Guelen et al., 2008). The highly organized heterochromatin is localized to the periphery of the nucleus, closely associated with the lamina (Dechat et al., 2008). However, not all the chromatin regions associated with lamina are repressed. Previously, it has been reported that a genetic locus, which has been targeted to the nuclear periphery by lamin B1, maintains its ability to be transcribed (Kumaran and Spector, 2008). In general, the lamina is more associated with inactively transcribed chromosome territories, such as gene-poor human chromosome 18, on the contrary, gene-rich chromosome 19 resides preferentially deep inside the nucleus (Croft et al., 1999). Perturbation of lamins, such as lamin A, leads to loss of peripheral heterochromatin, ectopic chromosome condensation and mis-positioning of centromeric heterochromatin (Galiová et al., 2008; Nikolova et al., 2004; Sullivan et

al., 1999). Meanwhile, global epigenetic histone markers are also altered, including decreased levels of the heterochromatin markers histone H3 lysine 9 trimethylation (H3K9me3) and H3K27me3 and increased levels of H4K20me3 (Dittmer and Misteli, 2011). Genome-wide mapping techniques have identified genome regions that preferentially associate with lamins, known as lamin-A-associated domains (LADs). These domains are generally gene-poor and are proposed to represent a repressive chromatin environment (Guelen et al., 2008).

1.1.4.2 Transcription and gene expression

Both A and B type lamins have been reported to involve in transcription gene expression regulation. In *Xenopus laevis* oocytes, RNA polymerase II (pol II) activity was inhibited by overexpression of N-terminally deleted lamins, accompanied by the disassembly of the endogenous lamin network, leading to an impairment of transcription (Gruenbaum et al., 2005; Spann et al., 2002). There are examples indicate the transcription and gene expression regulation of lamins are facilitated by transcription factors and lamin-associated proteins, such as LAP2 and emerin both of which belong to LEM-domain proteins (Lin et al., 2000). LAP2β, an INM residing lamin interacting proteins binds exclusively to lamin B (Foisner ' and Gerace, 1993), forms functional complexes with B-type lamins as well as the transcription factors germ-cell-less (GCL) and E2f-associated protein (DP) to inhibit E2F activity (Nili et al., 2001). Another member of LAP2 family, LAP2α, that interacts specifically to A-type lamins, associates with lamin A/C in a complex with retinoblastoma (Rb) that tethers un-phosphorylated Rb protein within the nucleus (Markiewicz et al., 2002).

Whereas mutant forms of Rb that cannot be tethered promote cancer through E2F mediated cell-cycle progression, suggesting the necessary of Rb nuclear tethering for its stability and function (Hinds et al., 1992). Actually, a large number of lamin A binding proteins are transcriptional factors, such as zinc finger protein MOK2 (Dreuillet et al., 2002) and sterol response element binding protein 1 (SREBP1) (Lloyd et al., 2002), which contribute to the transcription regulation role of lamin proteins. The INM protein emerin has been suggested to form at least two distinct lamin-anchored complexes by binding to GCL and barrier to autointegration factor (BAF) (Bengtsson and Wilson, 2004; Holaska et al., 2002). Moreover, the GCL-binding region in emerin can also bind to other gene regulators, such as BCL2-associated transcription factor (BTF) known a death-promoting repressor, implicating a role of emerin–lamin complexes in transcriptional regulation (Haraguchi et al., 2004).

1.1.4.3 Development and differentiation

It is well known that A- and B-type lamins are expression at different developmental stages (Gruenbaum et al., 2005; Stuurman et al., 1998). B-type lamins can be detected throughout the entire development. Whereas A-type lamins are undetectable until a later stage when differentiation initiates (Broers et al., 1997). The changes in lamin expression have been reported crossing species in early development of *Xenopus* (Benavente et al., 1985; Lourim et al., 1996; Stick and Hausen, 1985; Wolin et al., 1987), *Drosophila* (Riemer et al., 1995), chicken (Lehner et al., 1987) and mouse embryos (Röber et al., 1989; Stewart and Burke, 1987). It has been suggested that the repressed expression of lamin A/C in undifferentiated human

embryonic stem (ES) cells is responsible for the high deformability of the nuclei in these cells (Pajerowski et al., 2007). Depending on the site of the mutation, mutants of Dm0, the B-type *Drosophila* lamin, cause lethality at different embryonic or late pupal stages (Gruenbaum et al., 2003; Osouda et al., 2005). Furthermore, Vergnes et al. have shown that lamin B1 deficient mice die at birth with defective lungs and bones (Vergnes et al., 2004). On the other hand, lamin A/C deficient animals develop normally until birth, but have severe postnatal growth retardation and develop muscular dystrophy (Sullivan et al., 1999). All these evidences suggested that lamins are closely correlated with cell differentiation and development. In support, evidence has been shown that A-type lamins are highly involved with differentiation of many cell linages, including adipocytes, osteoblasts and adult stem cells. Lamins A/C regulate adipocyte differentiation together with the INM protein emerin through influencing the distribution of β-catenin in nucleocytoplasm (Tilgner et al., 2009). In addition, silencing lamins A/C expression causes impaired osteoblastogenesis and accelerated osteoclastogenesis in human bone marrow stromal cells (Akter et al., 2009; Rauner et al., 2009). Moreover, a dominant negative lamin A mutant, progerin, impairs the differential potential of human mesenchymal stem cells, probably by affecting the Notch-signaling pathway (Espada et al., 2008).

1.2 Hutchinson–Gilford progeria syndrome (HGPS)

1.2.1 Laminopathies

Since the first discovery of *LMNA* mutations cause autosomal dominant Emery-Dreifuss muscular dystrophy in 1999 (Bonne et al., 1999), an enormous

number of mutations in nuclear lamins, have successively been found to link with around 20 genetic disease (Dittmer and Misteli, 2011), collectively known as the laminopathies. Noteworthy, both the number of lamin mutations and associated diseases is continuing to grow. The majority of these diseases is heterozygous and at lease 17 (Dittmer and Misteli, 2011) of them are associated with more than 300 different mutations in *LMNA* producing around 200 mutant lamin A/C proteins (Dechat et al., 2008), existing in the forms of cardiomyopathy, muscular dystrophy, lipodystrophy and aging related progeria. The latter includes Hutchinson-Gilford progeria syndrome (HGPS), atypical Werner's syndrome (WS), restricted dermopathy (RD), and mandibuloacral dysplasia (MAD) (Broers et al., 2006; Kudlow et al., 2007; Worman and Bonne, 2007), suggesting a closely associated role of lamin A with human aging.

Contrary to *LMNA*, only two diseases are reported to be associated with mutations in the *LMNB1* and *LMNB2* genes, which is probably due to the ubiquitous expression and the importance for viability of B-type lamin. These include autosomal-dominant leukodystrophy caused by a duplication of *LMNB1* that resulting in higher *LMNB1* dosage/expression in brain tissues and acquired partial lipodystrophy caused by several rare *LMNB2* missense mutations (Hegele et al., 2006; Padiath et al., 2006).

Yet, how different mutations on the single *LMNA* gene affect its function and lead to a wild range of tissue specific diseases in the laminopathies still remain ambiguous. More investigations towards lamin A/C function and regulation are needed to unravel the puzzle.

1.2.2 HGPS

Among all the known laminopathies, HGPS manifests the most striking accelerated aging symptoms. The reported incidence of this disorder is 1 in 8 million, but could be as high as 1 in 4 million, which takes into consideration of unreported or misdiagnosed cases (Capell and Collins, 2006; Sarkar and Shinton, 2001). As of December 2016, there are 111 known HGPS cases worldwide (www.progeriaresearch.org), approximately forty of which are current (Pollex and Hegele, 2004). HGPS affects both genders. The patients tend not to live beyond their teenage years, with the cause of death predominantly due to atherosclerosis at an average age of 13 (Capell and Collins, 2006; Merideth et al., 2008).

1.2.2.1 Clinical manifestations

Children with HGPS typically appear normal at birth, but then they experience severe failure to thrive and gradually show symptoms of accelerated aging during the first year of life (Fig 1-4). After the age of 3, these children almost always exhibit delayed growth, short stature, and below-average weight comparing to their healthy peers. HGPS patients also display typical facial features such as a small jaw, prominent eyes, hair loss, craniofacial disproportion, delayed and crowded dentition, and prominent scalp veins. In addition, due to the lost of subcutaneous fat, their skin shows wrinkled and aged appearance. Other abnormalities include a thin, high-pitched voice, a pear-shaped thorax, a “horse-riding” stance, and stiff joints. The most devastatingly, this disease impairs the patient’s cardiovascular system, causing severe, progressive atherosclerosis, which eventually leads to heart attacks or strokes.

However, Children with HGPS experience normal motor and mental development (Merideth et al., 2008; Pollex and Hegele, 2004).

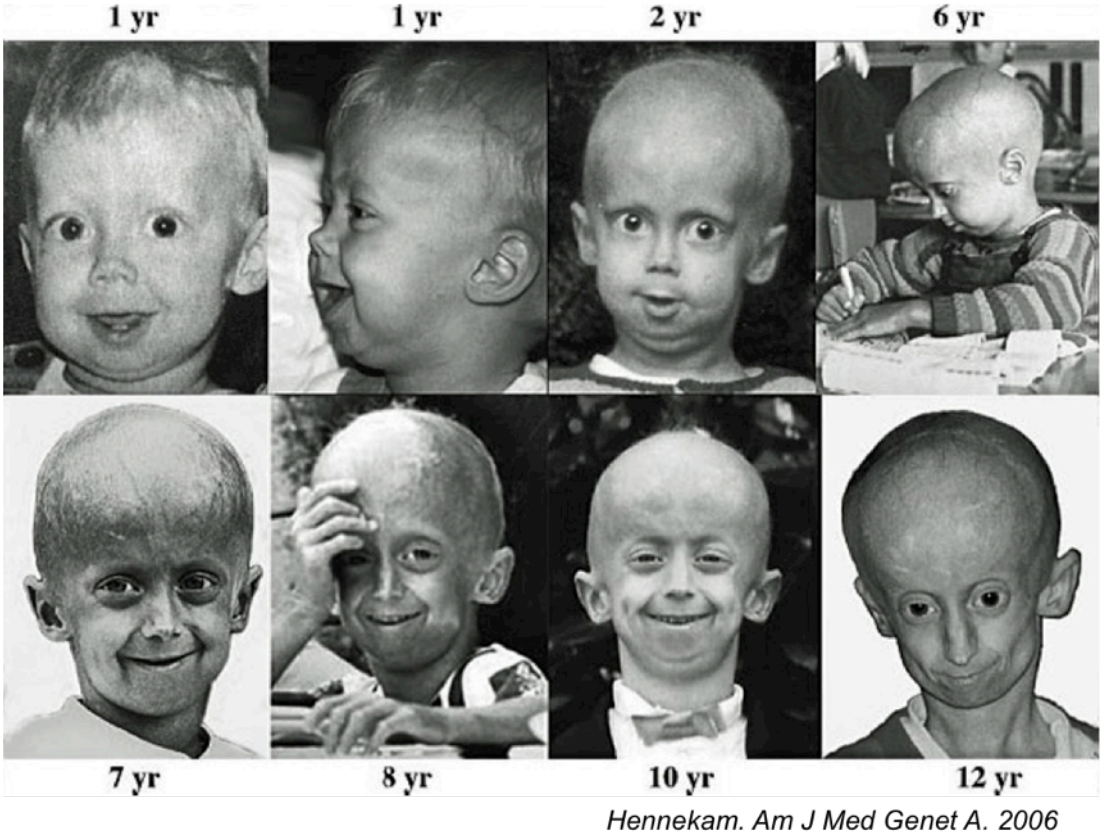

Figure 1-4. A Dutch progeria patient at the age of 1, 2, 6, 7, 8, 10, and 12 years.

1.2.2.2 Genetic cause

Progeria was first described by Jonathan Hutchinson and Hastings Gilford in 1886 and 1904, respectively, whose names were later give rise to the name of the disease - Hutchinson–Gilford progeria syndrome. Although it was documented 130 years ago, the molecular mechanism that causes HGPS was not unraveled until 2003 (Eriksson et al., 2003). At first, scientists hypothesized it might be a autosomal recessive disease based on the observed inheritance pattern that the parents of

progeria children were mostly healthy (Khalifa, 1989; Maciel et al., 1988). However, a whole-genome scan showed no evidence of homozygosity. Finally by using microsatellite genotyping, Eriksson and her colleagues narrowed down the HGPS-inducing gene to a region of 4.82Mb on proximal chromosome 1q, where roughly 80 known genes reside. One of the genes, *LMNA*, immediately drew their attention because its mutation were already known to associated with several genetic disorders in the form of cardiomyopathy, lipodystrophy, muscular dystrophy, tooth disorder, and mandibuloacral dysplasia, which are all observed in patients with HGPS.

Eventually, a signal nucleotide substitution from C to T at position 1824 on *LMNA* gene was identified in 18 out of 23 HGPS patient samples after sequencing. None of the patients' parents carried this mutation, suggesting it's a *de novo* point mutations. It is a synonymous substitution that does not alter the original amino acid sequence (G608G (GGC>GGT)), instead it introduces a cryptic splice donor site within exon 11 of *LMNA* gene, which leads to a in-frame deletion of extra 150 nucleotides from exon 11 with mRNA (Eriksson et al., 2003) (Fig 1-5). *LMNA* gene

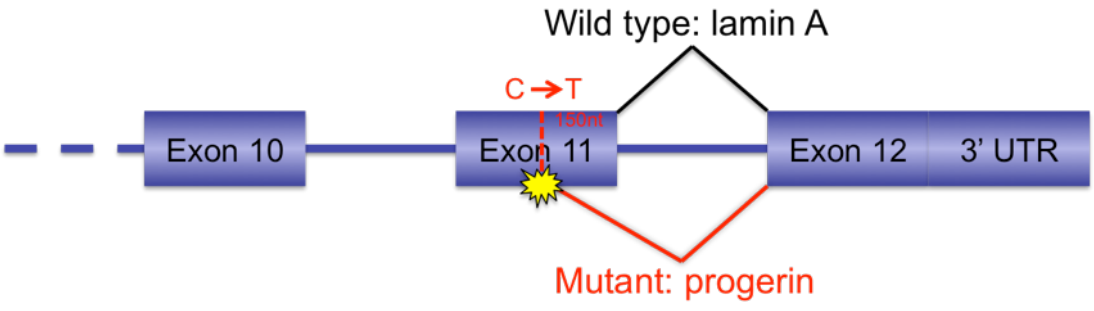

Figure 1-5. Activation of a cryptic splice donor site in exon 11 of LMNA gene of HGPS mutation. The *de novo* C to T mutation introduces a cryptic splice donor site within exon 11 of *LMNA* gene, which leads to a in-frame deletion of extra 150 nucleotides from exon 11 with mRNA, and eventually generates a mutant protein termed progerin.

has 12 exons and generates two protein isoforms, lamin A and lamin C. Lamin A is coded by exon 1-12 and lamin C by exon 1-10 (Dittmer and Misteli, 2011). As mentioned earlier, lamin A maturation undergoes CaaX modification at the C-terminus (Burke and Stewart, 2012; Rusiñol and Sinensky, 2006; Yang et al., 2005), in which a farnesyl group was first added to the cysteine of the CaaX box (CSIM) of lamin A precursor by a farnesyltransferase. Then the aaX group (SIM) is removed by Rce1 and/or Zmpste24 endoprotease (Rusiñol and Sinensky, 2006), followed by carboxymethylation of the terminal farnesylated cysteine (Dai et al., 1998). In the last step, Zmpste24 carries out a second cleavage to remove the terminal 15 amino acids, including the farnesyl group (CORRIGAN et al., 2005; Hennekes and Nigg, 1994). For HGPS patients, due to the synonymous substitution and the subsequent deletion on prelamin A mRNA, a mutant protein product that is 50 amino acids shorter than the wild type lamin A, named progerin, is generated. The effective cite of the second Zmpste24 cleavage falls right into the deleted 50-amino acid-region, therefore, this final cleavage step is blocked in HGPS, and progerin permanently maintain its farnesylated C-terminus in patient cells like B-type lamins (D'Apice et al., 2004; De Sandre-Giovannoli et al., 2003; Sinensky et al., 1994) (Fig 1-6). However, it is still not clear why the substitution happens spontaneously.

1.2.2.3 Cellular effects

Progerin is expressed in multiple tissues, mostly of mesenchymal origin including skin, bone, skeletal muscle, adipose tissue, heart and large and small arteries (Gordon et al., 2014a). The permanently farnesylated progerin acts in a dominant-negative way in lamin A expressing cells by irreversibly anchoring to the

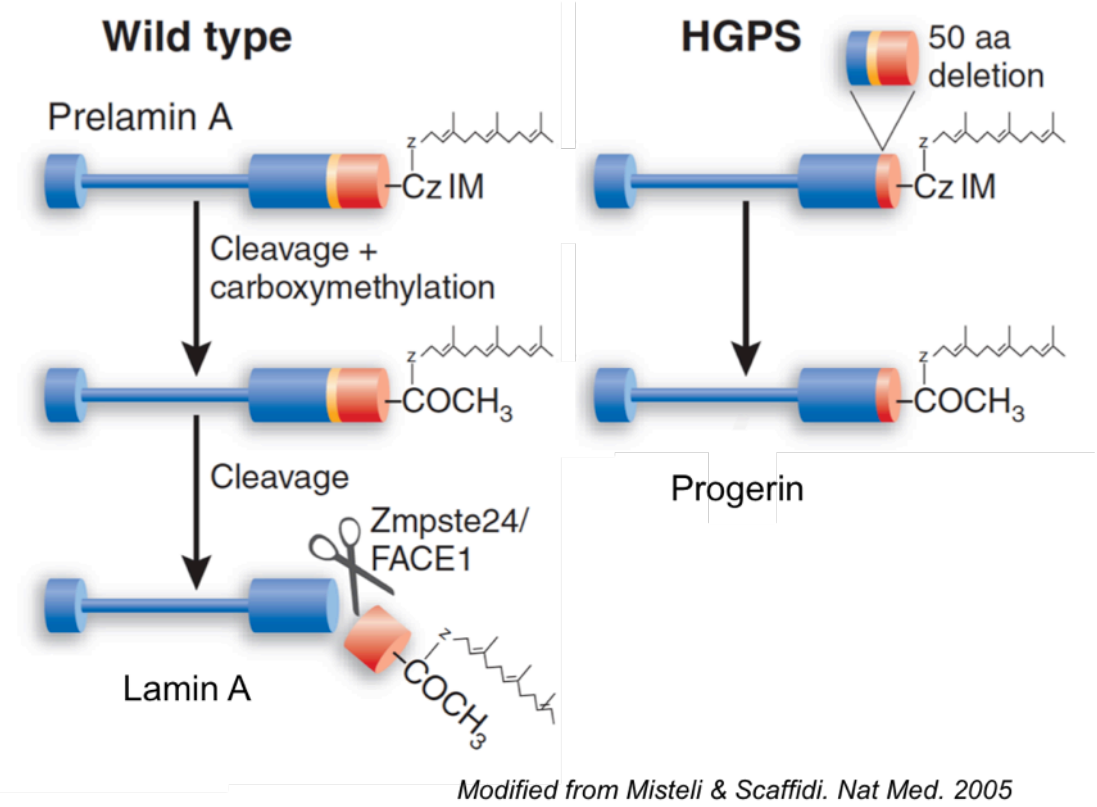

Figure 1-6. Lamin A–processing defects in HGPS. lamin A maturation undergoes several steps: farnesylation of the carboxyl terminus, cleavage of the three carboxyl terminal amino acids, carboxymethylation of the farnesylated cysteine and cleavage of the 15 terminal amino acids (red cylinder) by the endoprotease Zmpste24/FACE1. In HGPS cells, due to the 50 amino acid inframe deletion caused by the *de novo* mutation, the lamin A precursor loses the cleavage site (yellow line) for Zmpste24/FACE1. Therefore, a noncleavable truncated lamin A permanently carrying the farnesylated C-terminus is synthesized, named progerin.

nuclear envelope, thereby disrupting normal lamina function and eliciting numerous nuclear abnormalities in the cells of HGPS patients. These include the hallmark phenotype of HGPS - abnormal blebbed nuclei, clustering of nuclear pores, disrupted heterochromatin-lamin interactions, accumulation of DNA damage, defective DNA damage repair, telomere aberrations and mitochondrial dysfunction as well as alterations in downstream signaling and gene transcription, leading to differentiation defects and premature cellular senescence (Brunauer and Kennedy, 2015; Cao et al.,

2007; Eriksson et al., 2003; Goldman et al., 2004; McCord et al., 2013a; Vidak and Foisner, 2016; Zhang et al., 2014). In addition, progerin expression leads to decreased expression levels of lamin B1, heterochromatin protein 1 α (HP1α) and LAP2α, and loss of nucleoplasmic lamins. It has been reported that the A-type and B-type lamin segregation are lost in cells expressing progerin. Instead of polymerizing into distinct homopolymers, lamin A and B1 from mixed heteropolymers together with progerin, which potentially affect the normal function of both proteins (Delbarre et al., 2006). Moreover, it is well recognized that progerin inhibits the proliferation rate and lifespan of HGPS fibroblasts in culture (Goldman et al., 2004). They are hypersensitive to heat stress and exhibit broad epigenetic changes in histone methylation patterns that predate any nuclear shape changes (Paradisi et al., 2005; Shumaker et al., 2006).

1.2.2.4 Therapeutical strategies

Since progerin permanent bears the farnesylated C-terminus and aberrantly anchors to the NE, causing massive cellular abnormalities in the patient cells (Capell and Collins, 2006), many therapeutic strategies were targeting to the posttranslational modification stage, specifically, inhibition of the farnesylation process. That includes all the strategies that have been evaluated in progeria patients, for example, farnesyltransferase inhibitors (FTIs), which is the first compounds that were tested (Lo Cicero and Nissan, 2015). FTIs had previously been used as potential anticancer drugs and had acceptable side effects in children, which promises the shortest timeline from preclinical to clinical testing (Gordon et al., 2014a). FTI treatments improved abnormal blebbed nuclear shape in HGPS patient fibroblasts as well as

increased mouse lifespan and amended disease symptoms in progeria mouse models (Capell et al., 2008; Fong et al., 2006; Toth et al., 2005). Based on these benefits, a clinical trail with FTI lonafarnib for a minimum of 2 years enrolling 25 HGPS children was initiated in 2007. Although with certain variations, promising improvements were reported in weight gain, vascular stiffness, bone density and cardiovascular function in patients (Gordon et al., 2012b).

In addition to FTIs, statins and aminobisphosphonates that inhibit the synthesis of the farnesyl group have also been tested. Varela et al. have shown that combination of pravastatin (a statin) and zoledronate (a aminobisphosphonate) markedly improves the progeria symptoms in both HGPS fibroblasts and progeria mice model (Varela et al., 2008). Comparing to FTI, the combined treatment inhibits both farnesylation and geranylgeranylation of progerin and minimizes the possibility of alternative prenylation events that allow for prelamin A processing in HGPS patients bypassing the effects of FTIs (Varela et al., 2008). In 2009, clinical trials with the combination of the FTI lonafarnib, pravastatin, and zoledronic acid have been performed in 37 children with HGPS. Many patients showed improved weigh gain, reduced vascular stiffness and increased bone mineral density, but no addictive cardiovascular benefit with the addition of pravastatin and zoledronic acid comparing to lonafarnib monotherapy treatment (Gordon et al., 2012b; Gordon et al., 2014b; Gordon et al., 2016).

Alternative strategies affecting progerin from different biological angles have also been proposed. Rapamycin, a macrolide antibiotic promotes autophagy by inhibiting mTOR (mechanistic target of rapamycin) (Kim et al., 2015) and has been

used as an anticancer drug and an immunosuppressant in transplantation (Ehninger et al., 2014). It was reported to reverse premature senescence and nuclear shape abnormalities of HGPS fibroblasts by elevating progerin clearance through autophagy (Cao et al., 2011b). In addition, the antioxidant sulforaphane was shown to enhance progerin clearance by stimulating autophagic proteasomal activity in HGPS fibroblast (Gabriel et al., 2015).

Elevated ROS (reactive oxygen species) level has been reported in HGPS patient cells and leads to accumulated DNA damage in the cells (Lattanzi et al., 2012; Richards et al., 2011; Viteri et al., 2010). Thus, several ROS scavengers aiming to alleviate the abnormal ROS level have been tested as a potentially effective treatment for HGPS patients. N-acetyl cysteine (NAC) has been demonstrated to reduce the levels of un-repairable double strand breaks (DSB) and to improve the proliferative rate in HGPS fibroblasts (Richards et al., 2011). Treatment of methylene blue, an antioxidant compound known to stimulate mitochondrial function, showed beneficial effects in progeria fibroblast culture, including reduced ROS level and nuclear blebbings and improved overall mitochondrial health (Xiong et al., 2016). Recently, a rho-associated protein kinase (ROCK) inhibitor identified using high-throughput screening results in a reduced abnormal nuclear morphology and DNA DSBs along with decreased ROS level in the patient cells (Kang et al., 2017).

Splicing-directed therapies using morpholino antisense oligonucleotides were also conducted. Morpholinos are small modified oligonucleotides that can block splicing events by preventing access of the splicing machinery to the splice sites (Parra et al., 2011). Reduced progerin amounts and extended lifespan were observed

in fibroblasts of HGPS patients and HGPS mouse model respectively using morphlino oligos specifically binding to the neighboring region of the HGPS mutation (Osorio et al., 2011). More recent, retinoids were shown to reverse aging characteristic defects in HGPS primary cells, dependent to the retinoid acid receptors (RAR) (Kubben et al., 2016). Vitamin D was found to reduce progerin production in HGPS cells through vitamin D receptor pathway (Kreienkamp et al., 2014).

These approaches reducing progerin toxicity through different biological processes provide potential addictive or synergetic benefits of development of combination therapies for HGPS treatment.

1.3 Regulation of lamin A expression

The expression of lamin A is highly regulated during development and differentiation. Lamin A/C is absent from early embryo and from some undifferentiated (embryonic stem cells) and cancer cells (eg. leukemias and lymphomas) (Broers et al., 1997; Stadelmann et al., 1990). Although numerous researches have been implemented to study lamin A's function especially after the discovery of the cause of HGPS in 2003, there is not much information known about the regulation of *LMNA* gene expression during development and differentiation.

1.3.1 Transcriptional regulation

Regulatory motifs in LMNA promoter The gene structure of human *LMNA* was first analyzed by Feng Lin and Howard Worman in 1993 (Lin and

Worman, 1993). Analysis of *LMNA* 5'-proximal promoter region revealed that it does not contain typical TATA boxes immediately to the transcription start sites. This is sometimes the case for "housekeeping" genes that are not extensively regulated. Instead, two atypical TATA-like elements, several GC-rich stretches and a CCAAT box were found further upstream (Lin and Worman, 1993; Lin and Worman, 1997). They noticed that lamin A/C was present in extracts from all human tissues but visibly reduced on the whole brain compared to heart, placenta, lung, liver, skeletal muscle, kidney, and pancreas. Furthermore, several leukemias and lymphomas also have little or no level of lamin A/C expression. This differential expression of lamin A/C in various tissues and cell lines suggested that transcription from the gene encoding these two proteins is probably regulated by cell-type-specific factors. However, reporter gene assay of lamin A/C proximal promoter region did not show transcription activation differences between cells with or without endogenous lamin A/C, suggesting lamin A/C proximal promoter is not responsible for the cell-type-specific expression of lamin A/C (Lin and Worman, 1997). Therefore, some *cis* inhibitory elements may exist in regions outside of the proximal promoter, for example *LMNA* distal 5' and 3' regions and the large first intron, and act as a powerful promoter in cells that do not contain lamin A/C.

Other regulatory regions have been identified in *LMNA* promoter region. It has been reported that retinoic acid can induce lamin A/C expression in mouse embryonic carcinoma cells (Lebel et al., 1987). Later, Okumura and colleagues identified a retinoic acid responsive element (L-RARE) in the *LMNA* promoter that is regulated by the transcription factors c-Jun and Sp1/Sp3 (Okumura et al., 2004). In

addition, there are also other regulatory motifs in the *LMNA* promoter binding the transcription factors Sp1/3, c-Jun, and c-Fos, and the transcriptional coactivator CREB-binding protein (Janaki Ramaiah and Parnaik, 2006; Muralikrishna and Parnaik, 2001).

Due to the well-known mechanism of transcriptional inactivation by promoter CpG island hypermethylation in human tumors (Esteller, 2002; Herman and Baylin, 2003), scientists tested promoter hypermethylation for *LMNA* in order to find out whether it is accountable for lamin A/C inactivation in a few hematologic malignancies. Although some of leukemia and lymphoma cell lines showed positive results, most of the tested cell lines do not exhibit CpG island methylation in lamin A/C promoter, implying that other mechanisms might be involved in lamin A/C repression in these cells.

Regulatory role of LMNA first intron The first intron of *LMNA* is approximately 16 kb, taking up more than 60% of the entire *LMNA* gene. The second intron is roughly 2 kb and the rest nine introns are all less than 1 kb in length (Lin and Worman, 1993). Considering its unusually large size and possible regulatory motifs embedding, the first intron of *LMNA* was inspected for elements that are responsible for the differential expression of lamin A/C. Nakamachi et al. identified a cluster of cell-type-specific DNase I hypersensitive sites (DHSs) in a lamin A/C expressing mouse cell line, which is located within the 2.9kb of the 5' of the *LMNA* first intron. This fragment of the HSs lead to an increased transcription level of luciferase reporter constructs when stably integrated into the genome of lamin A/C expressing cells (Nakamachi and Nakajima, 2000b). Furthermore, *LMNA* first intron harbors the

transcription initiation site of lamin C2, which is a male germ-cell-specific A-type lamin generated from *LMNA* gene (Nakajima and Abe, 1995). Analysis of the upstream region of the lamin C2 translation start site revealed binding sites for the transcription factors, hepatocyte nuclear factor-3β and retinoic X receptor β (RXRβ) (Nakajima and Abe, 1995).

With the development of high throughput sequencing technology, more data sets, including DNase Digital Footprinting (DNase-DGF), DNaseI HS Sequencing (DNase-seq) and FAIRE-seq Open Chromatin (FAIRE-seq) etc., towards open chromatin regions are available and more potential regulatory regions such as DHS sites have been identified on *LMNA* gene. In addition, TF bindings and many other epigenetic marks like histone modifications and DNA methylation have been reported for *LMNA* first intron (refer to Figure 4-1 in chapter 4). All these data provide strong scientific supports and a perfect opportunity for us to further dissect the role of *LMNA* first intron in lamin A transcription regulation.

1.3.2 Post-transcriptional regulation

The location where nuclear lamins are processed has been a paradoxical issue in the field over 30 years (Fig 1-7). Although CaaX processing occurs at the cytosolic face of ER in the cytosol for most proteins with the CaaX box (Gelb et al., 2006; Winter-Vann and Casey, 2005), there are evidences suggest that lamin proteins, eg., lamin A, are more likely to be modified within the nucleus. For example, Kinetic studies suggest that nuclear import proceeds much more rapidly than maturation of lamin A (Beck et al., 1990; Goldman et al., 1992; Lehner et al., 1986). Lehner et al.

have showed that the maturation of lamin A was accompanied with the incorporation into the nuclear lamina, which is extracted as a Triton X-100-insoluble particulate subcellular fraction (Lehner et al., 1986). Moreover, very nascent unprocessed prelamin A proteins has been observed to accumulate within nucleoplasm upon farnesylation blockage. On reversal of this block, laminA was observed at the nuclear rim (Lutz et al., 1992; Sasseville and Raymond, 1995). More importantly, Michaelis group has revealed dual ER/INM localization of CaaX-processing enzymes Zmpste24 and Icmt, supporting the idea of nucleus being a physiological CaaX-processing

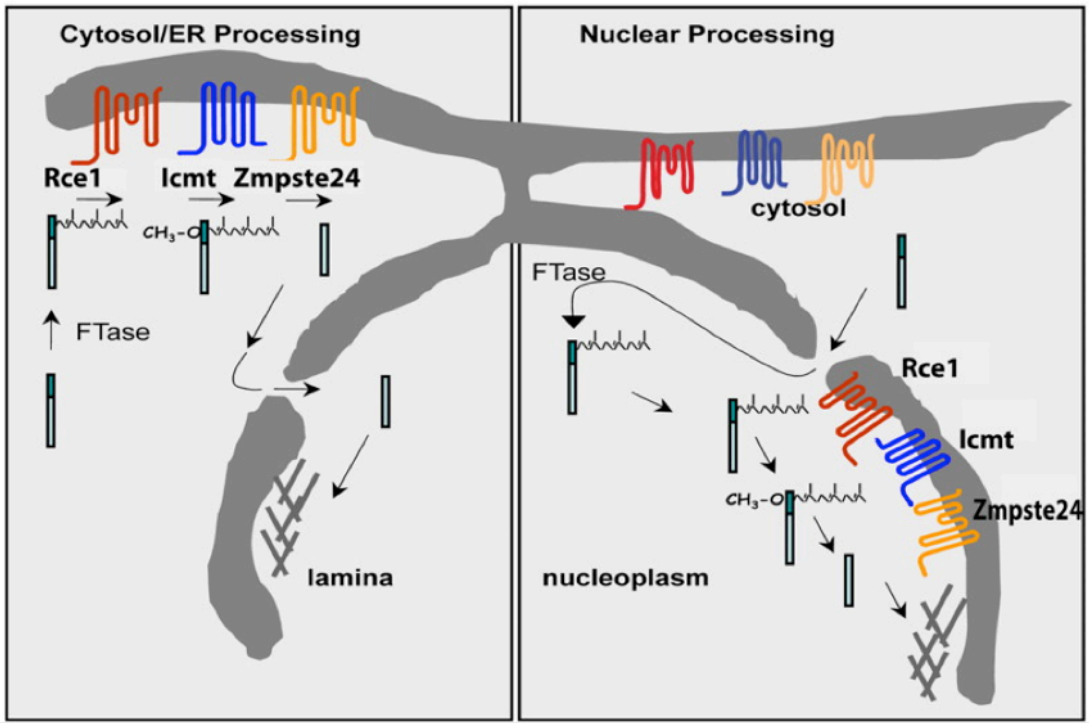

Barrowman et al. Mol Biol Cell. 2008

Figure 1-7. Two opposing models for the intracellular location of prelamin A processing. Left is the Cytosol/ER processing model of lamin A, which is supported by knowledge of CaaX enzyme localization to the cytosol (FTase) and ER membranes (Rce1, Icmt, Zmpste24). Right is the is Nuclear processing model, which has been hypothesized based on lamin A localization, kinetic studies and the INM localization of Zmpste24. (Barrowman et al., 2008)

compartment (Barrowman et al., 2008). Thus, instead of undergoing processing at the ER in the cytosol and then being imported into the nucleus, lamin A precursors are first translocated into the nucleus under the control of its nuclear localization sequence (NLS) followed by CaaXing modification on INM.

Additional to the processing localization paradox, post-transcriptional stability of lamin A mRNA was also investigated. In 2012, Jung et al. revealed the mechanism that contributes to the lamin A/C inactivation in mouse brain tissue. They noticed that most cells in the brain express lamin C but lamin A is mostly repressed, suggesting the transcription of *LMNA* gene is not inhibited. After ruling out the possibility of alternative splicing, the authors presented a mechanism involving lamin A 3'UTR, in which a brain specific microRNA, miR-9, targets to the 3'UTR of lamin A transcripts, mediating the degradation of lamin A mRNA in brain cells. Meanwhile, the expression of progerin, the lamin A mutant causing HGPS, was also repressed by this mechanism in HGPS mouse model. Their results provide explanations to the normal mental development of HGPS patients that is not disrupted by progerin due to the 3'UTR mediated downregulation (Jung et al., 2012). However, this mechanism is brain tissue specific and does not explain the lamin A repression observed in other tissues.

1.3.3 Protein turnover and stability

At the onset of mitosis, both A- and B-type lamins are reversibly disassembled in a phosphorylation-dependent manner to facilitate the nuclear breakdown (Fields and Thompson, 1995; Gerace et al., 1980). Lamin A/C carries

many mitotic phosphorylation sites, most of which are clustered in the head domain and near the nuclear localization signal (NLS) (Simon and Wilson, 2013). Specifically, phosphorylation of Ser-22 at head domain, as well as Ser-392, Ser-404 and Ser-406 at the coiled-coil domain by mitotic cyclin-dependent kinase CDK1 are responsible for the depolymerization of lamin A/C filaments during mitosis (Eggert et al., 1991; Heald and McKeon, 1990; Peter et al., 1990; Schneider et al., 1999; Thompson and Fields, 1996; Ward et al., 1990). The dephosphorylated lamin monomers are later re-incorporated into newly forming daughter cell nuclei in telophase and G1 stage (Dechat et al., 2008; Fields and Thompson, 1995; Moir et al., 2000; Thompson et al., 1997).

Lamin A degradation during apoptosis was accomplished by caspases (Lazebnik et al., 1995; Takahashi et al., 1996). This cleavage happens to the aspartic acid at position 230 (Asp 230) on lamin A protein (Takahashi et al., 1996). Asp230 resides in the 2B region of the lamin A central rod domain (Takahashi et al., 1996), which is one of the most highly conserved regions across all known intermediate filament proteins (Goldman et al., 2002). It has been shown that caspase-uncleavable lamin A mutant slowed down the apoptosis progression in HeLa cells, including nuclear shrinkage and chromatin condensation (Rao et al., 1996), implying that the caspase cleavage of lamin A is critical for the disassembly of the nuclear lamina and nuclear breakdown during apoptosis.

The mechanism controlling lamin proteins' turnover during interphase has always been a mystery. Being proteins providing structural stability, nuclear lamins are considered as long-lived proteins in the cells (Toyama et al., 2013). Furthermore,

It has been proposed that the mutant progerin might be more stable than wild type lamin A, due to the accumulation of progerin during cellular senescence (Goldman et al., 2004) and the greater progerin/lamin A ratio at protein level comparing to that at mRNA level in HGPS patient fibroblasts (Reunert et al., 2012). However, due to the low solubility nature of the lamins, it is a challenge to evaluate their stability using traditional methods that largely depend on the solubility of the protein.

Taken together, although studies mentioned above provide valuable information regarding the general parameters for A-type lamins expression, it is obvious that more extensive work is required in order to better understand the regulation and function of the A-type lamins during development and differentiation.

1.4 Significance of this study

As mentioned above, mutations of lamin A are associated with various phenotypes in laminopathies in the forms of cardiomyopathy, lipodystrophy, muscular dystrophy, tooth disorder, and mandibuloacral dysplasia. However, how lamin A mutants cause a wide range of phenotypes affecting multiple tissues and how lamin A is regulated are remaining uncertain. Therefore to address these questions, I studied the post-translational processing, post-translational degradation and transcriptional regulation in my dissertation in order to better understand the function and regulation of lamin A.

Previously, it has been reported that the anchorage of progerin to the INM disrupts normal NE disassembly during mitosis, leading to an accumulation of progerin-membrane aggregates in mitosis. Importantly, there is a noticeable delay in the recruitment of progerin aggregates back to the nucleus at the end of mitosis.(Cao et al., 2007; Dechat et al., 2007) Although progerin is nuclear-localized, the cytoplasmic accumulated progerin may also contribute to cell abnormalities. In chapter 2, I examined the possible effects of the cytoplasmic progerin by using nuclear localization signal (NLS)-deleted progerin and lamin A. Analysis of these mutants provides new insights into lamin A processing and a better understanding of gene misregulation in muscular dystrophy and cardiomyopathy.

It has been suggested that progerin possesses a higher stability than the wild type lamin A based on the accumulation of progerin in HGPS patient cell (Columbaro et al., 2005; Reunert et al., 2012). To test this hypothesis, I compared the relative stability of lamin A, lamin B1 and progerin using a novel comparison system based on viral 2A sequence in chapter 3. I not only provide strong evidence showing that progerin is more stable than wild type lamin A and lamin B1 in both fibroblasts and human bone marrow-derived mesenchymal stem cells, but also proposed an alternative method that is able to compare protein stability, especially the protein with low solubility, in a more simplified way

Chapter 4 focuses on investigating the transcriptional regulation of lamin A in lamin A non-expressing cells. In this section, the effect of LMNA first intron was functionally analyzed and tested. My data provides evidence showing that in HL60

cells, LMNA first intron plays an essential role in repressing *LMNA* expression by binding to the transcription factor Sp1 through a highly conserved region.

Taken together, my dissertation answers fundamental questions of lamin A processing and regulation, and provides new insights into understanding lamin A's function in various cellular processes.

Chapter 2: Nuclear localization signal deletion mutants of lamin A and progerin reveal insights into lamin A processing and emerin targeting

2.1 Introduction

Lamin A, encoded by the LMNA gene, is a major component of the nuclear lamina in animal cells. As a type V intermediate filament, lamin A forms a dynamic network underneath the inner nuclear membrane (INM), providing mechanical support to the nuclear envelope (Goldman et al., 2002). Besides the structural function, lamin A has been suggested to play essential roles in cell regulation, including chromatin organization, transcription and apoptosis (Capell and Collins, 2006; Csoka et al., 2004; McCord et al., 2013b). These roles are at least partially accomplished by direct or indirect interactions with chromosomes and various nuclear regulators, including emerin, an integral protein of the INM (Berk et al., 2013; Gruenbaum et al., 2002; Holaska and Wilson, 2006; Kubben et al., 2010; Wilson and Foisner, 2010).

Similar to other intermediate filament proteins, lamin A contains a short globular N-terminal head domain, a central α-helical coiled-coil rod domain and a long globular C-terminal tail domain. In addition, between the central rod domain and C-terminal tail domain, lamin A has a nuclear localization signal sequence (NLS), which signals its nuclear residence (Eriksson et al., 2009; Stuurman et al., 1998). Moreover, a CaaX motif (C, cysteine; a, aliphatic amino acid; X, any amino acid) is located at the C-terminus of lamin A, with an exact sequence of CSIM (cysteine-serine-isoleucine-methionine) (Holtz et al., 1989).

It has been shown that proper processing of the CaaX motif is critical for membrane association, localization and functionality of lamin A (Capell et al., 2005;

Gelb et al., 2006; Gruenbaum et al., 2005; Shumaker et al., 2005; Yang et al., 2005). After the DNA sequence is transcribed and translated into the lamin A precursor protein (prelamin A), the cysteine in the CSIM motif is farnesylated by a farnesyltransferase (FTase), followed by the removal of SIM by ZMPSTE24 and carboxylmethylation by Icmt. In the last step, the final 15 amino acids including the farnesylated C-terminus of prelamin A are excised by ZMPSTE24 to allow the release of mature lamin A from the INM (Boyartchuk et al., 1997; Dai et al., 1998; Goldman et al., 2002; Hennekes and Nigg, 1994; Sinensky et al., 1994; Wright and Philips, 2006). ZMPSTE24 is an integral membrane zinc metalloprotease, which has a dual affinity to both the INM and the cytosolic ER membrane (Barrowman et al., 2008; Barrowman et al., 2012; Bergo et al., 2002), and the INM has been shown to be the physiologically relevant compartment for prelamin A processing (Barrowman et al., 2008).

A wide range of human disorders known as laminopathies are associated with mutations of LMNA, among which Hutchinson–Gilford progeria syndrome (HGPS) has the most striking premature aging phenotypes (Capell and Collins, 2006; Eriksson et al., 2009; Vlcek and Foisner, 2007). HGPS is extremely rare, affecting 1 in 4–8 million live births. The patients appear normal at birth, but gradually show symptoms of accelerated aging after 12 months, and often die of heart attacks or strokes in their early teens (Capell and Collins, 2006). The culprit of HGPS is a lamin A mutant known as progerin which is caused by a de novo nucleotide substitution from C to T at position 1824 of LMNA. The mutation changes no amino acid (G608G), but induces a cryptic splicing donor site that generates a 150-nucleotide deletion on the

mRNA sequence. The resulting progerin protein thus bears a 50-amino acid in-frame deletion that lacks the normal cleavage site of ZMPSTE24 for C-terminal farnesyl group release (D'Apice et al., 2004; De Sandre-Giovannoli et al., 2003; Eriksson et al., 2003). Therefore, progerin permanently retains the farnesylated C-terminus and remains associated with the nuclear membrane, eliciting nuclear blebbings and other nuclear abnormalities in HGPS patient cells, including disrupted heterochromatin-lamin interactions and alterations in gene transcription (Cao et al., 2007; Goldman et al., 2004; McCord et al., 2013b). Inhibiting farnesylation of progerin with farnesyltransferase inhibitors (FTIs) or mutating CSIM into non-farnesylable SSIM relocalizes progerin away from the nuclear envelope (NE) and alleviates the prominent nuclear phenotypes (Capell et al., 2005; Toth et al., 2005; Yang et al., 2005; Yang et al., 2011).

Previously, it has reported that the anchorage of progerin to the INM disrupts the normal NE disassembly during mitosis, leading to an accumulation of progerin-membrane aggregates in mitosis. Importantly, there is a noticeable delay in the recruitment of progerin aggregates back to the nucleus at the end of mitosis (Cao et al., 2007; Dechat et al., 2007). To investigate the possible effects of the cytoplasmic progerin aggregates, I created nuclear localization signal (NLS)-deleted progerin and lamin A (PGΔNLS and LAΔNLS, respectively). Analysis of these mutants has revealed new insights into lamin A processing and emerin targeting.

2.2 Results

2.2.1 Deletion of NLS directs lamin A and progerin to the ER

In the current study, the NLS was deleted from lamin A (LA) and progerin (PG) cDNA sequences, (AAAAAGCGCAAACTGGAG), using a PCR-mediated mutagenesis method 48. These newly generated DNA segments were sequenced and sub-cloned into a pEGFP-C1 plasmid for expression (Fig 2-1 & 2-2A). To examine the proteins' sizes, I performed Western blot analyses on transiently transfected HeLa cells with EGFP-LA, EGFP-PG, EGFP-LAΔNLS or EGFP-PGΔNLS plasmids. As expected, the sizes of EGFP-tagged ΔNLS mutants were slightly smaller than their

Figure 2-1. Sequences and positions of the primers used for generation of the NLS mutants. The 150bp deletion in progerin cDNA is highlighted in orange. Primers used for NLS deletion by PCR mutagenesis are shown in blue. The sequences underlined in blue indicate that the primer sequences are consecutive. The red box indicates the position of the NLS deletion.

NLS bearing counterparts, and the endogenous lamin A/C showed a consistent level across all transfected cell lines (Fig 2-2B). Untransfected HeLa cells were used as a control.

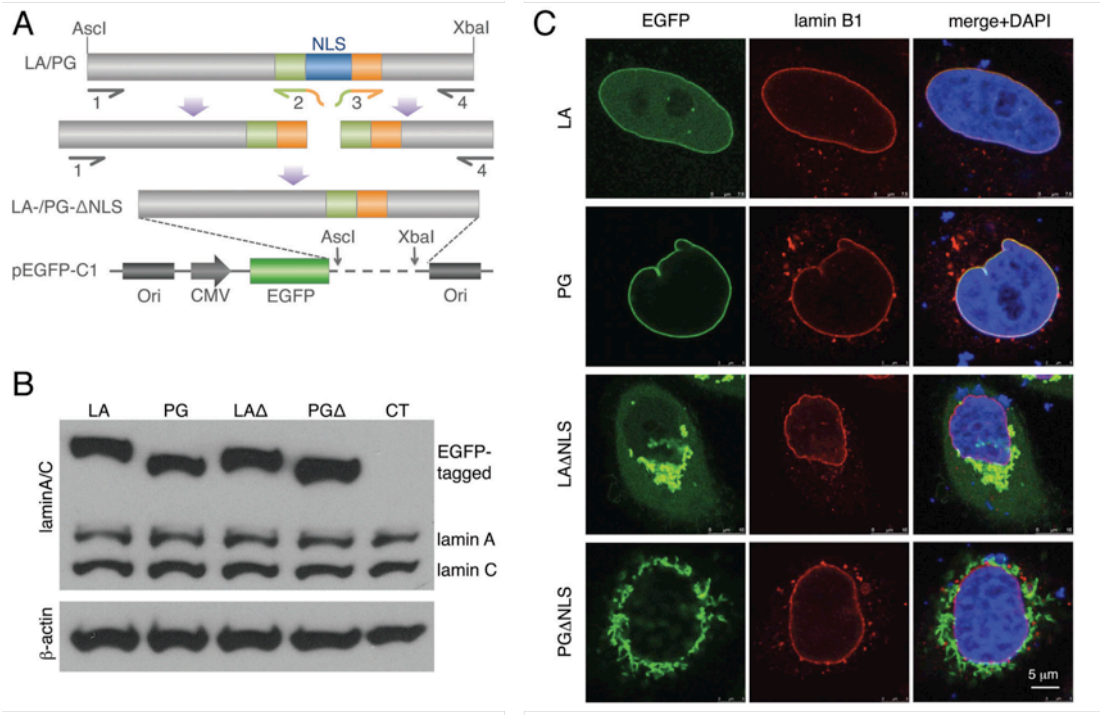

Figure 2-2. Characterization of the NLS-deleted lamin A and progerin. (A) A schematic diagram of the generation of the NLS deletion mutants. Lamin A and progerin NLS deletion (LAΔNLS and PGΔNLS) were created via PCR and subcloned into the AscI and XbaI sites of the pEGFP-C1 plasmid. (B) Western Blot analysis. Protein samples were immunoblotted with antibodies of lamin A/C and β-actin. Non-transfected HeLa cells were used as a control (CT). (C) Confocal fluorescence images. HeLa cells transiently expressing EGFP-LA, EGFP-PG, EGFP-LAΔNLS or EGFP-PGΔNLS (green) were fixed and stained with anti-lamin B1 (red) by immunofluorescence at 24 h post transfection. DNA was stained with DAPI (blue). A representative cell under each condition is shown. Scale bar, 5 μm.

Next, I examined the cellular localization of EGFP-LAΔNLS and EGFP-PGΔNLS. I predicted that, without the NLS, neither of them could enter the nucleus. Indeed, 24 hours post transfection, I found that the majority of the EGFP-LAΔNLS and EGFP-PGΔNLS stayed in the cytosol while EGFP-LA and EGFP-PG co-localized with lamin B underneath the INM (Fig 2-2C). Interestingly, I found that

these cytosolic LAΔNLS and PGΔNLS were concentrated at specific locations. Moreover, time-course experiments revealed that in the EGFP-LAΔNLS transfected cells, diffuse cytoplasmic EGFP signals became detectable after 24 hours post transfection, indicating that the EGFP-LAΔNLS accumulates gradually transformed into two distinct states with the passage of time: the insoluble state and the soluble cytoplasmic state. However, almost all PGΔNLS remained insoluble during the same time course (Fig 2-3).

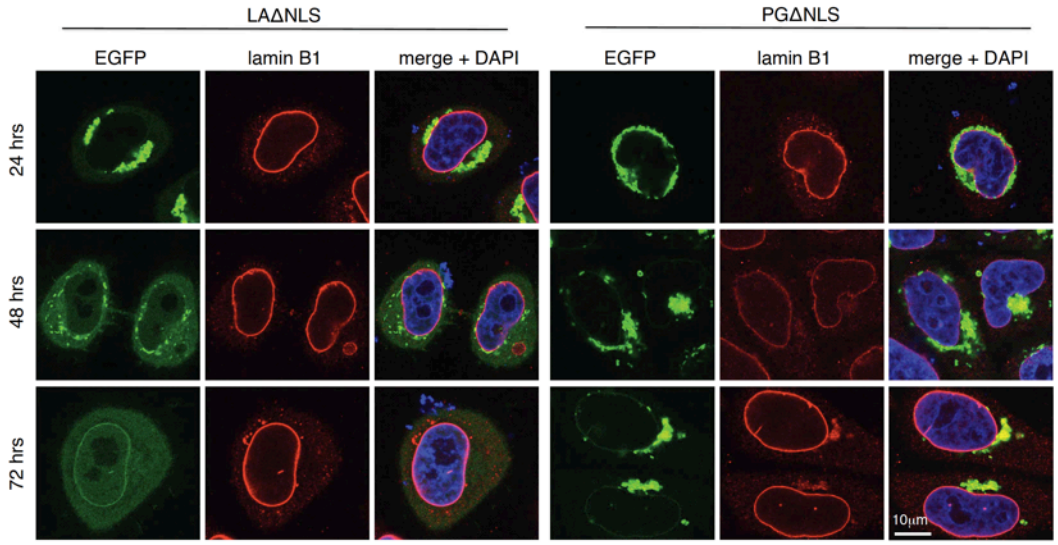

Figure 2-3. The time course experiment showing the localization changes of NLS-deleted mutants. The signals of EGFP-LA NLS and EGFP-PG NLS were fixed and photographed at 24, 48 and 72 hours posttransfection. We found that the aggregates of LA NLS gradually solubilized with the passage of time. In contrast, the PG NLS aggregates remained associated with the ER throughout the 72 hour experiment. Scale Bar: 10μm.

To elucidate the cytosolic localization of these NLS mutants, I co-stained the EGFP-tagged NLS mutants with the anti-KDEL and anti-GM130 antibodies, markers for the ER and Golgi apparatus respectively (Munro and Pelham, 1987; Nakamura et al., 1995). Microscopic analysis revealed that these mutant aggregates co-localized with a sub-domain of the ER while no overlaps were identified between LAΔNLS or

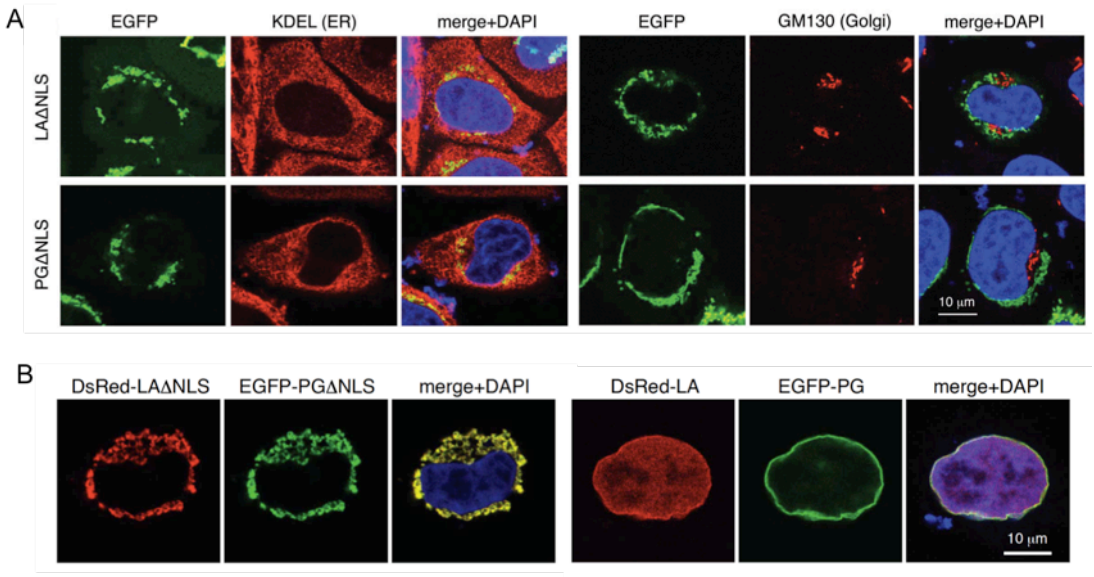

Figure 2-4. ER localization of NLS-deleted mutants. (A) Confocal fluorescence images of HeLa cells transiently expressing EGFP-LAΔNLS or EGFP-PGΔNLS (green) and stained with anti-KDEL (a marker for ER, in red) or anti-GM130 (a marker for Golgi, in red). Scale bar, 10 μm. (B) Confocal fluorescence images of HeLa cells cotransfected with either LAΔNLS and PGΔNLS or lamin A and progerin. Lamin A and LAΔNLS are in red and progerin and PGΔNLS are in green. The distribution of DNA was detected with DAPI in blue. In merged images, yellow indicates overlapping between red and green. Scale bar: 10μm. A representative cell under each condition is shown.

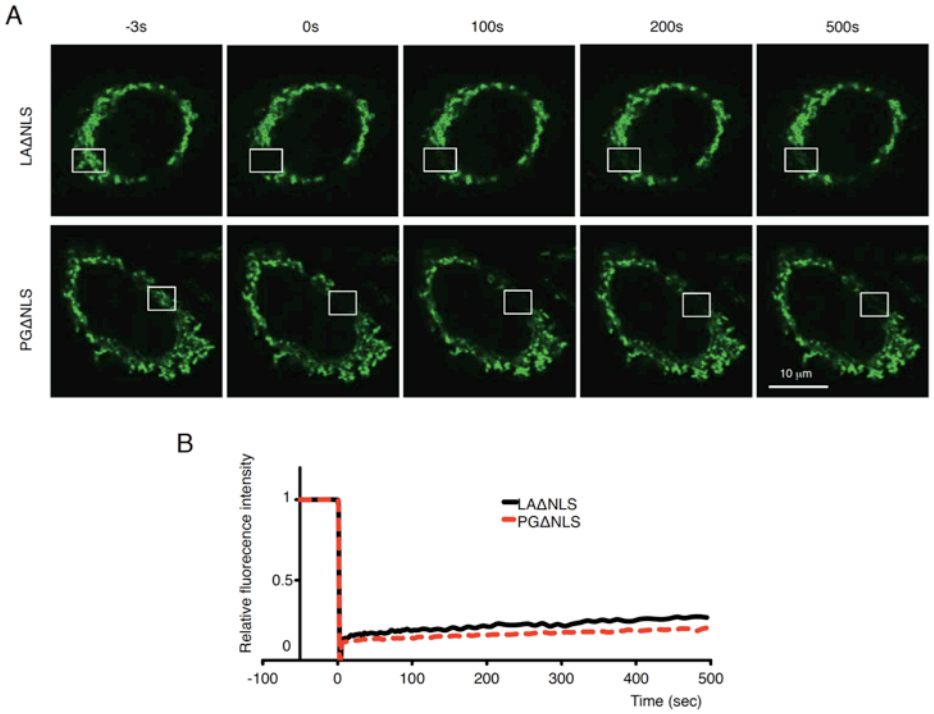

Figure 2-5. Fluorescence Recovery After Photo bleaching (FRAP) analysis of LAΔNLS and PGΔNLS aggregates. (A) Confocal images of the representative pictures at the denoted time points during the FRAP experiment. Squares indicate the photobleached areas. The NLS mutants are shown in green. Bars, 10μm. (B) Quantification of (A).

PGΔNLS and the Golgi marker GM130 (Fig 2-4A). In addition, I observed a complete overlap between the signals of DsRed-LAΔNLS and EGFP-PGΔNLS at 24 hours post transfection (Fig 2-4B), suggesting that both ΔNLS mutants localized to the same ER sub-domain. Consistently, FRAP experiments suggested a comparably slow motion of these ER-associated LAΔNLS and PGΔNLS (Fig 2-5). In summary, I found that without the NLS, both lamin A and progerin immediately attached to a sub-domain of the ER after being synthesized.

2.2.2 The C-terminal farnesyl group tethers LAΔNLS and PGΔNLS to the ER membrane

To understand why LAΔNLS and PGΔNLS showed affinities to the ER, I hypothesized that both ΔNLS mutants were farnesylated at the C-terminus, which tethered these proteins to the ER membrane. To test this hypothesis, I first determined the farnesylation status of LAΔNLS and PGΔNLS with a Click chemistry assay on transfected HeLa cells (see Methods). As expected(Capell and Collins, 2006; Sinensky et al., 1994), wild type mature lamin A was not farnesylated while progerin showed positive farnesylation signals due to its inability to be cleaved by ZMPSTE24 (Fig 2-6A&B). Notably, farnesylation signals were detected in both LAΔNLS and PGΔNLS, but the signal of LAΔNLS was significantly weaker compare to that of PGΔNLS (Fig 2-6A&B). I reason that the difference in farnesylation levels between LAΔNLS and PGΔNLS is likely caused by the cleavage of the C-terminal farnesyl group of LAΔNLS by the ER-associated ZMPSTE24, as ZMPSTE24 has been demonstrated to be a dually localized protein on both the ER membrane and the INM

(Barrowman et al., 2008). Supporting this notion, I observed a gradual increase of diffuse cytoplasmic LAΔNLS with time, which likely represented the cleaved form of LAΔNLS (Fig 2-3).

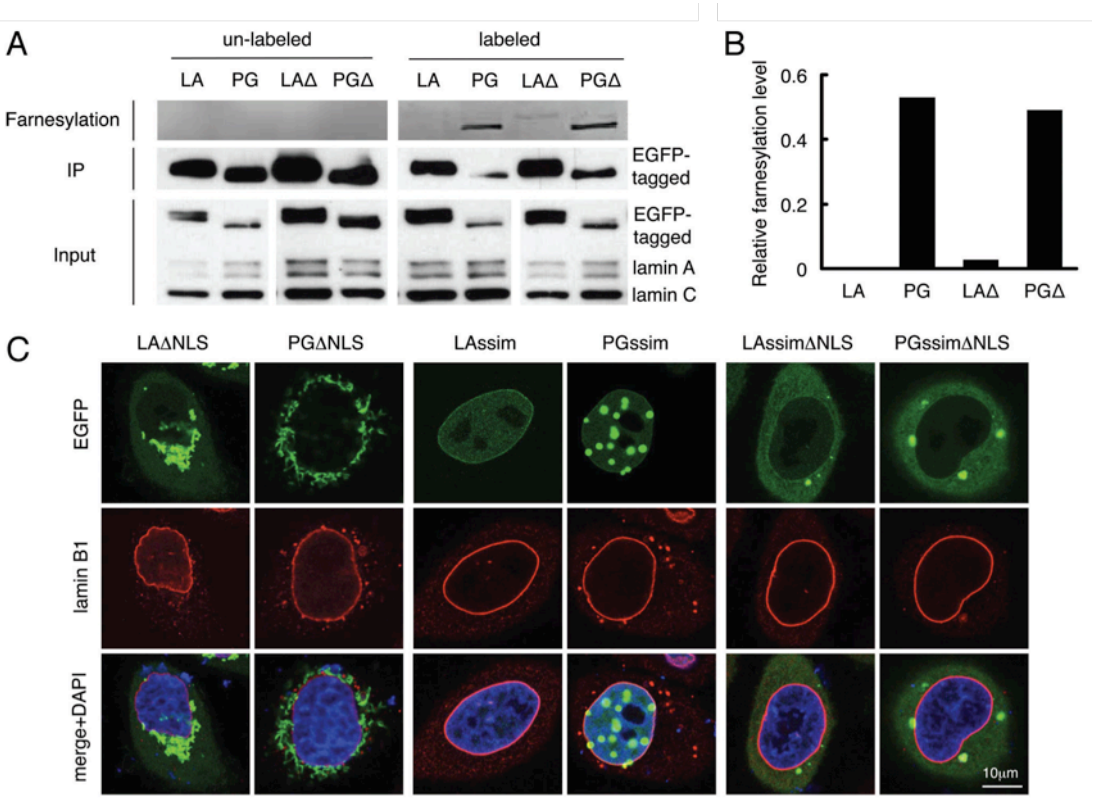

Figure 2-6. C-terminal farnesyl group tethers LAΔNLS and PGΔNLS to the ER membrane. (A) Click chemistry analysis. HeLa cells were transfected with EGFP-LA, EGFP-PG, EGFP-LAΔNLS or EGFP-PGΔNLS and labeled with Click-iT farnesyl alcohol, followed by precipitation with GFP-Trap beads and detection with 647 Alkyne. Strong farnesylation signals appeared in PG and PGΔNLS (PGΔ) lanes, and weak but detectable farnsylation showed in LAΔNLS (LAΔ) lane. (B) Quantification of farnesylation levels in (A). The relative farnesylation level was calculated as the ratio of the farnesylation signal to the corresponding IP'ed protein signal. (C) Confocal fluorescence images of LAssimΔNLS and PGssimΔNLS. Immunofluorescence was performed 24 h after transfection. Confocal images show EGFP (green), lamin B1 (red), and DNA (blue). A representative cell under each condition is shown. Scale bar, 10 μm.

To further test this idea, I asked whether blocking the farnesylation of LAΔNLS and PGΔNLS could lead to dissociation from the ER membrane. It has been shown that farnesylation is abolished when the C-terminal sequence of CSIM on lamin A and progerin is mutated into SSIM (Capell et al., 2005; Yang et al., 2006;

Yang et al., 2011). Thus, I generated the SSIM-ΔNLS double mutants of lamin A and progerin (LAssimΔNLS and PGssimΔNLS). As expected (Capell et al., 2005; Capell et al., 2008; Yang et al., 2008; Yang et al., 2011), the SSIM mutation alone directed lamin A and progerin into the nucleoplasm (Fig 2C). Importantly, when the two features ΔNLS and SSIM were combined, the proteins were released from the ER into the cytoplasm (Fig 2-6C), validating the idea that the farnesyl groups on the C-termini of LAΔNLS and PGΔNLS tethered them to the ER membrane.

Additional support was obtained with a drug-treatment experiment using farnesyltransferase inhibitors (FTIs). When I blocked farnesylation with FTIs, the non-farnesylated LAΔNLS and PGΔNLS became soluble in the cytoplasm (Fig 2-7).

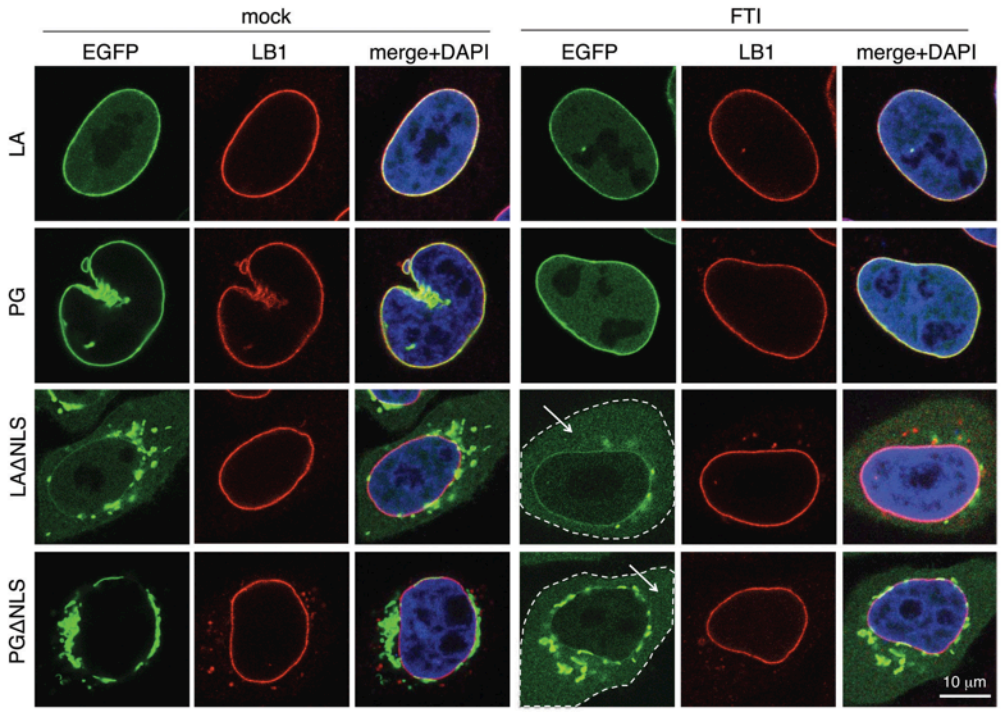

Figure 2-7. The effect of FTI treatment resembles that of LAssimΔNLS. FTI treatment was performed on HeLa cells at 4 h post-transfection for 16 h. The cytoplasm of the ΔNLS mutants transfected cells with FTI treatment are outlined by dashed lines. Soluble cytoplasmic EGFP signals are pointed by arrows. Confocal images show EGFP (green), lamin B1 (red), and DNA (blue). A representative cell under each condition is shown. Scale bar, 10 μm.

2.2.3 Nuclear targeting of emerin is disrupted by LAΔNLS and PGΔNLS

It has been suggested that emerin localization is dependent on A-type lamins (Vaughan et al., 2001). Thus, I investigated whether the distribution of emerin was altered by the ΔNLS mutants. In control LA and PG transfected HeLa cells, as expected, most of the endogenous emerin co-localized with LA or PG to the nuclear rim, outlining the shape of the nucleus (Fig 2-8A, first and third panels). However, in the ΔNLS mutant transfected cells, emerin became cytosolic and colocalized with the ΔNLS mutants to a sub-domain of the ER (Fig 2-8A, second and fourth panels), suggesting that emerin's nuclear localization is dependent primarily on lamin A. Notably, emerin's normal nuclear localization appeared to be more disrupted by PGΔNLS than by LAΔNLS, as the nuclear rim staining of emerin was almost absent in PGΔNLS transfected cells as it was still visible in LAΔNLS expressing cells (Fig 2-8A, second and fourth panels).

To determine the potential physical interactions between emerin and the ΔNLS mutants, an immunoprecipitation (IP) experiment was carried out using GFP-Trap beads. Non-transfected HeLa cells were used as a control. I found that emerin co-precipitated with EGPF-LA, EGFP-PG, EGFP-LAΔNLS and EGFP-PGΔNLS (Fig 2-8B). Consistent with the microscopic observation that PGΔNLS more effectively sequestered emerin from the nucleus than LAΔNLS (Fig 2-8A), quantification revealed that the interaction of emerin with PGΔNLS was almost twice as strong as with LAΔNLS (Fig 2-8C).

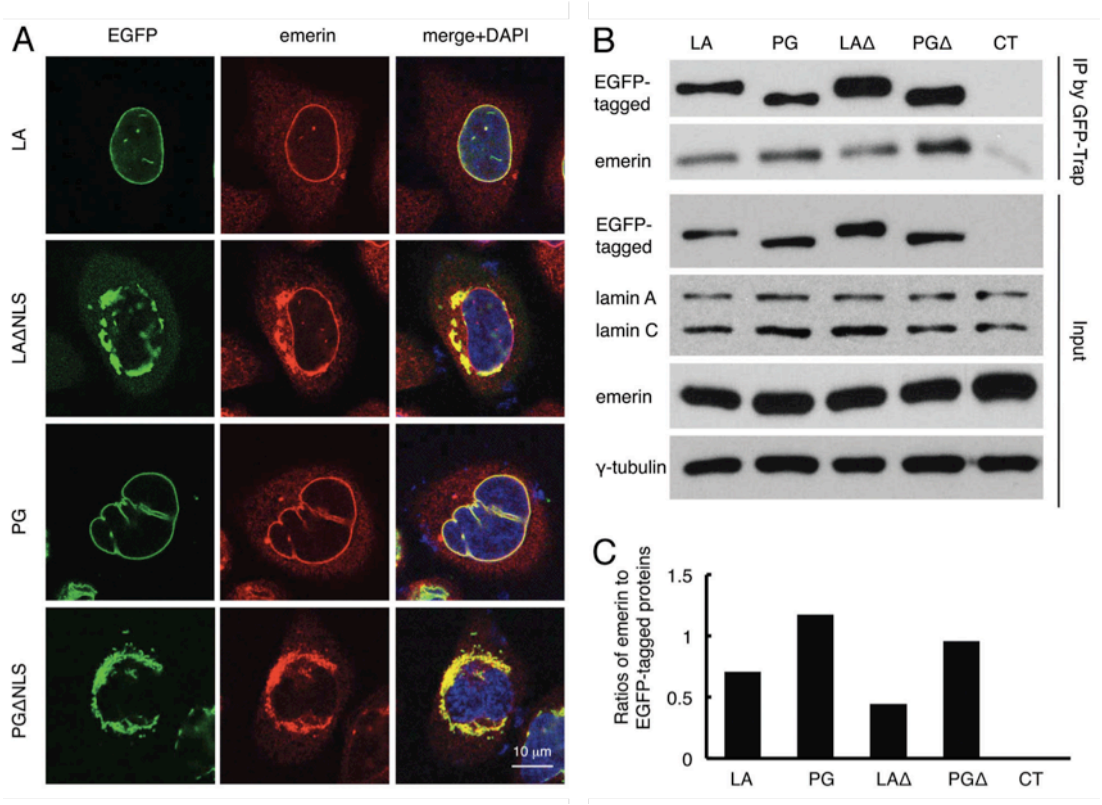

Figure 2-8. Disrupted emerin localization in cells expressing LAΔNLS or PGΔNLS. (A) Confocal fluorescence images. HeLa cells transiently expressing EGFP-LA, EGFP-PG, EGFP-LAΔNLS or EGFP-PGΔNLS (green) were fixed and stained with anti-emerin (red) at 24 h post transfection. A representative cell under each condition is shown. Scale bar, 10 μm. (B) IP with GFP-Trap®_A beads in the transfected HeLa cells. Un-transfected HeLa cells were used as a control (CT). (C) Relative intensity of emerin to EGFP-tagged proteins in each immunoprecipitated sample. Band intensities were analyzed using ImageJ. Relative intensities were presented as the ratio of emerin to EGFP. Two biological duplicates were conducted. A representative experiment was shown.

Taken together, these data showed that the NLS deletion mutants interacted and sequestered emerin away from its normal INM localization. Our data suggest that emerin is targeted to the nucleus primarily through its interactions with lamin A, and there is a stronger affinity between emerin and progerin or PGΔNLS than emerin and lamin A or LAΔNLS.

2.3 Discussion

2.3.1 The processing of prelamin A by the INM and ER localized ZMPSTE24

ZMPSTE24, as one of the key players in the lamin A maturation process, is an integral membrane protein (Barrowman et al., 2008; Barrowman et al., 2012; Bergo et al., 2002). The cytosolic face of the ER membrane was considered its primary residency until recently when Barrowman and colleagues clearly demonstrated that ZMPSTE24 was also localized to the INM, and that the nucleus was the physiologically relevant compartment where the C-terminal cleavage of prelamin A occurred (Barrowman et al., 2008).

In this study, I generate the cytoplasmic-resident lamin A mutant LAΔNLS. This mutant rapidly tethers to a sub-domain of the ER via its farnesyl tail after being synthesized on the ribosomes (Figs 2-4 and 2-6). Notably, I find that over a course of 72 hours post transfection, the ER-associated LAΔNLS becomes gradually released into the cytoplasm (Figs 2-6 & 2-7), which is likely to be resulted from the removal of the farnesylated C-terminus. In support of this notion, I detect a reduced level of farnesylation in LAΔNLS compared to PGΔNLS, and the double mutant LAssimΔNLS and PGssimΔNLS and FTI treatment experiments further support that the cytoplasmic soluble fraction of LAΔNLS is not farnesylated (Figs 2-6 & 2-7). Based on the previous finding that ZMPSTE24 is a dually localized enzyme (Barrowman et al., 2008), I would like to suggest that the cleavage of LAΔNLS's farnesylated tail is executed by the ER-associated ZMPSTE24.

Interestingly, the Click Chemistry labeling experiment reveals unexpected differences in enzymatic activities of the ER-associated and the INM-associated ZMPSTE24. As shown in Fig 2-6 A&B, the processing of the wild-type lamin A is achieved in an extremely rapid manner on the INM, leading to no detection of the farnesylated prelamin A. In contrast, the processing of the ER-associated LAΔNLS by the ER-associated ZMPSTE24 appears to be much slower, which resulted in a clearly detectable fraction of the farnsylated LAΔNLS at 48 hours post transfection. This difference in enzymatic efficiency is intriguing, implying a possibility that some unknown nuclear factors might serve as activators to facilitate ZMPSTE24-mediated prelamin A processing on the INM.

Previously, Barrowman and colleagues have examined the ZMPSTE24 processing kinetics of a lamin A-tail construct that is fused with a large carrier protein HA-pyruvate kinase either with or without the NLS (Barrowman et al., 2008). Without the NLS, the lamin A-tail construct produced a cytosolic protein. Consistently with my observation, Barrowman and colleagues found that ZMPSTE24 was functional in both the INM and the ER locations. Interestingly, they found that the rate of ZMPSTE24 processing of this lamin A fusion protein was quite similar in both locations (Barrowman et al., 2008). The potential differences in the two studies may be caused by many variables including differential access of membrane-bound proteins versus cytosolic proteins and differential enzymatic activity of ZMPSTE24 to LAΔNLS versus Pyruvate kinase-lamin A tail fusion protein. Future studies, with controls of these variables, will be required to directly compare the processing kinetics of the ER and INM localized ZMPSTE24 to lamin A.

2.3.2 Emerin nuclear localization is disrupted by PGΔNLS

Mutations and aberrant targeting of emerin cause a number of diseases including muscular dystrophy, cardiomyopathy and Emery-Dreifuss muscular dystrophy, which is characterized by muscle weakening, contractures of major tendons and potentially lethal cardiac defects (Astejada et al., 2007; Holaska and Wilson, 2006; Lee et al., 2001; Mislow et al., 2002). Emerin primarily localizes to the INM. Previously, Ostlund and colleagues suggested that the N-terminal nucleoplasmic domain of emerin was both necessary and sufficient for targeting emerin to the INM (Ostlund et al., 1999). However, using SW13 cells that did not express lamin A, Vaughan et al. showed that the INM localization of emerin was dependent on the lamin A complex containing both lamins A and B (Vaughan et al., 2001). In support of this argument, it has been shown biochemically that that emerin is in complexes with both A and B type lamins (Clements et al., 2000; Vaughan et al., 2001).

In this study, I compartmentalize B type lamins and endogenous lamin A/C to the nucleus and LAΔNLS and PGΔNLS to the ER. With this geographic separation, I compare the effects of LAΔNLS, PGΔNLS and endogenous lamins on emerin's nuclear targeting. My analyses reveal that at the presence of wildtype lamins A, B and C, emerin's nuclear localization is still mainly dependent on LAΔNLS and PGΔNLS (Fig 2-8). Notably, my study suggests that emerin is dominantly extracted from the INM by the ER-localized progerin. In support, the IP experiment further suggests that emerin exhibits a stronger binding affinity to progerin or PGΔNLS than to lamin A or

LAΔNLS, respectively (Fig 2-8). Future work will focus on determining whether other INM proteins are also affected by PGΔNLS.

Given the emerging roles of the emerin-lamin A complex in regulating muscle- and heart-specific gene expression (Ho et al., 2013), I believe that these new insights gained from this study will promote a better understanding of gene misregulation in muscular dystrophy and cardiomyopathy.

Chapter 3: Comparing lamin proteins post-translational relative stability using a 2A peptide-based system reveals elevated resistance of progerin to cellular degradation

3.1 Introduction

As mentioned earlier, HGPS patients were born with normal appearance, but gradually developed accelerated aging symptoms and abnormalities affecting multiple tissues due to the accumulation of progerin (Merideth et al., 2008; Pollex and Hegele, 2004). Previously, higher progerin to lamin A ratio at protein level comparing to that at mRNA level has been reported, which was thought due to the decreased amount of lamin A in progeria patients (Moulson et al., 2007; Reunert et al., 2012). A fibroblast cell line from a 9-year-old HGPS patient with more also showed a greater ratio of progerin to lamin A when compared with fibroblasts from younger HGPS patients (Columbaro et al., 2005). Furthermore, increased progerin protein levels have been observed during cellular senescence of HPGS patience fibroblasts (Goldman et al., 2004). The increased ratio of progerin to lamin A often accompanies with increased severity of the progeria phenotype (Reunert et al., 2012). Therefore, it has been assumed that progerin might be more stable than wild type lamin A, possibly due to the farnesyl residue still attached to the protein.

The commonly used approach of measuring protein stability is pulse-chase analysis, which metabolically labels the protein of interest in the cells with a radioactive precursor for a short period, then chased with an excess of nonradioactive precursor molecules in the culture medium, followed by immunoprecipitation and SDS-PAGE to quantify the radiolabeled protein (Fritzsche and Springer, 2014; Zhou, 2004). However, successful deployment of this method, particularly the step of immunoprecipitation, largely depends on the solubility of the target protein. Although this method has been widely used to examine pre-lamin stability

(Bertacchini et al., 2013), the tendency of lamin proteins to polymerize into higher order insoluble structures in vitro at relatively low critical concentrations (Dechat et al., 2010) has a potential to interfere with the accurate assessment of lamin protein stability using this methodology. To overcome this limitation, I adapted the novel method originally employed by Rodriguez-Contreras and colleagues (Rodriguez-Contreras et al., 2015) to demonstrate differential glucose transporter stability under various growth conditions in the protozoan parasite Leishmania mexicana. This simplified approach exploits the unique properties of viral 2A peptide sequences (De Felipe et al., 2006) in a manner that does not require immunoprecipitation or radiolabelling of cells, and consequently avoids the complications arising from the treatment of cells with the translation inhibitor cycloheximide.

The 2A peptide was initially discovered and characterized in the foot and mouth disease virus (FMDV) which was shown to mediate the production of two polypeptides (i.e., 2A and 2B) from the virus' complex single open reading frame (ORF). Translation of the 19 amino acid 2A peptide coding sequence causes an intra-ribosomal "skipping" event between the final Gly residue of the 2A peptide and the first Pro residue of the next polypeptide, causing the release of the first polypeptide and reinitiating translation of the second polypeptide starting with Pro (Fig 3-1A) (for simplicity, this process will be referred to as "cleavage") (de Felipe et al., 2010; De Felipe et al., 2006; Donnelly et al., 2001; Ryan et al., 1991). Functional 2A peptide-like sequences have been discovered in several other viruses and retrotransposons, and various versions of the sequence have been exploited in molecular biology, gene therapy, and biotechnology applications because they enable the production of

multiple polypeptides from single open reading frames (De Felipe et al., 2006). Because the two polypeptides resulting from a 2A-mediated

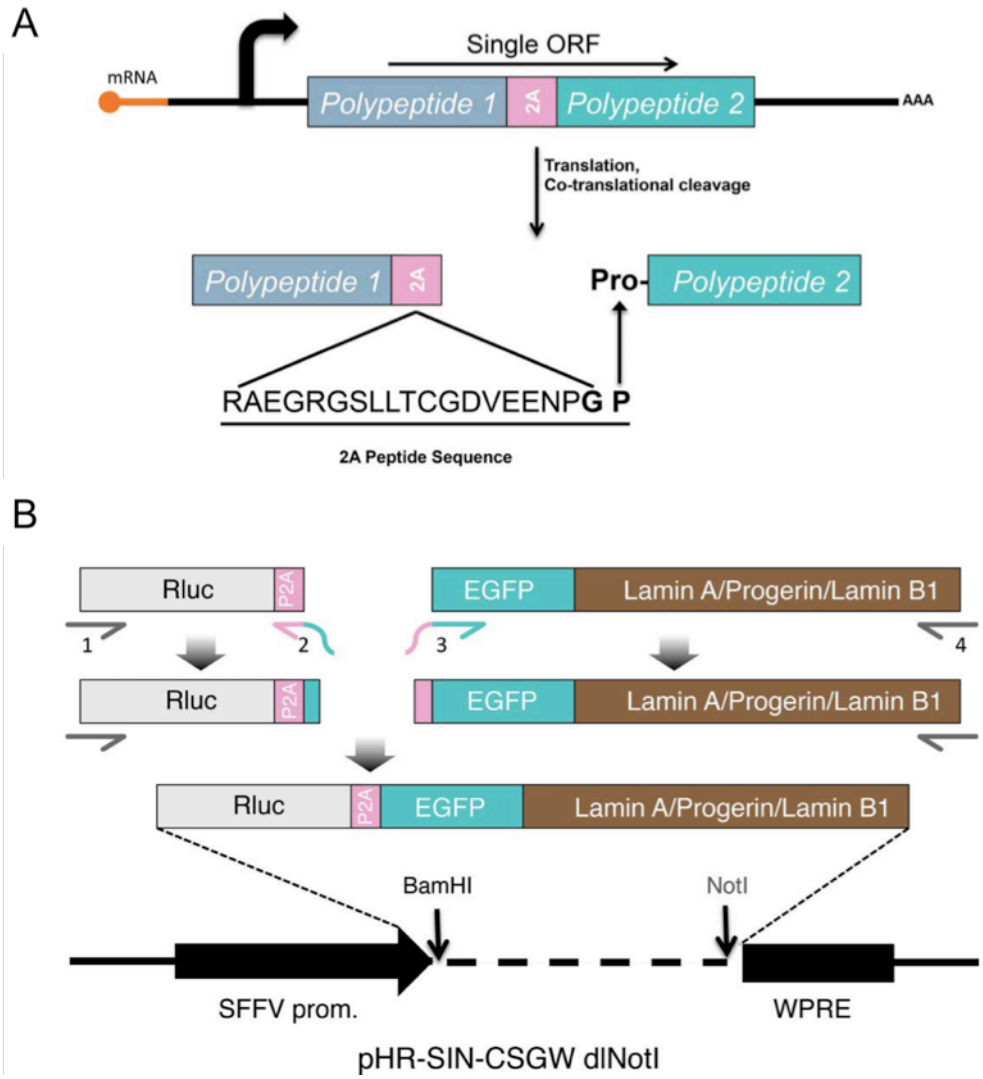

Figure 3-1. Schematic diagrams of processing and creation of 2A constructs. (A) Processing of 2A-linked constructs. DNA sequences of Polypeptide 1 and 2 are connected by a 2A motif and transcribed into a single ORF. The two polypeptides are then separated during translation by a co-translational, intraribosomal cleavage right before the proline at the end of the 2A sequence, adding a proline at the N-terminus of polypeptide 2. (B) Generation of luciferase-P2A-lamin (lamin A, progerin, lamin B1) constructs. Segments of luciferase- P2A and EGFP tagged lamins were amplified and linked together via PCR. The subsequent long fragment was subcloned between the BamHI and NotI sites on the lentivector of pHR-SIN-CSGW dlNotI plasmid.

co-translational cleavage event are inherently transcriptionally and translationally co-regulated, their relative abundance in the cell is determined solely by their post-translational stability. Differences in the abundance ratio of the polypeptides among cell types or under differential growth conditions will reflect alterations in the post-translational stability of one or both polypeptides. It has been reported that the 2A sequence from Porcine teschovirus-1 (P2A) has the highest cleavage efficiency among all four commonly used 2A sequences (Kim et al., 2011a). Therefore I chose to use P2A in our study.

I reasoned that fusing Renilla luciferase (Rluc) to various EGFP-tagged lamin proteins (lamin A, progerin, and lamin B1) via a P2A peptide sequence (Fig 3-1B) would allow the relative post-translational stabilities of the lamin proteins to be assessed by comparing the EGFP-lamin:Rluc ratios for each lamin type, since the stability of Rluc should be the same in all of the constructs. Different antibodies may present a discrepancy in protein detection efficiency, but fusing EGFP to each lamin eliminates this variability and allows uniform detection with an anti-EGFP antibody. Lamin stability was investigated in lamin A expressing fibroblasts and bone marrow mesenchymal stem cells (hBM-MSCs). My results are consistent with the notion that progerin is more stable than wild type lamin A. Moreover, FTI treatment significantly reduced the post-translational stability of progerin to the level of wild type lamin A, which may provide new insights into future directions for the clinical therapy of HGPS.

3.2 Results

3.2.1 Progerin possesses higher post-translational stability than lamin A protein in primary fibroblasts and human bone marrow-derived mesenchymal stem cells (hBM-MSCs).

To connect Rluc and EGFP-tagged lamin proteins with P2A sequence, I applied a series of PCR reactions as illustrated in the schematic Figure 1B. The subsequent Rluc-P2A-lamin constructs were then subcloned into the lentiviral expression vector for lentiviruses production in HEK293T cells as previously described (Xiong et al., 2016). To compare these lamins' relative stabilities using this P2A platform, I first transduced the lentiviruses in primary human fibroblasts and human bone marrow-derived mesenchymal stem cells (hBM-MSCs) (Fig 3-2), both of which express comparable amounts of endogenous lamin A (Fig 3-3). In both cell types, the majority of the EGFP-lamin proteins were successfully dissociated from Rluc protein under the effect of P2A motif, with a small fraction of uncleaved products (P2A-LA: 8.8%; P2A-PG:10.7%; P2A-LB1: 25.3%) (Fig 3-3). The expression of each EGFP-lamin was further validated using lamin-specific antibodies (Fig 3-2 A&C). The localization of each EGFP-lamin protein was identical to that of the corresponding endogenous lamin (Fig 3-2 B&D), suggesting that these EGFP-lamins are properly integrated into the nuclear lamina network in fibroblasts and hBM-MSCs.

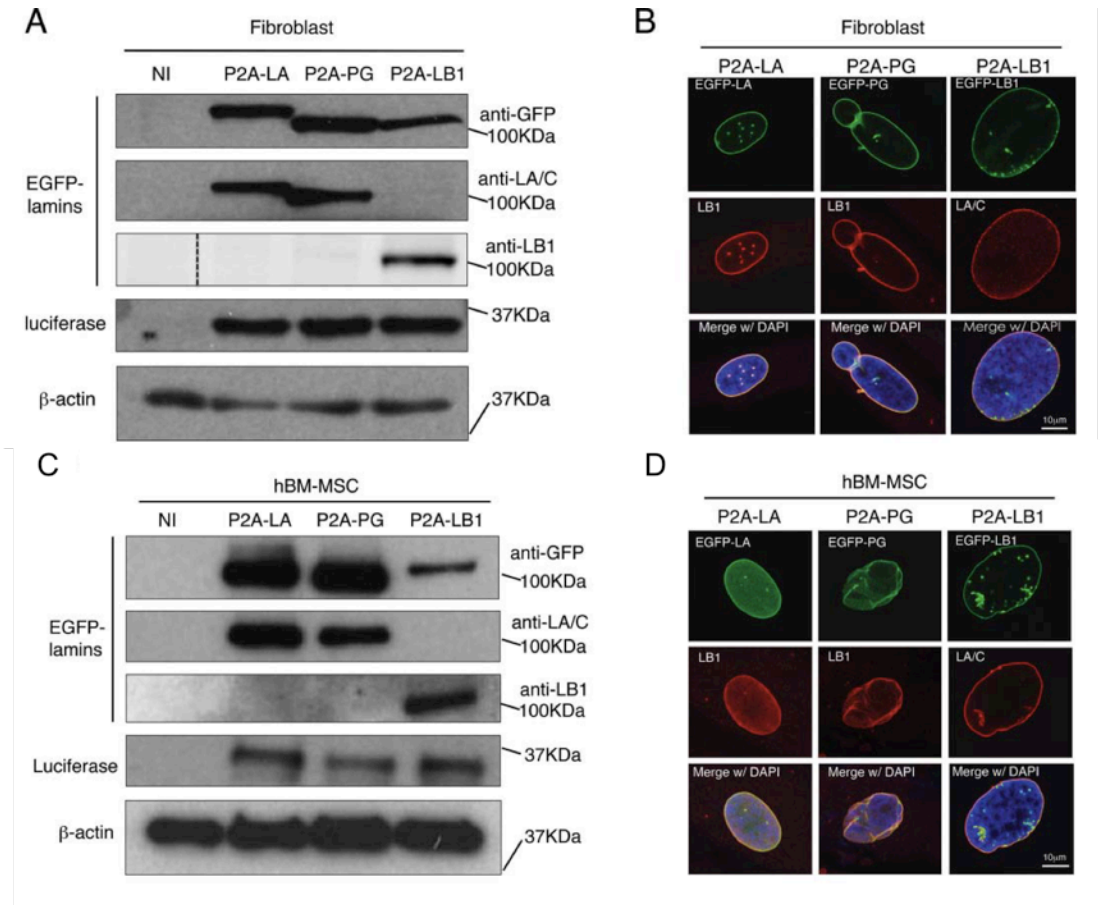

Figure 3-2. Characterization of 2A constructs in both human fibroblasts and hBM-MSCs (A) Western blotting analysis of viral infected human fibroblasts. Protein samples were immunoblotted with antibodies of GFP, lamin A/C, lamin B1, luciferase and b-actin. Non-infected fibroblast cells were used as a negative control. (B) Confocal fluorescence images. Infected fibroblasts expressing 2A-lamins (green) were fixed and stained with anti-lamin B1 (red) by immunofluorescence at 48 hours post infection. DNA was stained with DAPI (blue). A representative cell under each condition is shown. Bars, 10 mm. (C) Western blotting analysis of viral infected hBM-MSCs. Protein samples were immunoblotted with antibodies of GFP, lamin A/C, lamin B1, luciferase and b-actin. Non-infected hBM-MSCs cells were used as a negative control. (D) Confocal fluorescence images of infected hBM-MSCs expressing 2A-lamins (green) and stained with anti-lamin B1 (red) by immunofluorescence at 48 hours post infection. DNA was stained with DAPI (blue). A representative cell under each condition is shown. Bars, 10 mm. P2A-LA, P2A-PG and P2A-LB1 refer to the constructs of luciferase-P2A-lamin A, luciferase-P2A-progerin and luciferase-P2A-lamin B1.

Next, time course experiments were applied to investigate the post-translational protein stability of the EGFP-lamins within a 7-day period after transduction. A gradual accumulation of the three EGFP-tagged lamins was noticeably observed in both fibroblasts and hBM-MSCs (Fig 3-4 A&B). Particularly

in the fibroblasts, the proteins exhibited a rapid accumulation rate with greater slopes at earlier time points (day 2 - 4), and then reached the plateau by day 5 (EGFP-PG and EGFP-LB1) or 6 (EGFP-LA) (Fig 3-4E). A similar trend was also observed in hBM-MSCs (data not shown).

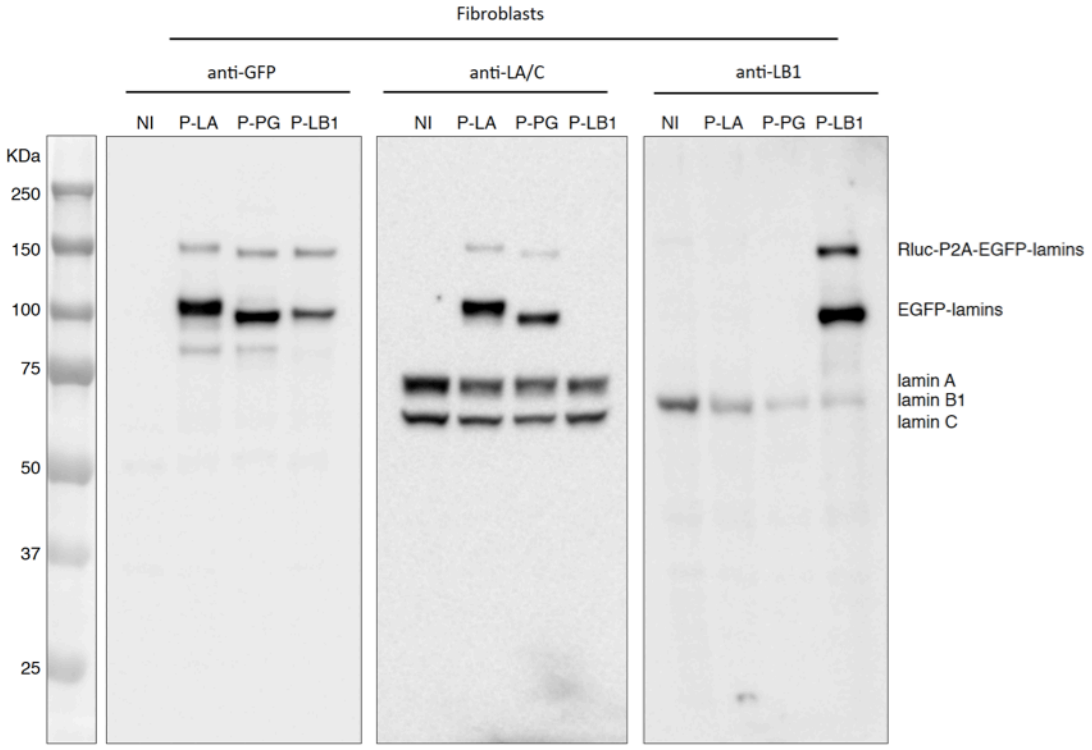

Figure 3-3. Full gel image of fibroblasts expressing Rluc-P2A-EGFP-lamin A (P-LA), Rluc-P2A-EGFP-progerin (P-PG) and Rluc-P2A-EGFP-lamin B1 (P-LB1).

To analyze the post-translational stability of these EGFP-tagged lamin variants, the EGFP signal was normalized to Rluc for quantification and the analysis presents an average of the plateau period from day 5 to day 7. The Rluc and the EGFP-tagged lamin/progerin are encoded within the same mRNA, and their translation initiates from the same ATG. Because the P2A-mediated "cleavage" that separates these two proteins occurs during translation, the post-translational stability

of the Rluc and EGFP-lamin proteins is completely independent. Normalization to the co-translated Rluc control renders the contribution of all transcriptional and post-

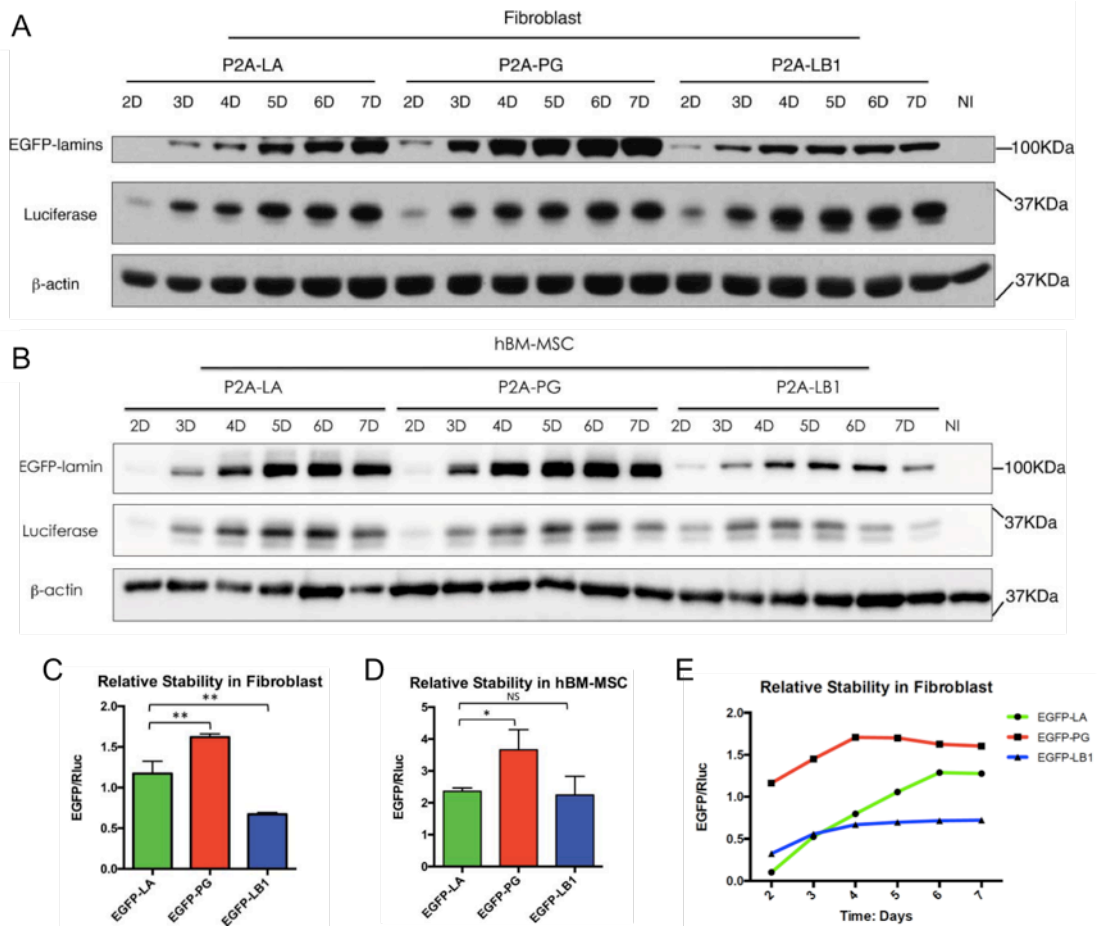

Figure 3-4. Comparing relative stability of lamin A, progerin and lamin B1 in fibroblasts and hBM-MSCs. (A) Western blotting analysis on time course of viral infected human fibroblasts. Protein samples were immunoblotted with antibodies of GFP, luciferase and b-actin. (B) Time course of viral infected hBM-MSCs were analyzed by Western blotting. Antibodies of GFP, luciferase and b-actin were utilized for immunoblotting. (C) and (D) are quantifications of lamins' relative stabilities in (A) and (B), respectively. The relative stability was calculated as the intensity ratio of EGFP/luciferase. Bar graph shows the average of day 5 to day 7 data. Results were generated from 3 biological replicates. *P < 0.05, **P < 0.01. (E) Representative plot of EGFP/Rluc ratio during time course experiment for fibroblasts. P2A-LA, P2A-PG and P2A-LB1 refer to the constructs of luciferase-P2A-lamin A, luciferase-P2A-progerin and luciferase-P2A-lamin B1.

transcriptional regulatory mechanisms, except post-translational protein stability. Thus, we reason that the steady state levels of EGFP-lamins (from day 5 to day 7)

should directly reflect the post-translational stability of these proteins when normalized to Rluc. I further suggest that differences in the EGFP/Rluc ratio between the various EGFP-lamin/progerin fusions should reflect differences in relative post-translational stability. Based on this method, I found that among the three lamins, EGFP-progerin possessed the greatest relative stability in both cell types, followed by EGFP-lamin A and EGFP-LB1 (Fig 3-4 C&D). Interestingly, EGFP-lamin B1 was the least stable lamin variant in fibroblasts (Fig 3-4 C) and exhibited a stability similar to EGFP-LA in hBM-MSCs (Fig 3-4 D), despite the fact that it, like progerin, remains farnesylated.

3.2.2 Endogenous lamin A may not alter the post-translational stability of exogenously expressed A type lamin proteins

Because the 2A peptide-mediated reporter system relies on overexpression of exogenous EGFP-lamin proteins, which are expected to interact with endogenously encoded lamins, I wanted to determine if the presence of endogenous lamin A/C influenced the stability of the EGFP-lamin proteins. To address this issue, I used wild type mouse embryonic fibroblasts (MEF) and lamin A null MEF lines for lentiviral transduction. Like in fibroblasts and hBM-MSCs (Figs 3-2 & 3-4), the fused proteins were successfully expressed and "cleaved" in both types of MEFs (Fig 3-5A).

Next, the post-translational stability of EGFP-LA and EGFP-PG was determined by time course experiments from 4 days to 6 days post-transduction when the steady state expression was achieved (Fig 3-5B). The quantification analysis was done by averaging all the EGFP/Rluc ratio of each lamin protein (Fig 3-5C), as in Fig

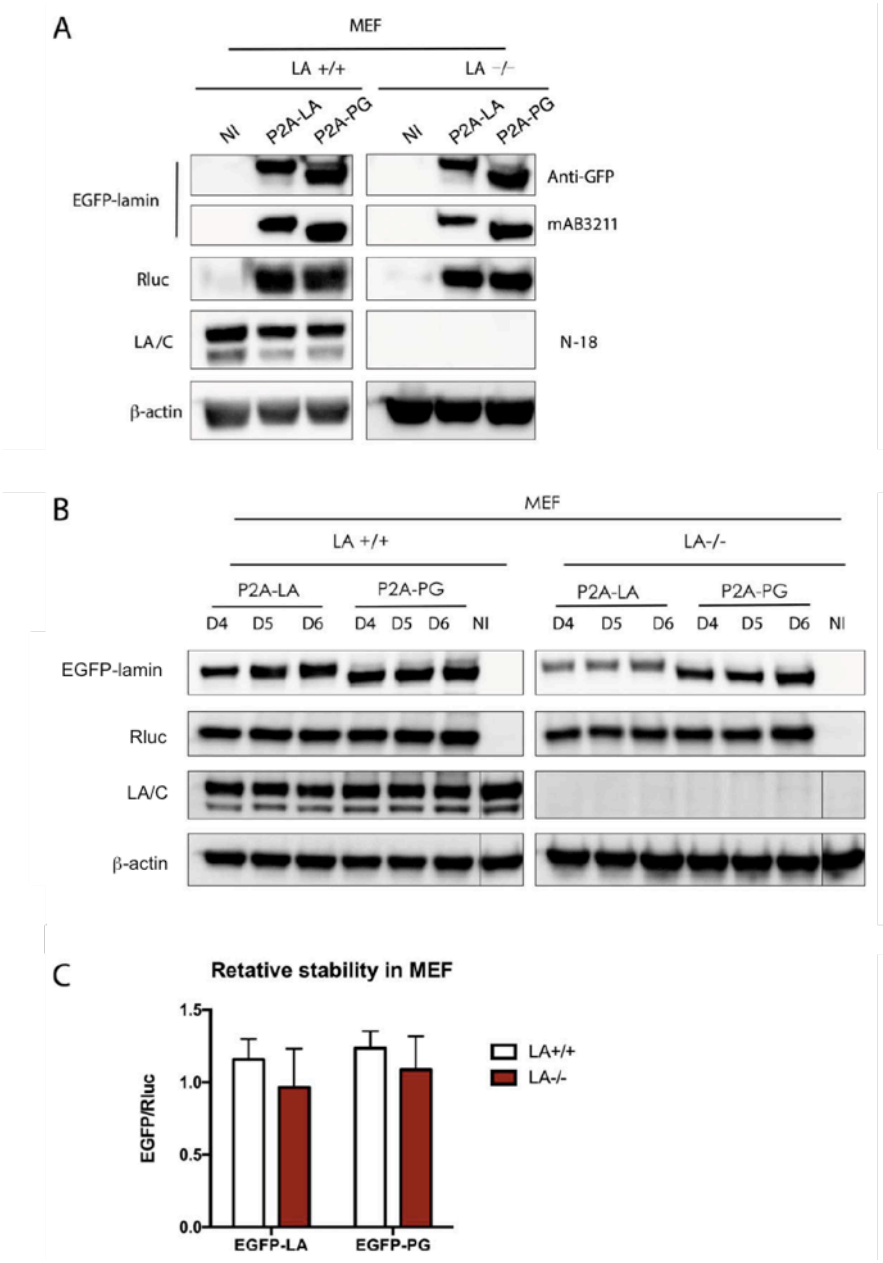

Figure 3-5. Examining lamin relative stabilities in both LAC/C and LA-/- MEFs. (A) Western blotting analysis of viral infected MEF cells. Proteins were probed with antibodies of GFP, human lamin A/C (mAB3211, which only recognizes human lamin A/C), lamin A/C (N-18), luciferase and b-actin. Non-infected cells were used as a negative control. (B) Time course of viral infected hBM-MSCs were analyzed by Western blotting. Antibodies of GFP, luciferase, human lamin A/C and b-actin were utilized for immunoblotting. (C) The quantification was calculated as the intensity ratio of EGFP/luciferase. Bar graph shows the average of day 4 to day 6 data. Results were generated from 3 biological replicates. P2A-LA, P2A-PG and P2A-LB1 refer to the constructs of luciferase-P2A-lamin A, luciferase-P2A-progerin and luciferase-P2A-lamin B1.

3-4. I found that the relative protein levels of EGFP-LA and EGFP-PG in wild type and LA null MEFs were essentially identical, suggesting the post-translational degradation of exogenously expressed human A type lamins was not impacted by the presence of endogenous mouse lamin A.

It should be noted that these wild type or lamin A null MEF cells were derived from mouse embryos. This species-mismatched cell line might explain why I did not observe a significant increase in the relative amount of human progerin compared to human lamin A. While the results from this experiment implies that the presence of endogenous lamin A/C does not affect the post-translational stability of the exogenously expressed EGFP-lamins, MEFs lines are not the optimal system and further validation using a human LA/C null fibroblast or MSC lines are desired.

3.2.3 FTI treatment reduces progerin stability in fibroblasts

Farnesyltransferase inhibitors (FTI) block farnesylation of progerin, relocalize the protein away from the nuclear envelope, and alleviate the prominent nuclear phenotypes in human progeria fibroblasts (Capell et al., 2005; Gordon et al., 2012a; Toth et al., 2005; Yang et al., 2006). The past studies on FTI did not elaborate how inhibition of farnesylation by FTI affects post-translational lamin protein stability, specifically in the lamins with farnesyl tail such as progerin and lamin B1. To study this, the P2A-EGFP-lamin system was applied in fibroblast cells treated with FTI for six days (Fig 3-6A). During the treatment, nucleoplasmic aggregates of EGFP-lamin A, EGFP-progerin or EGFP-lamin B1 were observed (Fig 3-7). The quantification was presented as averaged data of the EGFP/Rluc ratio from day 4 to day 6, when the

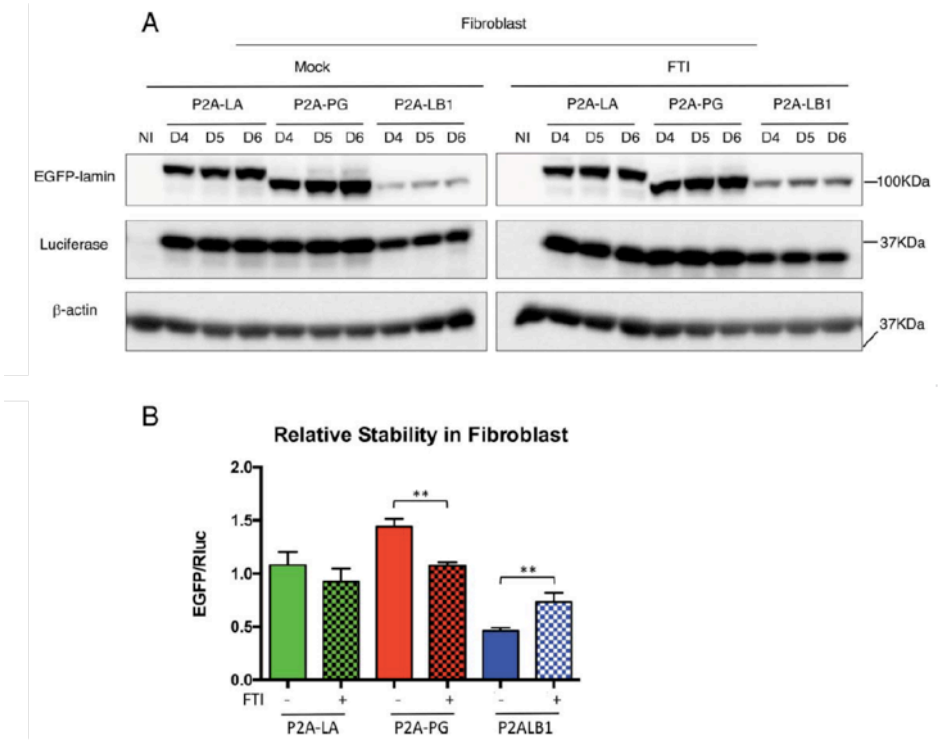

Figure 3-6. Effects of FTI on lamins relative stabilities in human fibroblasts. (A) Western blotting analysis of viral infected fibroblasts upon the treatment of FTI. DMSO treated cells were mock control. (B) Quantification of the relative stability in (A) is presented as EGFP/luciferase ratios. Bar graph shows the average of day 4 to day 6 data. Results were generated from 3 biological replicates. * $P < 0.05$, ** $P < 0.01$. P2A-LA, P2A-PG and P2A-LB1 refer to the constructs of luciferase-P2A-lamin A, luciferase-P2A-progerin and luciferase-P2A-lamin B1.

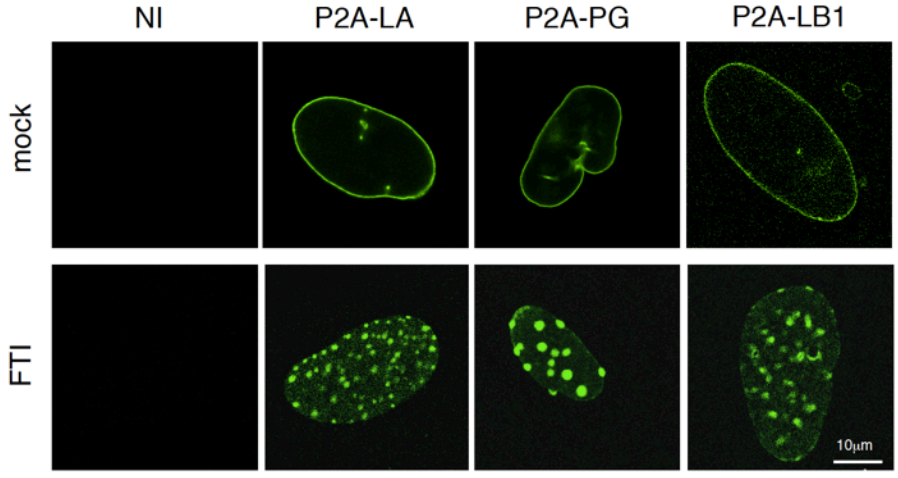

Figure 3-7. Representative confocal images of FTI treated fibroblasts for 4 days. Green indicates EGFP signals. P2A-LA, P2A-PG and P2A-LB1 refer to the constructs of luciferase-P2A-lamin A, luciferase-P2A-progerin and luciferase-P2A-lamin B1.

protein steady state was achieved (Fig 3-6B). Interestingly, I found that FTI significantly reduced progerin's stability to the level of wild type lamin A, whereas lamin A had no significant changes in stability after FTI treatment (Fig 3-6B).

To my surprise, the other farnesylated lamin, EGFP-LB1, displayed an opposite response to FTI treatment, where its post-translational stability was largely increased by farnesylation inhibition. Yet, Adam and his colleagues have previously reported reduced endogenous lamin B1 expression in fibroblasts treated with FTI (Adam et al., 2013a). To address this potential discrepancy, I compared endogenous

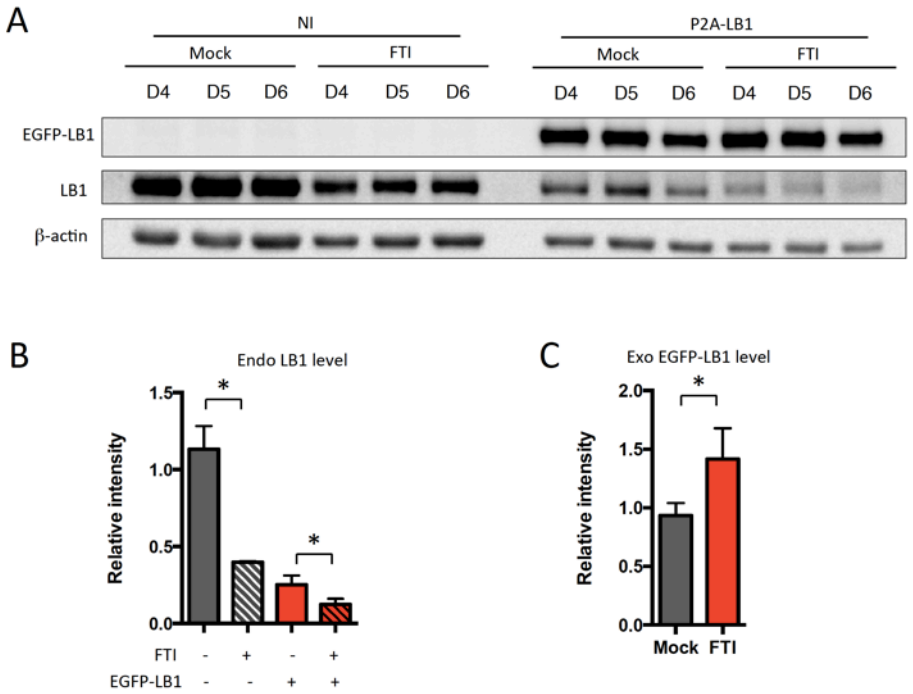

Figure 3-8. Effects of FTI on relative protein abundance of endogenous lamin B1 and exogenously expressed EGFP-lamin B1 in human fibroblasts. (A). Western blotting analysis of viral infected and un-infected fibroblasts upon the treatment of FTI. DMSO treated cells were mock control. (B) Quantification of the relative protein abundance of endogenous lamin B1. (C) Quantification of the relative protein abundance of exogenously expressed EGFP-lamin B1. Bar graph shows the average of day 4 to day 6 data. Results were generated from three biological replicates. * $p<0.05$. P2A-LA, P2A-PG and P2A-LB1 refer to the constructs of luciferase-P2A-lamin A, luciferase-P2A-progerin and luciferase-P2A-lamin B1.

LB1 and exogenous LB1 protein levels in FTI treated and untreated fibroblast cells (Fig 3-8). In agreement with Adam et al., the endogenous LB1 protein decreased with FTI treatment in both non-infected and P2A-LB1 lentiviral-infected fibroblasts (Fig 3-8 A&B). Consistently, I observed an increased level of exogenously expressed EGFP-LB upon FTI treatment (Fig 3-8C). As suggested by Adam et al., the decreased endogenous lamin B1 level was likely due to the down-regulated lamin B1 mRNA by FTI treatment. Whereas for EGFP-lamin B1, its transcription is driven by a spleen focus-forming virus (SFFV) promoter, which may be independent of the influence of FTI. Therefore, the accumulation of EGFP-lamin B1 in the FTI treatment, as revealed by the P2A method, indeed reflects only the post-translational protein stability of EGFP-lamin B1.

3.3 Discussion

In this study, I employed a viral P2A-sequence based comparison system to demonstrate that progerin is post-translationally more stable than wild type lamin A in fibroblasts and hBM-MSCs. My results are in agreement with the previous observation that progerin protein accumulates during cellular aging (Cao et al., 2011a; Eriksson et al., 2003; Goldman et al., 2004). FTI significantly reduced progerin's post-translational stability to the level of wild type lamin A, which provides additional evidence to support the beneficial effects of FTI in HGPS cells, animal models and patient clinical trials (Capell et al., 2008; Gordon et al., 2012a; Yang et al., 2006). Interestingly, my study showed that EGFP-lamin B1's post-

translational stability was increased upon the treatment of FTI. A previous study reported a reduction in endogenous lamin B1 protein in FTI-treated cells, which was likely due to the down-regulation of lamin B1 mRNA level by FTI (Adam et al., 2013b). In my experiment, the transcription of the exogenous EGFP-lamin B1 was driven by an SFFV promoter which does not show a noticeable response to FTI treatment (Fig 3-8). Furthermore, in the P2A system, the normalization of EGFP-lamins to the Rluc control accounts for any differences in mRNA abundance or translation rate. Thus, only the post-translational stability of EGFP-lamin B1 was assessed and compared across samples. My study suggests that normally farnesylated LB1 is less stable than the non-farnesylated LB1. Previous findings have shown that disrupted farnesylation by mutations in the CAAX motif of LB1 mislocalize the protein to the nucleoplasm (Maske et al., 2003; Verstraeten et al., 2011). A recent study has reported that lamin B1 degradation involves nucleus-to-cytoplasm vesicular transport that delivers lamin B1-LC3 to the lysosomes (Dou et al., 2015). Based on these data, a possible explanation is that the removal of the farnesyl tail from lamin B1 may disassociate the protein away from the nuclear lamina, which disrupts the LC3-mediated exporting vesicle formation, causing an increase in the stability of lamin B1.

I show that the P2A sequence efficiently mediated the disassociation of Rluc and EGFP-tagged lamin proteins in different cell lines, including fibroblasts, hBM-MSCs and MEFs, suggesting the extensive applicability of this method. The normalization of steady-state levels of EGFP-tagged lamins to those of the cotranslationally separated Rluc protein controlled for differences in transcription,

mRNA stability, and translation rates between samples, and allowed differences in post-translational stability between the various lamins to be inferred. The main advantages of the P2A peptide-mediated post-translational reporter system are that it is much simple to implement, it avoids potentially confounding pleiotropic effects from cycloheximide inhibition of translation, and it provides a means to look at the relative stability of insoluble proteins. One of the main drawbacks of the technique in its current configuration is that it cannot provide a direct measurement of protein half-life, and only allows relative changes in protein stability to be inferred for a protein under different growth conditions (Rodriguez-Contreras et al., 2015), or between protein variants as presented here for the lamins. Rodriguez-Contreras and colleagues used a variation of the P2A-peptide technique to examine changes in stability of the LmxGT1 glucose transporter in response to glucose starvation, and demonstrated that the fold-change in LmxGT1 stability determined via this technique was essentially identical to the fold-change in half-life determined via the cycloheximide block technique (Rodriguez-Contreras et al., 2015). This serves as a validation of the underlying concepts of the technique, and emphasizes the direct relationship between protein half-life and steady state protein abundance. I have noticed that the dynamics of normalized protein accumulation (lamin/luc) over time were highly reproducible and specific for each lamin type (Fig 3-4E). Since the rate of increase in protein abundance should be directly proportional to the half-life of the protein, it may be possible to use this rate to calculate protein half-life in a manner similar to the "approach to steady-state labeling" method described previously (GREENBERG, 1972). In that method the cells were labeled with a continuous supply of [3H] uridine

and the rate of specific mRNA that accumulated at a steady-state level was measured. Then the half-life of the mRNA was calculated based on the time required to reach its steady-state. This method can be explored in the future.

Chapter 4: *LMNA* first intron mediates transcription suppression through Sp1 binding

4.1 Introduction

The expression of lamin A is suppressed in undifferentiated cells like embryonic stem cells, and some highly proliferative cells, such as leukemias and lymphomas, and is induced upon cell differentiation (Broers et al., 1997; Stadelmann et al., 1990). This tissue- and stage-specific expression pattern implies that lamin A expression is highly regulated.

It was first thought that the regulation of lamin A expression is primarily occurred at the transcriptional level (Hamid et al., 1996; Lin and Worman, 1997; Mattia et al., 1992). Several transcriptional regulation motifs and transcription factor binding sites have been found on the *LMNA* promoter region. For example, a retinoic acid-responsive element (L-RARE) was identified within the *LMNA* promoter, which is bound by several transcription factors including c-Jun and Sp1/Sp3 (Okumura et al., 2004) and responsible for retinoic acid-mediated activation of lamin A/C in mouse embryonic carcinoma cells (Lebel et al., 1987). There are also other regulatory motifs in the *LMNA* promoter that may interact with the transcription factors Sp1/3, c-Jun, and c-Fos, and the transcriptional coactivator CREB-binding protein (Janaki Ramaiah and Parnaik, 2006; Muralikrishna and Parnaik, 2001). The CpG island hypermethylation of *LMNA* promoter has also been examined. However, it does not explain lamin A/C inactivation for all the tested hematologic malignancies (Agrelo et al., 2005).

Meanwhile, studies of lamin A/C post-transcriptional regulation have also been conducted. The devoid of lamin A/C expression in undifferentiated P19 mouse

embryonal carcinoma cells is considered to be a post-transcriptional event, due to the unchanged *LMNA* transcription rate during retinoic acid-induced differentiation (Lanoix et al., 1992). Furthermore, Jung and his colleagues illustrated that a brain-specific microRNA, miR-9, mediates the suppression of lamin A expression by targeting to the 3'UTR of lamin A transcripts in brain cells (Jung et al., 2012). Apparently, there are still many uncertainties about the regulation of lamin A/C during differentiation and development. More extensive studies are required in order to further unravel the puzzle.

Therefore, other regions outside of the promoter were explored. The *LMNA* first intron, which is ~16kb in length, contains the transcription initiation site of the male germ-cell-specific lamin C2 isoform (Nakajima and Abe, 1995). DNase hypersensitive site clusters were shown to be present within the first intron and associated with lamin A/C expression (Nakamachi and Nakajima, 2000b). Binding sites for transcription factors hepatocyte nuclear factor-3β and retinoic X receptor β (RXRβ) have also been reported (Nakajima and Abe, 1995).

In this chapter, I investigate the regulation of lamin A expression in human promyelocytic leukemia HL60 cells by elucidating the role of *LMNA* first intron in transcription control of *LMNA* gene expression through a combination of bioinformatic and molecular biology approaches. I found out that a highly conserved region in the *LMNA* first intron is closely associated with lamin A/C repression in HL60 cells. This function is mediated by the binding of the transcription factor Sp1.

Please note that I refer fibroblasts as lamin A/C positive cells and HL60 as lamin A/C negative cells based on the lamin A/C expression status throughout this chapter.

4.2 Results

4.2.1 Conserved regions with potential transcriptional regulatory activities are identified in the *LMNA* first intron

Using UCSC genome browser, we found that the first intron of *LMNA* gene is very special. Not mention its unusual size of 16kb, which takes up 60% of the whole *LMNA* gene length, the first intron bears many features that are not usually seen in introns. For example, bindings of transcription factors and histone modifications have been reported in *LMNA* first intron, including the markers that are commonly associated with active transcription of nearby genes, such as H3K4me3 and H3K27ac (Fig 4-1). In addition, by comparing the conserved sequences among 44 mammalian species using the data from UCSC genome browser, the first intron of *LMNA* was shown to contain many conserved regions (shown as peaks in the figure) whose conservatory is compatible with that in exons (Fig 4-1). On the contrary, other *LMNA* introns (eg. the second intron) do not show these features.

To investigate the role of *LMNA* first intron in lamin A expression regulation, I first identified a total of five highly conserved regions (Con 1-5) across the entire *LMNA* first intron using bioinformatic approaches (Fig 4-2A). Next, luciferase activity assays of Con 1, 3, 4, and 5 were performed on transiently transfected HeLa cells to test the transcription regulatory activity of the conserved regions (Fig 4-2A).

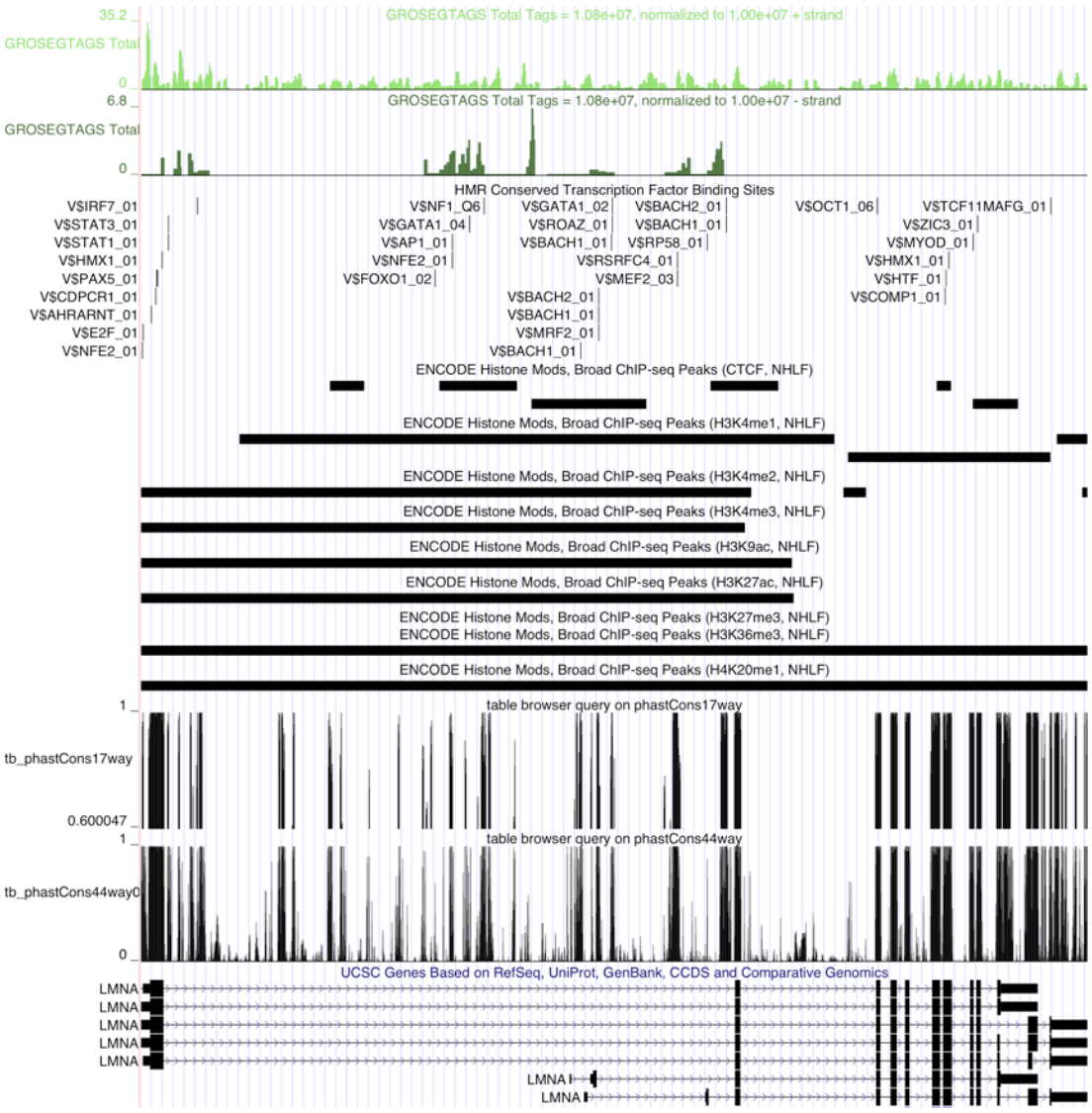

Figure 4-1: Screen shot of *LMNA* gene structure information from UCSC genome browser. From the bottom to the top: *LMNA* gene Refseq and common isoforms; Conservatory generated from 44 mammalian species; A few histone modification marks across the gene; Conserved transcription factor binding sites; GRO-seq of both sense and antisense strands.

These luciferase constructs were created by inserting each of the conserved regions independently to the upstream of the basal promoter in a luciferase reporter plasmid. Conserved region 2 (Con 2) was not tested due to certain cloning difficulties. The results showed that the conserved region 1 (Con1), which is around 1.2kb downstream of *LMNA* transcription start site (TSS), exhibited the highest luciferase

activity of 7-fold upregulation comparing to the control group. On the contrary, conserved region 5 (Con 5), which is about 270bp to the 3' of *LMNA* first intron, significantly reduced the luciferase activity to a barely detectable level. The other two tested regions, Con 3 and 4, had no notable effects on the transcription of luciferase constructs (Fig 4-2B). These data suggested that both Con 1 and Con 5 might contain

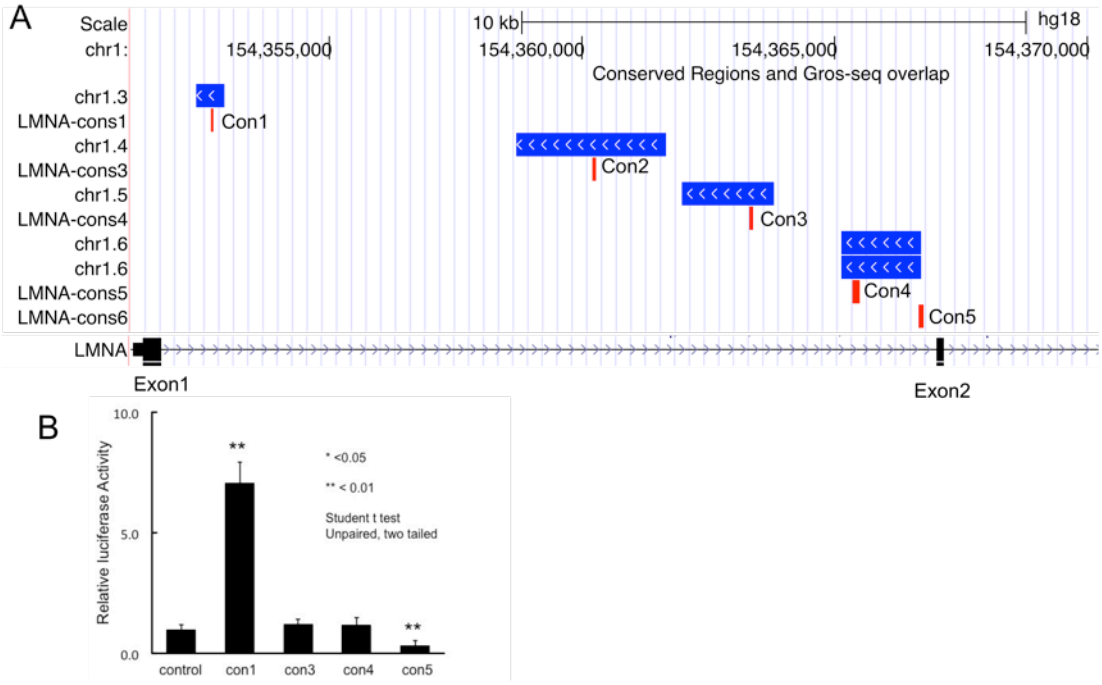

Figure 4-2. Functional analysis of LMNA first intron. (A) Five highly conserved regions identified within the first intron of *LMNA*. (B) Relative luciferase activities of the five conserved regions in transfected HeLa cells. Quantification was done by student t test. * $p<0.05$, ** $p< 0.01$.

motifs that possess certain transcription regulatory activity. My attention was immediately drawn to Con 5, because it showed a transcription repression activity, which may contribute to the repressed lamin A expression in certain cell types. Therefore my following study is mainly focused on Con 5.

4.2.2 Sp1, together with its co-factors E2F1 and HDAC2, are predicted to be the potential regulatory element binding to Con 5 in the lamin A first intron

To further investigate the role of Con 5 in lamin A transcription regulation, I functionally analyzed Con 5 in two types of cell lines, fibroblasts which express a high levels of lamin A, and the leukemia cell line HL60 which has very low lamin A expression (Fig 4-3B). By analyzing the ENCODE DNase-seq data of fibroblasts and HL60 cells, I found that the chromatin around Con 5 region is open for protein binding in both of the cell lines. Next, a Position Weight Matrix (PWM) scan was used to predict transcription factors (TFs) that may bind to Con 5 region. False positive binding candidates were removed by analyzing of DNase-DGF data of the Con 5 region across several cell lines. Last, the candidate list was further narrowed down by comparison against the ENCODE ChIP-seq data around Con 5 region. Only two true-positive candidates were left, Sp1 and REST. REST (RE1-Silencing Transcription factor) was subsequentially excluded after considering that it functions in the repression of neural genes in non-neuronal cells (Chong et al., 1995; Coulson, 2005), whereas *LMNA* does not belong to that category. Transcription factor Sp1 (specificity protein 1) is a ubiquitously-expressed transcription factor involved in many cellular processes, including differentiation, proliferation, cell cycle regulation, apoptosis and tumorigenesis (BLACK et al., 2001; Tan and Khachigian, 2009). It often interacts with two other cofactors, such as E2F1 and HDAC2, to regulate gene expression (Doetzlhofer et al., 1999; Lin et al., 1996; Won et al., 2002). Therefore I also include E2F1 and HDAC2 in my following study.

Next, the expression levels of Sp1, E2F1 and HDAC2 were examined at mRNA and protein levels in both fibroblasts and HL60 cells. A real-time quantitative reverse transcription PCR was first employed to measure the mRNA expression level of lamin A and the three candidates. As expected, lamin A was highly expressed in the fibroblasts, but largely repressed in HL60 cells (Fig 4-3A). To my surprise, the mRNA levels of Sp1, E2F1 and HDAC2 were low in fibroblasts but significantly higher in HL60 cell (Fig 4-3A). In support, Western Blotting analysis demonstrated highly consistent results (Fig 4-3B&C). Fibroblasts displayed an intensive amount of lamin A/C proteins but little amount of the Sp1, E2F1 and HDAC2. On the contrary, these candidates showed strong bands in HL60 cells, whose lamin A/C proteins were barely detectable (Fig 4-3B&C). Those data suggested that the three candidates were

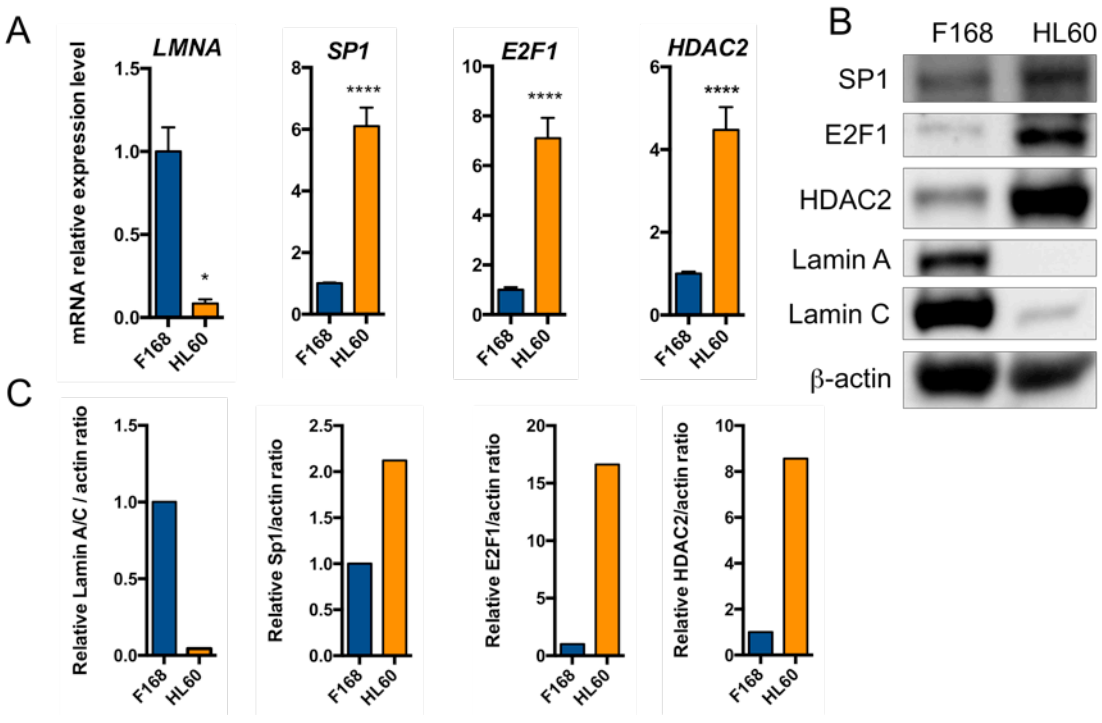

Figure 4-3. Reciprocal expression pattern between endogenous lamin A and the protein candidates Sp1, E2F1 and HDAC2 . (A) mRNA expression levels of *LMNA*, SP1, E2F1 and HDAC2 in fibroblasts and HL60 cells. * $p<0.05$, **** $p<0.0001$. (B) Western Blot analysis of fibroblasts and HL60. Protein samples were immunoblotted with antibodies of Sp1, E2F1, HDAC2, lamin A/C and β-actin. (C) Quantification of (B).

differentially expressed between fibroblasts and HL60s. Based on the reciprocal expression pattern between lamin A and the three candidates in fibroblasts and HL60s, I hypothesize that Sp1 may play a role in repressing lamin A expression by binding to the Con5 region in the *LMNA* first intron in HL60 cells. It may form a repressive complex with E2F1 and/or HDAC2 at Con5.

4.2.3 Sp1, E2F1 and HDAC2 expression levels are inversely associated with the lamin A amounts in HL60 and fibroblasts

To further explore the functional association of the three protein candidates with lamin A expression, I decided to manipulate the levels of Sp1, E2F1 or HDAC2 protein and examine their effects on lamin A expression. First, Sp1, E2F1 and HDAC2 were knocked down by 40-50% individually using siRNAs in HL60 cells (Fig 4-4A). As a consequence, increased lamin A/C mRNA levels were detected upon the inhibition of these candidates, among which Sp1 exhibited the most significant effect (Fig 4-4A). The unregulated lamin A/C expression was confirmed]\ at the protein level by Western Blotting analysis (Fig 4-4B). Although the expression of *LMNA* gene is nearly absent in HL60 cells, detection of traces of lamin A/C proteins has been reported in previous studies (Kaufmann, 1992; Lin and Worman, 1997; Olins et al., 2001). With relative long exposure time I was also able to observe low but detectable level of lamin A/C in scramble siRNA treated group (Fig 4-4B&C). Consistent with qPCR data, increased lamin A/C protein amount was detected in target protein siRNA treated samples (Fig 4-4B&C).

In addition to HL60 cells, the effects of the three candidates on lamin A expression regulation were also explored in lamin A expressing human fibroblasts.

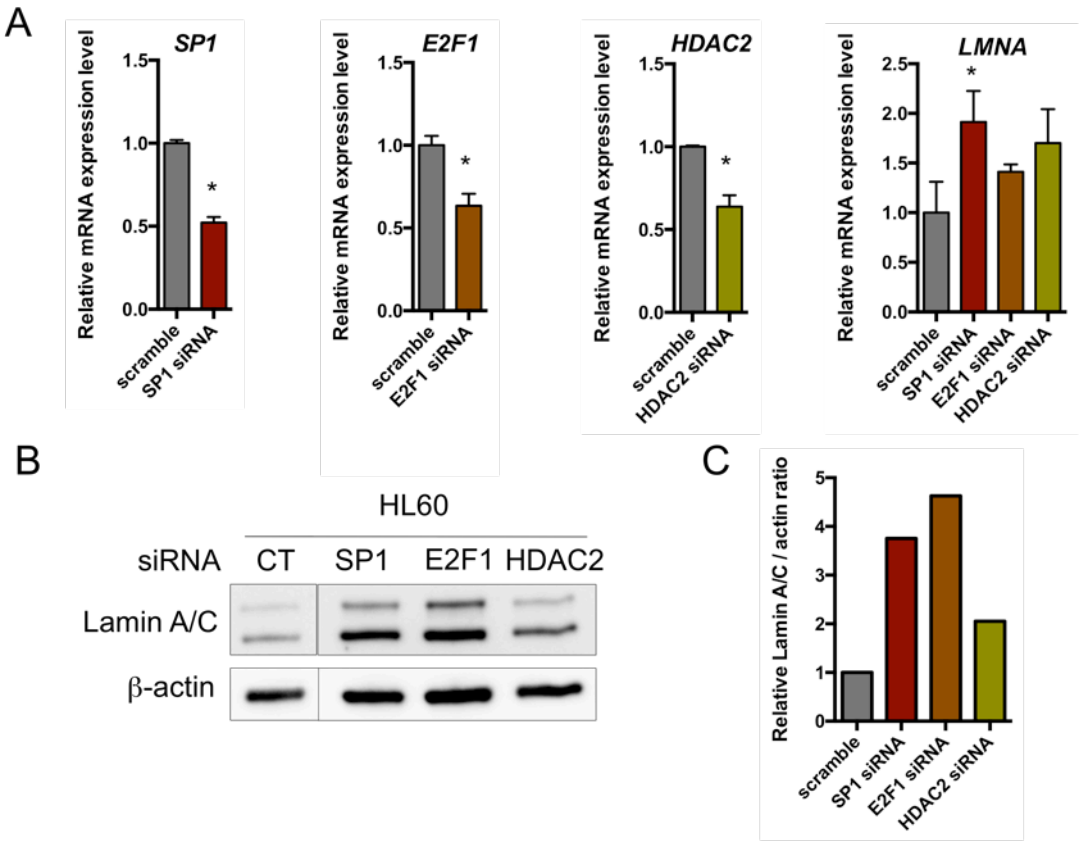

Figure 4-4. siRNA knocking down of Sp1, E2F1, HDAC2 induces lamin A transcription in HL60. (A) mRNA expression levels of *LMNA*, Sp1, E2F1 and HDAC2 in HL60 cells. * $p<0.05$. (B) Western Blot analysis. Protein samples were immunoblotted with antibodies of lamin A/C and β-actin. (C) Quantification of lamin A/C protein expression levels from (B).

Unlike HL60 cells, fibroblasts have relatively low level of Sp1, E2F1 or HDAC2 (Fig4-3). To further determine the reciprocal correlation between lamin A and the candidate proteins, I independently overexpressed GFP tagged Sp1, E2F1 and HDAC2 in fibroblasts (Fig 4-5). As a result, a 20-30% decrease of *LMNA* mRNA was detected in the candidate protein overexpression groups (Fig 4-5A). Moreover, lamin A/C protein levels were reduced to approximately half of the control group (Fig 4-5B&C). Together, our data suggested an inverse relationship between Sp1, E2F1 and HDAC2 and lamin A expression, which may contribute to the repressed lamin A transcription in HL60 cells.

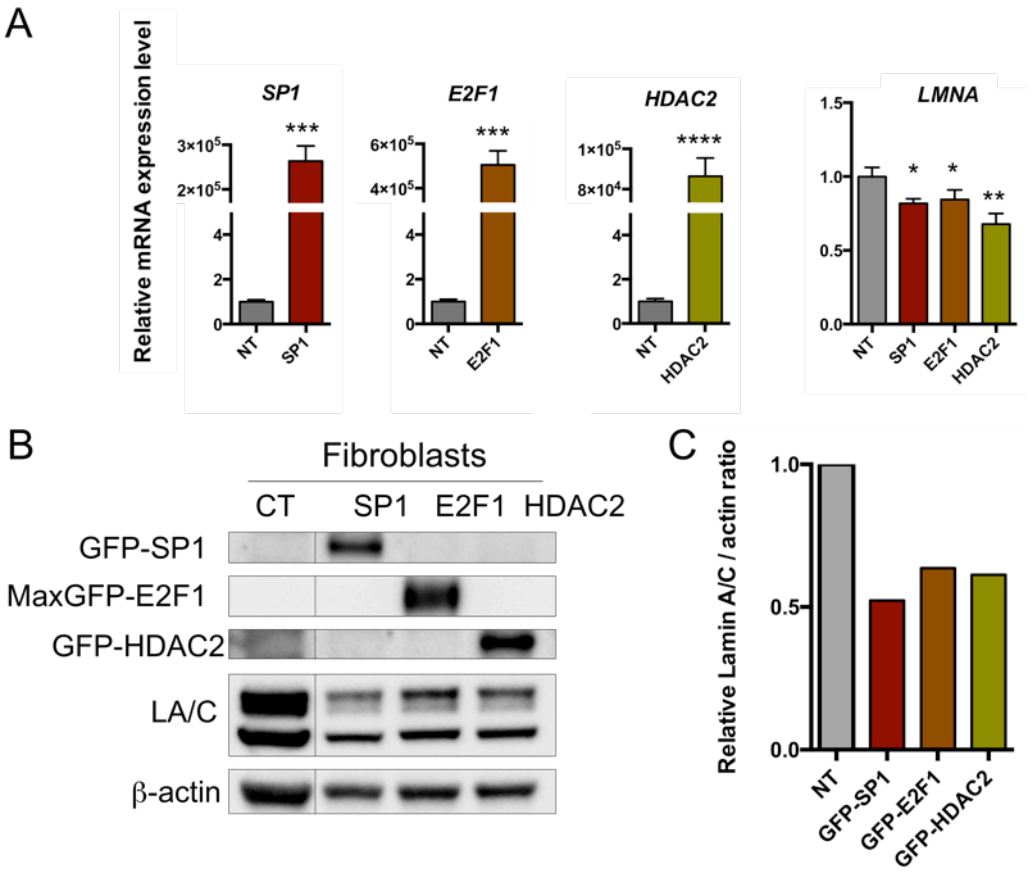

Figure 4-5. Overexpression of SP1, E2F1, HDAC2 decrease lamin A transcription in fibroblasts. (A) mRNA expression levels of *LMNA*, SP1, E2F1 and HDAC2 in fibroblasts cells. * $p<0.05$, ** $p<0.01$, *** $p<0.001$, **** $p<0.0001$. (B) Western Blot analysis. Protein samples were immunoblotted with antibodies of Sp1, E2F1, HDAC2, lamin A/C and β-actin. (C) Quantification of lamin A/C protein expression levels from (B).

4.2.4 Repressive effects of SP1 on lamin A expression depends on its binding to Con5 in *LMNA* first intron

My data suggestes that Sp1, E2F1 and HDAC2 are closely associated with lamin A expression repression. My next goal is to understand the underlying mechanism of this regulation. I started with Sp1, which is one of the most well characterized transcriptional factors (Vizcaíno et al., 2015). It was first recognized as a constitutive transcription activator of housekeeping genes and other TATA-less

genes (Azizkhan et al., 1993; Pugh and Tjian, 1990; Suske, 1999), and later on found to be involved in many other processes, including cell growth control and tumorigenesis (Li and Davie, 2010). To elucidate whether the transcription regulatory activity of Sp1 depends on the Con 5 region, I knocked down Sp1 using siRNA in HeLa cells (Fig 4-6A) and re-examined the luciferase activity of Con 5 (Fig 4-6B). Surprisingly, the luciferase activity of Con 5 was significantly increased upon the Sp1 siRNA silencing when comparing to the cells transfected with scrambled siRNA (Fig 4-6B, Con5). Conversely, HeLa cells transfected with the control luciferase vectors (CT) did not show distinct alternation on the luciferase activities between scrambled and Sp1 siRNA treated groups (Fig 4-6B, CT). These results imply that the transcription repression of Sp1 is largely Con 5-dependent, likely through a direct binding between Sp1 and Con 5 DNA sequence. However, this speculation needs further investigation. To determine the interaction between Sp1 and Con 5 sequence in HL60s and GFP-Sp1 overexpressed fibroblasts, chromatin immunoprecipitation (ChIP) will be performed.

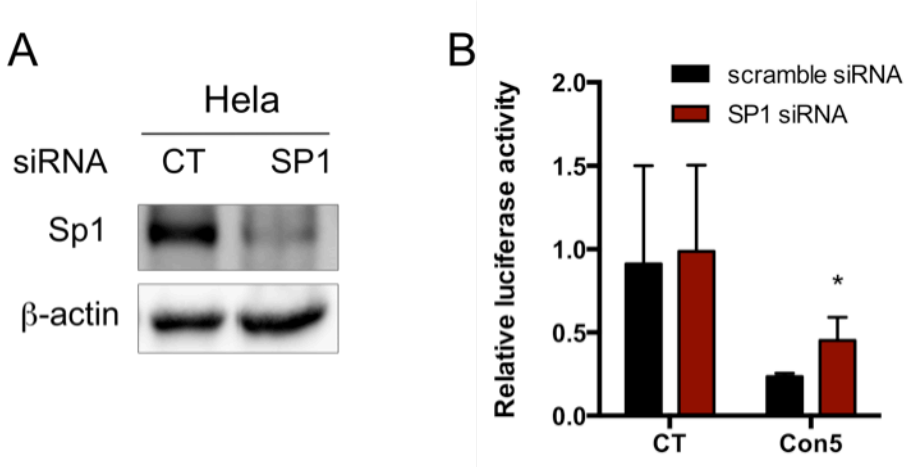

Figure 4-6. Identification of SP1/Con5 association. (A) Western Blot analysis on siRNA transfected HeLa. Protein samples were immunoblotted with antibodies of Sp1 and β-actin. (B) Relative luciferase activities of Con5 in Sp1 siRNA transfected HeLa cells. Quantification was done by student t test. * $p<0.05$.

4.3 Discussion

Lamin A and C are the two major isoforms generated from *LMNA* gene. Although being found in many somatic cell cultures and a variety of tissues, expression of lamin A is highly repressed in undifferentiated cells and cells with high proliferative rates (Broers et al., 1997; Stadelmann et al., 1990). The regulation of lamin A during differentiation and development has been a long-lasting question that required more studies to elucidate. Besides the proximal promoter region, regulatory motifs have been suggested to reside in regions of 5' distal region, 3' UTRs and the large first intron of *LMNA* (Lin and Worman, 1993; Nakamachi and Nakajima, 2000a). In addition to its unusual size, the first intron of *LMNA* surprisingly exhibits many features similar to exons, including high conservatory, active histone modifications, transcription factor bindings, etc., suggesting a potential functionality. Therefore in this study, I zoomed into the very special first intron of *LMNA*, and explored its role in the suppression of lamin A expression. Based on the comparison among 44 mammalian species, a total of five highly conserved regions were identified in the first intron. Con 5 region showed a high level of transcription repression activity in luciferase activity assay. Moreover, it is predicted to be differentially bound by Sp1, E2F1 and HDAC2 in lamin A nonexpressing cells but not in lamin A positive cells. These findings led us to further investigate the connection between lamin A expression and the three candidates. Surprisingly, lamin A expression was inversely affected by the three proteins in lamin A-expressing fibroblasts and lamin A-nonexpressing HL60 cells. In particular Sp1 has a repression function on lamin A expression that was shown to be largely associated with the

interaction with the Con5 region. Together, my study reveals the repressive role of *LMNA* first intron in lamin A expression and provide strong evidence for introns being involved in gene regulation.

The relevance of introns in gene regulation of intermediate filaments has been reported. An example of such an analysis is keratin 18 (K18), which is expressed in diverse simple epithelial tissues and in various carcinomas (Blumenberg). It was shown that both enhancer and silencer elements embedded in the first intron of the K18 gene are responsible for the regulation of the gene expression during cell differentiation induced by retinoic acid (Pankov et al., 1994). The Con5 region identified in my study can be considered as an inhibitory element that contributes to the cell-type-specific expression of lamin A. However, it still needs be determined whether the first intron is involved in lamin A regulation during differentiation and development.

Chapter 5: Summarization and future directions

5.1 Summarization

My doctoral research presented in this dissertation studies lamin A processing and regulation in from the following three aspects:

First, based on a noticeable delay observed in the recruitment of progerin back to the nucleus at the end of mitosis, I examined the potential effects of cytoplasmic lamin A and progerin using molecular and biochemistry approaches in chapter 2. To start, I generate the cytoplasmic-resident lamin A and progerin mutants LAΔNLS and PGΔNLS by deleting the NLS from both lamin A and progerin. I found that both mutants are farnesylated and rapidly tethers to a sub-domain of the ER through the farnesyl tail after being synthesized. Additionally, I noticed that the ER-associated LAΔNLS becomes gradually released into the cytoplasm, which is likely due to the removal of the farnesylated C-terminus by ER-associated ZMPSTE24. Whereas PGΔNLS, which cannot be processed by ZMPSTE24, remains ER-associated. A much higher level of farnesylation was observed for LAΔNLS comparing to wild type lamin A, suggesting a differences in enzymatic activities between the ER-associated and the INM-associated ZMPSTE24. Moreover, the nuclear localization of an INM protein emerin is largely disrupted by LAΔNLS and, especially, PGΔNLS. Since mutations of emerin have been connected with cardiomyopathy and muscular dystrophy, my data indicates that the cytoplasmic progerin may also lead to these pathologic phenotypes observed in HGPS patients.

Second, I compared the relative protein stabilities among lamin A, progerin and lamin B1, to answer the long-standing questions in chapter 3: whether progerin is

more stable than wild type lamin A, and what effects does farnesyl tail have on protein stability. To overcome the limitation of traditional methods on stability testing of proteins with low solubility like nuclear lamins, I first established a comparison platform based on a viral 2A sequence, which mediates the co-translational cleavage of multiple polypeptides from a single ORF. In this system, I used Renilla luciferase as a normalization factor and linked it with different EGFP-tagged lamin proteins through the 2A motif. By normalizing EGFP to luciferase, I have control of the transcription rate, mRNA stability and translation rate between different lamin constructs. Thus, the relative stability of the lamins can be easily compared by Western Blotting analysis. Taking the advantage of this system, I compared the relative stability of lamin A, progerin and lamin B1 in different cell types, including human fibroblasts and bone marrow-MSCs. My data clearly shows that progerin possesses a significantly higher post-translational relative stability than both lamin A and lamin B1 in both tested cell lines. In addition, the relative stability of exogenous expressed proteins is not altered by the endogenous lamins, indicating the feasibility of my comparison system. Inhibition of farnesylation by FTI treatment largely reduced the relative stability of progerin. This can be added to the explanation of the clinical rescuing effects on HGPS patients. More interestingly, the relative stability of lamin B1, which naturally carries a farnesylated C-terminus, was not decreased upon FTI treatment. Instead, it was slightly increased. Therefore, my data implies that elimination of farnesyl tail does not always equal to elevated protein stability. For some proteins, the farnesyl group might be necessary for their function and cellular degradation.

From there I went back to the very fundamental level and explored the transcription regulation of lamin A gene in chapter 4. Unlike other introns in *LMNA* gene, *LMNA* first intron exhibits many features that normally are observed in exons, such as TF bindings, active histone modifications and conservatory. To investigate whether it is involved in lamin A regulation, I first functionally analyzed the first intron using a bioinformatics approach. A total of five highly conserved regions were identified across 46 mammalian species, among which the first conserved region (Con1) presented the highest transcriptional regulation activity. Next, I narrowed down three DNA binding proteins that specifically bind to Con5 region and highly expressed in lamin A non-expressing cell lines but not in lamin A expressing cells. These proteins, Sp1, E2F1 and HDAC2, showed a reciprocal expression pattern with lamin A between human fibroblasts (lamin A positive) and HL60 cells (lamin A negative). Therefore, I hypothesized that Sp1, E2F1 and/or HDAC2 might negatively regulate lamin A expression by binding to the Con5 region on *LMNA* gene. To study the connection between Sp1, E2F1, and HDAC2 and lamin A expression, I further manipulated the level of these three proteins and observed the corresponding changes of lamin A expression: overexpression of Sp1, E2F1, or HDAC2 led to a decreased lamin A expression in fibroblasts, whereas silencing of these three proteins resulted in a increase of lamin A expression in HL60 cells. Moreover, by combination of Sp1 siRNA treatment and luciferase activity assay, I provided the evidence that the transcriptional regulatory activity of Sp1 is Con5 dependent. This dependence might be accomplished by the interaction between Sp1 and Con5, which plays a role on lamin A expression repression HL60 cells.

5.2 Future directions

Mutations in LMNA are mainly responsible for two groups of diseases, affecting highly specialized tissues: dystrophies of skeletal and/or cardiac muscles, and partial lipodystrophies (Vigouroux and Bonne, 2013). Especially for HGPS mutation, these defects exhibit in combination and with the most severities. However, the pathophysiology of the diseases linked to LMNA mutations remains unclear. Considering the widespread expression of lamin A/C in differentiated cells, it is puzzling that these diseases are exhibited in a tissue-specific manner. One possibility is the alternated protein-protein interactions between lamin A and the mutations of the binding partners of lamin A. One example is the emerin protein, whose mutants have been shown to be associated with X-linked Emery-Dreifuss muscular dystrophy (XL-EDMD) (Bione et al., 1994). This disease is overall clinically identical with other two muscular dystrophies caused by *LMNA* mutations (Fenichel et al., 1982; Miller et al., 1985; Wehnert and Muntoni, 1999). In addition, the NE localization of emerin largely depends on lamin A. The protein is mislocalized to the ER and functionally lost from the NE with LMNA mutations (Broers et al., 2006; Worman and Bonne, 2007). My study in chapter 2 also reinforced the connection between lamin A and emerin and their roles in regulating muscle- and heart-specific gene expression. LAP2α is another lamin A interacting protein. A mutation in LAP2α is known to cause dilated cardiomyopathy by disrupting its binding to lamin A (Taylor et al., 2005). In addition to the aforementioned interactions, lamin A interacts with many proteins, which may participate in chromosomal organization, nucleus assembly, transcription, replication, signaling, and many other activities. If their localization and function require lamin A,

it can be assumed that these proteins might also explain the tissue-specific symptoms caused by lamin A mutations. Therefore, further exploration of this understudied area may lead to improved and potentially therapeutic understanding of many human genetic diseases.

In chapter 3, I compared the relative stability among several lamin proteins. However the mechanisms of degradation of lamin proteins during interphase largely remain unknown. The ubiquitin–proteasome and autophagy–lysosome pathways are the two main routes of protein and organelle clearance in eukaryotic cells (Rubinsztein, 2006). Ubiquitin can be attached to another ubiquitin, creating a 'chain' that marks the target for proteolytic degradation. By contrast, attachment of a single ubiquitin can influence target proteins in diverse ways and regulates many specific cellular pathways and nuclear functions (Simon and Wilson, 2013). There are widespread ubiquitylation signals of human A- and B-type lamins that have been revealed by high-throughput mass spectrometry analysis (Kim et al., 2011b; Wagner et al., 2011). Moreover, lamins are directly cleaved by caspases 1 and 6, granzymes A and B and CRNSP (Ca+2-regulated nuclear scaffold protease) at sites located near many ubiquitylation sites during apoptosis (Clawson et al., 1992; Simon and Wilson, 2013; Takahashi et al., 1996; Zhang et al., 2001). Yet it is still unclear whether polyubiquitination is involved in lamins degradation. Recently, an autophagy-mediated degradation of lamin B1 has been reported, in which the autophagy protein LC3 interacts with lamin B1 and mediates its degradation upon oncogenic insults through nucleus-to-cytoplasm transport that delivers lamin B1 to the lysosome (Dou

et al., 2015). However, this mechanism is under the condition of oncogenesis. Whether it is applicable to more generalized situation remains to be determined.

Finally, the regulation of lamin A during differentiation and development is understudied. The proximal promoter of *LMNA* gene is the most well-investigated region. However, previous studies showed that it is not responsible for the cell-type-specific expression of lamin A. The 5' dismal promoter region, the 3' UTR area and the first intron of *LMNA* are the proposed candidate regions that may participate in lamin A regulation. Although a microRNA, miR9, was identified to target to *LMNA* 3'UTR and facilitate the mRNA degradation in brain cells, it is possible that there are other tissue-microRNAs functions in other cell types. Moreover, based on high conservatory of *LMNA* first intron, more intensive studies are required to explore its role on lamin A regulation. Questions like whether these highly conserved regions identified in my study have different regulatory activity in different cell types under various differentiation states, what is the function of the actively transcribed regions on the antisense strand of *LMNA* first intron showed by GRO-seq, how do E2F1 and HDAC2 repress lamin A expression and do they form repressive complexes with Sp1 at Con5 region need to be further studied. Furthermore, the potential of the 5' dismal promoter region is still waiting to be explored.

Chapter 6: Materials and methods

6.1 Plasmid construction

In chapter 2, plasmids of pEGFP-C1-LAΔNLS, pEGFP-C1-PGΔNLS, pEGFP-C1-LASSIMΔNLS, and pEGFP-C1-PGSSIMΔNLS were constructed based on the pEGFP-C1 vector (Clontech). The NLS sequence (AAAAAGCGCAAACTGGAG) was removed from cDNA of Lamin A (LA), progerin (PG), LA-SSIM and PG-SSIM by PCR splicing. Primers used were two targeting each ends of LMNA, LMNA 5F (5'-AGACCCCGTCCCAGCGGCGCGC-3') and LMNA 3R (5'-GTCGACTCTAGATTACATGATGCTGCAGTTCTG-3'), and two flanking NLS regions complementary each other, LMNA 5R (5'-TGCGGCTCTCAGTGGAGGTGACGCTGCCC-3') and LMNA 3F (5'-GGGCAGCGTCACCTCCACTGAGAGCCGCA-3'). The 5'- and 3'- regions of LMNA were amplified using primer pairs "LMNA 5F + LMNA 5R" and "LMNA 3F + LMNA 3R" respectively, followed by a second amplification using the overlapping 5'- and 3'- fragments as templates to generate NLS-deleted sequences. The NLS deleted sequences were then sub-cloned into the AscI and XbaI sites of pEGFP-C1. A plasmid of pDsRed-monomer-C1-LA was created based on the pDsRed-monomer-C1 vector (Clontech). The full length of lamin A, progerin, LAΔNLS or PGΔNLS was amplified using LMNA 5F and LMNA 3R, followed by sub-cloning into the *BspEI* and *BamHI* sites of pDsRed-monomer-C1. In chapter 3, the lentiviral vector pHR-SIN-CSGW *dlNotI* was obtained as previously described (Xiong et al., 2016). Briefly, Rluc-P2A in pRP-M-Rluc-P2A-GFP plasmid and EGFP-lamins in above mentioned lamin plasmids were amplified by PCR using primer sets P1 (5'-GGTCCAGCGGATCCATGGCTTCCAAGGTG-3') and P2 (5'-GCCCTTGCTCACCATCGGACCTGGGTTCTC-3'), targeting Rluc-P2A, as well as

P3 (5'-GAGAACCCAGGTCCGATGGTGAGCAAGGGC-3') and P4 (for LA/PG: 5'-GGTAGCCTGCGGCCGCAGATTACATGATGCTGCAGTTCTGG-3', for LB1: 5'-GGTAGCCTGCGGCCGCTTACATAATTGCACAGCTTCTATTGG-3'), targeting EGFP-lamins. The primer P2 completely overlapped with P3, which allowed the fragments of Rluc-P2A and EGFP-lamins to automatically ligate together in a second round of PCR reaction using P1 and P4. The ligated large fragments were subsequently sub-cloned into the BamHI and NotI sites of pHR-SIN-CSGW dlNotI. In chapter 4, plasmids of pN3-Sp1FL and pMax-E2F1 were purchased from Addgene; pEGFP-C1-HDAC2 was purchased from MRC PPU Reagents and Services. Sp1 cDNA was amplified by 4 consecutive PCR using primer pairs in order to add a linker between the sequence of EGFP and SP1: 5'-CTGAAGAGGACATGAGCGACCAAGATC-3' and 5'-GTTATCTAGATCCTCAGAAGCCATTGC-3' for the 1st PCR; 5'-GCAAAAGCTCATTTCTGAAGAGGACATG-3' and 5'-GTTATCTAGATCCTCAGAAGCCATTGC-3' for the 2nd PCR; 5'-GACTCAGATCCATGGAGCAAAAGCTC-3' and 5'-GTTATCTAGATCCTCAGAAGCCATTGC-3' for the 3rd PCR; 5'-AGCTGTACAAGTCCGGACTCAGATCC-3' and 5'-GTTATCTAGATCCTCAGAAGCCATTGC-3' for the 4th PCR. The final amplified product was subcloned into the *BsrGI* and *XbaI* sites of pEGFP-C1. The *Renilla* luciferase reporter vector pGL4.74[hRluc/TK] was purchased from Promega. The five conserved regions from *LMNA* first intron were independently subcloned into

pGL4.23 GW Reverse vector using pCR™8/GW/TOPO® TA Cloning® Kit (Invitrogen) according to the manufacture's instruction.

The sequences of the five conserved regions in *LMNA* first intron are listed below:

Name	DNA Sequence
Con1	CCCAGCGGGGCCAGGCAGTCTTTGCTCGGGCCCATCCTCTTAGCTGCTGACGTTTTGATCTT TGTCTTATTGAAGTGCTGGAATACAGTGACATTTTTGAAATCCAGCCGTTGGAAGATTCAG GCCACTCCCACTTTACCCACCCCTGCCCCACCCTACCCCACCCTACTCAACTGCACCTTCTT CTTTTCTAAAAAAGC
Con2	GTGCCCTGGCCTCCGGCCTCAGGCTTCTCCTGCCTCTGTACAATGCCACGTTGATACGCCCA GCAGCTGTGACTCAGGCCTGGCCCCCTGCCAGGCCCAGCACTTCTACTGGAGTTGCGTCTG AACATGTCAACAGGCTTCCTATCCCTCTCTCAGCACCAGTTCTCCCCACTTCAGCCCCTCCC TCTGCCTGGAATTAA
Con3	ATGCAAGGGAAAGGACTGGCACTCTGCTGGCACAGCACCCGGCCTGGGGCAGGACACGGG CGAAGCCAGGGTCTCCCCTGTGAGCACTAGAGGATTTCCCGACCCCTGCCCGGGTATTGTG TGCCTGAGCATGAGTCACCTGAGGGGCCCAGGTTCCCACCCTTCCCAGCTCCTCTGGCCTG CCCCACCCTGTCCTCCCT
Con4	GTTTTTCTTCATTTTCCCTCCTCCCCCTGCAGCTGCTTCAGCTTCGGAAAAGTTCTGAAGTCA TGGAAAGTTGGGGCTGTGCTCCCAGCCAGGGGCTAGGCCGGATGGCAGCCAAAACCTGAG CTGGGTTTTGACTTTATTTTTAGCTTTTCTGACTGAGACAGAGGAGGGAATACATTCTCCGG TTCTGGAAGGGGCTC
Con5	GGGCTCAGATCGAGAAGTGCTAGGGACATGTGGGCCATGAGCTTAGTTGTCAGGCTCCTCA GAGGGAGGGAAGCTTGGCCAAAGGGAAGTGAGTAGAGTCCAGGGAGAAGGCTAAGTAAG GCCCTGTGTGGGAAGGGGCAGGAGACAAAGGTACCCCTGTCTCTTTGGGAAAGAATGGGA GGAGAGAGAGGGAAAAGCATTCATATCACGG

6.2 Cell culture and FTI treatment

HeLa cells were cultured in DMEM (Lonza) containing 10% heat-inactivated FBS (BenchMark) at 37°C supplied with 5% CO_2. HL60 cells were maintained in RPMI-1640 medium (ATCC® 30-2001™) containing 10% FBS supplied with 5% CO_2. Human primary skin fibroblasts were obtained from the Progeria Research Foundation and cultured in MEM (Life Technologies) supplemented with 20% FBS

(Gemini Bio-Products) and 2 mm l-glutamine (Life Technologies) at 37 °C supplied with 5% CO_2. Human bone marrow mesenchymal stem cells (hBM-MSCs) purchased from Rooster Bio were maintained in aMEM (Corning) supplemented with 10% heat-inactivated FBS (Seradigrn), 2 mm l-glutamine and 1% MEM non-essential amino acid (NEAA) (Life Technologies) in 5% CO_2 at 37 °C. Control and lamin A null mouse embryonic fibroblasts were kindly provided by Dr. Jan Lammerding and grown in DMEM (Lonza) supplemented with 10% FBS. In the FTI treatment experiment, FTI (J&J) at a final concentration of 2 μM was added to culture media. In chapter 2, it was added to culture media 7 hours after transfection for a total of 24 hours. In chapter 3, it was added at the time of viral infection for a time period of 6 days. Medium was changed every other day with Lonafarnib supplementation.

6.3 Plasmid and siRNA transfection

HeLa cells were transiently transfected using FuGENE® 6 Transfection Reagent (Promega) following the manufacturer's instructions. In chapter 2, approximately 1.5×10^5 cells were seeded and incubated at 37°C for one day, then transfected with 2μg of the designated plasmids. For the luciferase activity assay in chapter 4, around 2.5×10^4 cells were seeded and transfected with 0.5μg experimental plasmid and 0.2μg pGL4.74 internal control plasmid. Cell were incubated at 37°C for two day prior to the luciferase activity assay. HL60 cells were transfected by Nucleofactor™ 2b machine (Lonza) using Cell Line Nucleofector® Kit V (Lonza) according to the manufacturer's instructions. Briefly, 2×10^6 cells were transfected with 30pmol of siRNA using the program T19 on the mechine. Medium was changed

with fresh medium every other day afterwards. Transfection on primary skin fibroblasts were accomplished by using Lipofectamine® 2000 reagent (ThermoFisher Scientific). Cells were transfected with 1.6μg of plasmids at 70-90% confluency in growth medium. Fresh medium was added the next day.

6.4 Virus generation and viral infection

HEK293T cells were co-transfected with lentiviral plasmids and two virus packaging vectors, pHR-CMV-8.2ΔR and pCMV-VSVG, utilizing Fugene 6 (Promega). Culture supernatants were collected on 48 hrs and 72 hrs post-transfection, and filtered through 0.45-μm filters to remove any nonadherent 293T cells, followed by concentration at 25k RPM for 2 hours in 4°C by OptimaTM L-100K Ultracentrifuge (Beckman Coulter). The virus pellets were re-suspended in 1 ml of cold DMEM/F12 (Lonza), then stored at −80 °C. Next, fibroblasts, hBM-MSCs, MEFs or iPSCs were infected by lentiviruses in media supplemented with Polybrene (Santa Cruze Biotechnology) with the final concentration of 8 μg/ml. The medium was changed every other day post-infection until the cells were harvested.

6.5 Antibodies

The antibodies used in Western blotting analysis, immunofluorescence and immunoprecipitation were: mouse-anti-human Lamin A/C (MAB3211, Millipore), goat-anti-Lamin A/C (N-18, Santa Cruz Biotechnology), goat- anti-Lamin B (sc-6217, Santa Cruz Biotechnology), mouse anti-β-Actin peroxidase conjugated (A3854,

Sigma), mouse-anti-KDEL (ab12223, Abcam), mouse anti-GM130 (610822, BD Transduction Laboratories), rabbit-anti-emerin (ab14208-20, Abcam), mouse-anti-γ-tubulin (019K4794, Sigma), rabbit-anti-GFP antibody (ab290, Abcam), mouse-anti-Renilla Luciferase Antibody (MAB4410, Millipore), goat-anti-Sp1 (sc-59 X, Santa Cruz Biotechnology), E2F1 (05-379, Millipore), HDAC2 (ab12169, Abcam).

6.6 Western Blotting

Cell pellets were dissolved in Laemmli Sample Buffer containing 5% β-mercaptoethanol (Bio-Rad) to obtain whole cell lysates. Protein samples were then electrophoretically resolved on 10% SDS-PAGE gels and subsequently transferred onto nitrocellulose membranes (Bio-Rad) for primary and secondary antibodies detection. Bands were visualized by enhanced chemiluminescence (In chapter 2: Pierce® ECL Western Blotting Substrate, Thermo SCIENTIFIC; In chapter 3 and 4: ClarityTM Western ECL Substrate, Bio-Rad). Quantification was performed by ImageJ in chapter 2 (National Institutes of Health, Bethesda, Maryland, USA) or Image Lab™ Software in chapter 3 and 4 (Bio-Rad).

6.7 Immunofluorescence staining and microscopy

Cells were washed twice with tris-buffered saline (TBS) and fixed in 4% paraformaldehyde/phosphate buffered saline (PBS) for 20 min at room temperature. Subsequently, the cells were permeabilized with 0.5% Triton X-100 in PBS for 5 min at room temperature. After being washed twice with TBS, cells were blocked in 4%

BSA/TBS for 1 hour, and probed with the primary antibodies overnight at 4°C. The cells were then washed five times with TBS, followed by secondary antibody incubation at room temperature for 1 hour in the dark. Secondary antibodies used were Alexa Fluor® 594 donkey anti-rabbit IgG (Invitrogen), Alexa Fluor® 594 donkey anti-goat IgG (Invitrogen) and Alexa Fluor® 594 donkey anti-mouse IgG (Invitrogen). After being washed five times with TBS, the cells were stained with DAPI and mounted using VECTASHIELD® Mounting Medium with DAPI (H-1200, VECTOR). Immunofluorescence microscopy was performed on a Leica SP5 X Confocal Microscope (Leica Microsystems, Inc., Wetzlar, Germany).

6.8 Immunoprecipitation

At 24 hours after transfection, the transfected HeLa cell pellets were lysed in ice-cold 1% Triton buffer (1% Triton, 50mM Tirs pH 7.4, 150mM NaCl, 5mM MgCl2, 1 X protease inhibitor cocktail (Roche)), and then centrifuged at 2700g at 4°C for 10 minutes to obtain supernatants. EGFP-tagged proteins were immunoprecipitated from the supernatants with GFP-Trap®A beads (Chromoteck) according to manufacturer's instructions. Both input supernatants and immunoprecipitates were then resolved on 10% SDS-PAGE gels and subsequently transferred onto nitrocellulose membranes (Bio-Rad) for staining with primary and secondary antibodies.

6.9 Click chemistry assay

HeLa cells transfected with designated pEGFP-C1 based plasmids were incubated with Click-iT farnesyl alcohol azide (C10248, Invitrogen) for 14 hours for labeling. Cell lysates were collected and immunoprecipitated using GFP-Trap®_A beads (Chromotek) according to the manufacturer's instructions, followed by farnesyl detection using Alexa Fluor® 647, alkyne (A10278, Invitrogen). Protein samples were then separated with non-reducing 10% SDS-PAGE gels. After being fixed with methanol/acetic acid, the SDS-PAGE gels were scanned under a Typhoon imager.

6.10 Fluorescence recovery after photobleaching (FRAP) assay

HeLa cells transfected with designated constructs were grown on glass-bottom dishes and cultured at 37°C prior to analysis. Photobleaching experiments were performed using a Leica SP5 X Confocal Microscope (Leica Microsystems, Inc., Wetzlar, Germany). All procedures were done at 37°C. Confocal images were taken every three seconds for the first 40 images and every ten seconds for the next 80 images. Quantification was conducted using Leica SP5 software.

6.11 RNA extraction, cDNA synthesis, and quantitative RT–PCR

Total RNA from various cell lines was extracted with Trizol (Life Technologies, Carlsbad, California, United States) and purified using the RNeasy Mini kit (Qiagen, USA) according to the manufacturer's instructions. The RNA yield was determined using the NanoDrop 2000 spectrophotometer. One microgram of

total RNA was converted to cDNA using iScript Select cDNA Synthesis kit (BioRad, USA). Quantitative RT-PCR was performed in triplicate using SYBR Green Supermix (BioRad) on CFX Connect™ rea-time system (BioRad).

6.12 Chromatin immunoprecipitation (ChIP)

Primary fibroblasts cells were grown until confluency for a week in 145 mm dishes. Protein complexes were then crosslinked by addition of formaldehyde to the culture medium to a final concentration of 1% for 10 minutes. The reaction was stopped by addition of glycine (final concentration 125µM). Fixed cells were rinsed, scraped in PBS, pelleted, and flash frozen in liquid nitrogen. Cell pellets were thawed on ice and resuspended in Lysis buffer 1 (50 mM HEPES-KOH, pH 7.5, 140 mM NaCl, 1 mM EDTA, 10% glycerol, 0.5% NP-40, 0.25% Triton X-100, 1x protease inhibitors) and rocked for 10 min at 4°C. Cells were spun down (2000 rpm for 2 min at 4°C), resuspended in Lysis buffer 2 (10 mM Tris-HCl, pH 8.0, 200 mM NaCl, 1 mM EDTA, 0.5 mM EGTA, 1x protease inhibitors), and pelleted by centrifugation at 4°C. Pellets were resuspended in 3 mL Lysis buffer 3 (10 mM Tris-HCl, pH 8.0, 100 mM NaCl, 1 mM EDTA, 0.5 mM EGTA, 0.1% Na-Deoxycholate, 0.5% N lauroylsarcosine, 1x protease inhibitors), and sonicated on ice for 6 times 25 seconds at 30% amplitude with a microtip attached to a Branson digital sonifier 450. Immunoprecipitations (IPs) were performed overnight with 30µg of antibody coupled to Dynal Protein G Magnetic Beads (Invitrogen). Beads were then washed with 5 times in RIPA buffer (50 mM HEPES-KOH, pH 7.55, 500 mM LiCl, 1mM EDTA,

1.0% NP-40, 0.7% Na-Deoxycholate, 1x protease inhibitors) and once in icecold PBS. DNA was eluted in Elution buffer (50 mM Tris-HCl, pH 8.0, 10 mM EDTA, 1.0% SDS) and resuspended in 10mM Tris HCl pH 8.

6.13 Luciferase activity assay

Luciferase activity of *LMNA* first intron conserved region was tested using the Dual-luciferase reporter assay system (Promega, E1910) following the manufacture's instruction. Briefly, cells transfected with luciferase reporter constructs were lysed in passive lysis buffer. Total of 20ul of cell lysate was mixed with 100ul LARII, followed by firefly luminescence measurement using a SpectraMax® M5 Series Multi-Mode Microplate Reade (Molecular Devices). Next, 100ul of Stop & Glo Reagent was added to the mixture, followed by the reading of Renilla luminescence. The final luciferase activity was calculated as the ratio of firefly luminescence to Renilla luminescence.

6.14 Conserved region identification and putative transcription factor binding prediction in LMNA first intron

To narrow down the potential targets, five conserved regions were extracted using UCSC genome browser, based on 46 species conservatory data - PhastCons scores. In evolution theory, it is reasonable to make the assumption that those significant conserved regions could be functional. More specifically they could potentially be

transcription enhancers, playing roles for regulation while bound by some related transcription factors. In order to uncover their regulatory functions and related binding transcription factor partners, we applied PWM-scan tool to predict putative transcription factor candidates and their potential binding sites within the five conserved regions. In addition, to provide more confidence for those predictions, we removed false positive predictions based on chromatin state information (open chromatin based on DNase data) and two histone modification markers (H3K27ac and H3K4me1), which are all shown to be correlated with active enhancers.

Bibliography

Adam, S. a, Butin-Israeli, V., Cleland, M. M., Shimi, T. and Goldman, R. D. (2013a). Disruption of lamin B1 and lamin B2 processing and localization by farnesyltransferase inhibitors. *Nucleus* **4**, 142–50.

Adam, S. a, Butin-Israeli, V., Cleland, M. M., Shimi, T. and Goldman, R. D. (2013b). Disruption of lamin B1 and lamin B2 processing and localization by farnesyltransferase inhibitors. *Nucleus* **4**, 142–50.

Agrelo, R., Setien, F., Espada, J., Artiga, M. J., Rodriguez, M., Pérez-Rosado, A., Sanchez-Aguilera, A., Fraga, M. F., Piris, M. A. and Esteller, M. (2005). Inactivation of the lamin A/C gene by CpG island promoter hypermethylation in hematologic malignancies, and its association with poor survival in nodal diffuse large B-cell lymphoma. *J. Clin. Oncol.* **23**, 3940–7.

Akter, R., Rivas, D., Geneau, G., Drissi, H. and Duque, G. (2009). Effect of Lamin A/C Knockdown on Osteoblast Differentiation and Function. *J. Bone Miner. Res.* **24**, 283–293.

Astejada, M. N., Goto, K., Nagano, A., Ura, S., Noguchi, S., Nonaka, I., Nishino, I. and Hayashi, Y. K. (2007). Emerinopathy and laminopathy clinical, pathological and molecular features of muscular dystrophy with nuclear envelopathy in Japan. *Acta Myol. myopathies cardiomyopathies Off. J. Mediterr. Soc. Myol.* **26**, 159–64.

Azizkhan, J. C., Jensen, D. E., Pierce, A. J. and Wade, M. (1993). Transcription from TATA-less promoters: dihydrofolate reductase as a model. *Crit. Rev.*

Eukaryot. Gene Expr. **3**, 229–54.

Barrowman, J., Hamblet, C., George, C. M. and Michaelis, S. (2008). Analysis of prelamin A biogenesis reveals the nucleus to be a CaaX processing compartment. *Mol. Biol. Cell* **19**, 5398–408.

Barrowman, J., Hamblet, C., Kane, M. S. and Michaelis, S. (2012). Requirements for efficient proteolytic cleavage of prelamin A by ZMPSTE24. *PLoS One* **7**, e32120.

Beck, L. A., Hosick, T. J. and Sinensky, M. (1990). Isoprenylation is required for the processing of the lamin A precursor. *J. Cell Biol.* **110**, 1489–99.

Belmont, A. S., Zhai, Y. and Thilenius, A. (1993). Lamin B distribution and association with peripheral chromatin revealed by optical sectioning and electron microscopy tomography. *J. Cell Biol.* **123**, 1671–85.

Benavente, R., Krohne, G. and Franke, W. W. (1985). Cell type-specific expression of nuclear lamina proteins during development of Xenopus laevis. *Cell* **41**, 177–90.

Bengtsson, L. and Wilson, K. L. (2004). Multiple and surprising new functions for emerin, a nuclear membrane protein. *Curr. Opin. Cell Biol.* **16**, 73–79.

Bergo, M. O., Gavino, B., Ross, J., Schmidt, W. K., Hong, C., Kendall, L. V, Mohr, A., Meta, M., Genant, H., Jiang, Y., et al. (2002). Zmpste24 deficiency in mice causes spontaneous bone fractures, muscle weakness, and a prelamin A processing defect. *Proc. Natl. Acad. Sci. U. S. A.* **99**, 13049–54.

Berk, J. M., Maitra, S., Dawdy, A. W., Shabanowitz, J., Hunt, D. F. and Wilson, K. L. (2013). O-Linked β-N-acetylglucosamine (O-GlcNAc) regulates emerin

binding to barrier to autointegration factor (BAF) in a chromatin- and lamin B-enriched "niche". *J. Biol. Chem.* **288**, 30192–209.

Bertacchini, J., Beretti, F., Cenni, V., Guida, M., Gibellini, F., Mediani, L., Marin, O., Maraldi, N. M., de Pol, A., Lattanzi, G., et al. (2013). The protein kinase Akt/PKB regulates both prelamin A degradation and Lmna gene expression. *FASEB J.* **27**, 2145–55.

Bione, S., Maestrini, E., Rivella, S., Mancini, M., Regis, S., Romeo, G. and Toniolo, D. (1994). Identification of a novel X-linked gene responsible for Emery-Dreifuss muscular dystrophy. *Nat. Genet.* **8**, 323–327.

BLACK, A. R., BLACK, J. D. and AZIZKHAN-CLIFFORD, A. J. (2001). Sp1 and Krüppel-Like Factor Family of Transcription Factors in Cell Growth Regulation and Cancer. *J. South. Afr. Stud.* **27**, 363–379.

Blumenberg, M. Transcriptional Regulation of Keratin Gene Expression.

Bonne, G., Schwartz, K., Barletta, M. R. Di, Varnous, S., Bécane, H.-M., Hammouda, E.-H., Merlini, L., Muntoni, F., Greenberg, C. R., Gary, F., et al. (1999). Mutations in the gene encoding lamin A/C cause autosomal dominant Emery-Dreifuss muscular dystrophy. *Nat. Genet.* **21**, 285–288.

Boyartchuk, V. L., Ashby, M. N. and Rine, J. (1997). Modulation of Ras and a-factor function by carboxyl-terminal proteolysis. *Science* **275**, 1796–800.

Bridger, J. M., Foeger, N., Kill, I. R. and Herrmann, H. (2007). The nuclear lamina. Both a structural framework and a platform for genome organization. *FEBS J.* **274**, 1354–61.

Broers, J. L., Machiels, B. M., Kuijpers, H. J., Smedts, F., van den Kieboom, R.,

Raymond, Y. and Ramaekers, F. C. (1997). A- and B-type lamins are differentially expressed in normal human tissues. *Histochem. Cell Biol.* **107**, 505–17.

Broers, J. L. V., Ramaekers, F. C. S., Bonne, G., Yaou, R. Ben and Hutchison, C. J. (2006). Nuclear Lamins: Laminopathies and Their Role in Premature Ageing. *Physiol. Rev.* **86**, 967–1008.

Brunauer, R. and Kennedy, B. K. (2015). Progeria accelerates adult stem cell aging. *Science (80-.).* **348**,.

Burke, B. and Stewart, C. L. (2012). The nuclear lamins: flexibility in function. *Nat. Rev. Mol. Cell Biol.* **14**,.

Cao, K., Capell, B. C., Erdos, M. R., Djabali, K. and Collins, F. S. (2007). A lamin A protein isoform overexpressed in Hutchinson-Gilford progeria syndrome interferes with mitosis in progeria and normal cells. *Proc. Natl. Acad. Sci. U. S. A.* **104**, 4949–54.

Cao, K., Blair, C. D., Faddah, D. A., Kieckhaefer, J. E., Olive, M., Erdos, M. R., Nabel, E. G. and Collins, F. S. (2011a). Progerin and telomere dysfunction collaborate to trigger cellular senescence in normal human fibroblasts. **121**,.

Cao, K., Graziotto, J. J., Blair, C. D., Mazzulli, J. R., Erdos, M. R., Krainc, D. and Collins, F. S. (2011b). Rapamycin reverses cellular phenotypes and enhances mutant protein clearance in Hutchinson-Gilford progeria syndrome cells. *Sci. Transl. Med.* **3**, 89ra58.

Capell, B. C. and Collins, F. S. (2006). Human laminopathies: nuclei gone genetically awry. *Nat. Rev. Genet.* **7**, 940–52.

Capell, B. C., Erdos, M. R., Madigan, J. P., Fiordalisi, J. J., Varga, R., Conneely, K. N., Gordon, L. B., Der, C. J., Cox, A. D. and Collins, F. S. (2005). Inhibiting farnesylation of progerin prevents the characteristic nuclear blebbing of Hutchinson-Gilford progeria syndrome. *Proc. Natl. Acad. Sci. U. S. A.* **102**, 12879–84.

Capell, B. C., Olive, M., Erdos, M. R., Cao, K., Faddah, D. a, Tavarez, U. L., Conneely, K. N., Qu, X., San, H., Ganesh, S. K., et al. (2008). A farnesyltransferase inhibitor prevents both the onset and late progression of cardiovascular disease in a progeria mouse model. *Proc. Natl. Acad. Sci. U. S. A.* **105**, 15902–7.

Chong, J. A., Tapia-Ramírez, J., Kim, S., Toledo-Aral, J. J., Zheng, Y., Boutros, M. C., Altshuller, Y. M., Frohman, M. A., Kraner, S. D. and Mandel, G. (1995). REST: a mammalian silencer protein that restricts sodium channel gene expression to neurons. *Cell* **80**, 949–57.

Clawson, G. A., Norbeck, L. L., Hatem, C. L., Rhodes, C., Amiri, P., McKerrow, J. H., Patierno, S. R. and Fiskum, G. (1992). Ca(2+)-regulated serine protease associated with the nuclear scaffold. *Cell Growth Differ.* **3**, 827–38.

Clements, L., Manilal, S., Love, D. R. and Morris, G. E. (2000). Direct Interaction between Emerin and Lamin A. *Biochem. Biophys. Res. Commun.* **267**, 709–714.

Columbaro, M., Capanni, C., Mattioli, E., Novelli, G., Parnaik, V. K., Squarzoni, S., Maraldi, N. M. and Lattanzi, G. (2005). Rescue of heterochromatin organization in Hutchinson-Gilford progeria by drug treatment. *Cell. Mol. Life Sci.* **62**, 2669–2678.

CORRIGAN, D. P., KUSZCZAK, D., RUSINOL, A. E., THEWKE, D. P., HRYCYNA, C. A., MICHAELIS, S. and SINENSKY, M. S. (2005). Prelamin A endoproteolytic processing *in vitro* by recombinant Zmpste24. *Biochem. J.* **387**, 129–138.

Coulson, J. M. (2005). Transcriptional Regulation: Cancer, Neurons and the REST. *Curr. Biol.* **15**, R665–R668.

Croft, J. A., Bridger, J. M., Boyle, S., Perry, P., Teague, P. and Bickmore, W. A. (1999). Differences in the localization and morphology of chromosomes in the human nucleus. *J. Cell Biol.* **145**, 1119–31.

Csoka, A. B., English, S. B., Simkevich, C. P., Ginzinger, D. G., Butte, A. J., Schatten, G. P., Rothman, F. G. and Sedivy, J. M. (2004). Genome-scale expression profiling of Hutchinson-Gilford progeria syndrome reveals widespread transcriptional misregulation leading to mesodermal/mesenchymal defects and accelerated atherosclerosis. *Aging Cell* **3**, 235–243.

D'Apice, M. R., Tenconi, R., Mammi, I., van den Ende, J. and Novelli, G. (2004). Paternal origin of LMNA mutations in Hutchinson-Gilford progeria. *Clin. Genet.* **65**, 52–4.

Dai, Q., Choy, E., Chiu, V., Romano, J., Slivka, S. R., Steitz, S. A., Michaelis, S. and Philips, M. R. (1998). Mammalian prenylcysteine carboxyl methyltransferase is in the endoplasmic reticulum. *J. Biol. Chem.* **273**, 15030–4.

de Felipe, P., Luke, G. A., Brown, J. D. and Ryan, M. D. (2010). Inhibition of 2A-mediated "cleavage" of certain artificial polyproteins bearing N-terminal signal sequences. *Biotechnol. J.* **5**, 213–23.

De Felipe, P., Luke, G. A., Hughes, L. E., Gani, D., Halpin, C. and Ryan, M. D. (2006). E unum pluribus: Multiple proteins from a self-processing polyprotein. *Trends Biotechnol.* **24**, 68–75.

De Sandre-Giovannoli, A., Bernard, R., Cau, P., Navarro, C., Amiel, J., Boccaccio, I., Lyonnet, S., Stewart, C. L., Munnich, A., Le Merrer, M., et al. (2003). Lamin a truncation in Hutchinson-Gilford progeria. *Science* **300**, 2055.

Dechat, T., Shimi, T., Adam, S. A., Rusinol, A. E., Andres, D. A., Spielmann, H. P., Sinensky, M. S. and Goldman, R. D. (2007). Alterations in mitosis and cell cycle progression caused by a mutant lamin A known to accelerate human aging. *Proc. Natl. Acad. Sci. U. S. A.* **104**, 4955–60.

Dechat, T., Pfleghaar, K., Sengupta, K., Shimi, T., Shumaker, D. K., Solimando, L. and Goldman, R. D. (2008). Nuclear lamins: major factors in the structural organization and function of the nucleus and chromatin. *Genes Dev.* **22**, 832–53.

Dechat, T., Adam, S. A., Taimen, P., Shimi, T. and Goldman, R. D. (2010). Nuclear lamins. *Cold Spring Harb. Perspect. Biol.* **2**, a000547.

Delbarre, E., Tramier, M., Coppey-Moisan, M., Gaillard, C., Courvalin, J.-C. and Buendia, B. (2006). The truncated prelamin A in Hutchinson-Gilford progeria syndrome alters segregation of A-type and B-type lamin homopolymers. *Hum. Mol. Genet.* **15**, 1113–1122.

Dittmer, T. A. and Misteli, T. (2011). The lamin protein family. *Genome Biol.* **12**, 222.

Doetzlhofer, A., Rotheneder, H., Lagger, G., Koranda, M., Kurtev, V., Brosch, G., Wintersberger, E. and Seiser, C. (1999). Histone Deacetylase 1 Can

Repress Transcription by Binding to Sp1. *Mol. Cell. Biol.* **19**, 5504–5511.

Donnelly, M. L., Luke, G., Mehrotra, A., Li, X., Hughes, L. E., Gani, D. and Ryan, M. D. (2001). Analysis of the aphthovirus 2A/2B polyprotein "cleavage" mechanism indicates not a proteolytic reaction, but a novel translational effect: a putative ribosomal "skip". *J. Gen. Virol.* **82**, 1013–25.

Dou, Z., Xu, C., Donahue, G., Shimi, T., Pan, J.-A., Zhu, J., Ivanov, A., Capell, B. C., Drake, A. M., Shah, P. P., et al. (2015). Autophagy mediates degradation of nuclear lamina. *Nature* **527**, 1–17.

Dreuillet, C., Tillit, J., Kress, M. and Ernoult-Lange, M. (2002). In vivo and in vitro interaction between human transcription factor MOK2 and nuclear lamin A/C. *Nucleic Acids Res.* **30**, 4634–42.

Eggert, M., Radomski, N., Tripier=, D., Traub, P. and Jost, E. (1991). Identification of phosphorylation sites on murine nuclear lamin C by RP-HPLC and microsequencing. **292**, 205–209.

Ehninger, D., Neff, F. and Xie, K. (2014). Longevity, aging and rapamycin. *Cell. Mol. Life Sci.* **71**, 4325–46.

Ellis, D. J., Jenkins, H., Whitfield, W. G. and Hutchison, C. J. (1997). GST-lamin fusion proteins act as dominant negative mutants in Xenopus egg extract and reveal the function of the lamina in DNA replication. *J. Cell Sci.* **110**,.

Eriksson, M., Brown, W. T., Gordon, L. B., Glynn, M. W., Singer, J., Scott, L., Erdos, M. R., Robbins, C. M., Moses, T. Y., Berglund, P., et al. (2003). Recurrent de novo point mutations in lamin A cause Hutchinson-Gilford progeria syndrome. *Nature* **423**, 293–8.

Eriksson, J. E., Dechat, T., Grin, B., Helfand, B., Mendez, M., Pallari, H.-M. and Goldman, R. D. (2009). Introducing intermediate filaments: from discovery to disease. *J. Clin. Invest.* **119**, 1763–71.

Espada, J., Varela, I., Flores, I., Ugalde, A. P., Cadiñanos, J., Pendás, A. M., Stewart, C. L., Tryggvason, K., Blasco, M. A., Freije, J. M. P., et al. (2008). Nuclear envelope defects cause stem cell dysfunction in premature-aging mice. *J. Cell Biol.* **181**, 27–35.

Esteller, M. (2002). CpG island hypermethylation and tumor suppressor genes: a booming present, a brighter future. *Oncogene* **21**, 5427–5440.

Fawcett, D. W. (1966). On the occurrence of a fibrous lamina on the inner aspect of the nuclear envelope in certain cells of vertebrates. *Am. J. Anat.* **119**, 129–45.

Fenichel, G. M., Sul, Y. C., Kilroy, A. W. and Blouin, R. (1982). An autosomal-dominant dystrophy with humeropelvic distribution and cardiomyopathy. *Neurology* **32**, 1399–401.

Fields, A. P. and Thompson, L. J. (1995). The regulation of mitotic nuclear envelope breakdown: a role for multiple lamin kinases. *Prog. Cell Cycle Res.* **1**, 271–86.

Foisner ', R. and Gerace, L. (1993). Integral Membrane Proteins of the Nuclear Envelope Interact with Lamins and Chromosomes, and Binding Is Modulated by Mitotic Phosphorylation. *Cell* **73**, 1267–1279.

Fong, L. G., Frost, D., Meta, M., Qiao, X., Yang, S. H., Coffinier, C. and Young, S. G. (2006). A Protein Farnesyltransferase Inhibitor Ameliorates Disease in a Mouse Model of Progeria. *Science (80-.).* **311**,.

Fritzsche, S. and Springer, S. (2014). Pulse-chase analysis for studying protein synthesis and maturation. *Curr. Protoc. Protein Sci.* **78**, 30.3.1-23.

Furukawa, K. and Hotta, Y. (1993). cDNA cloning of a germ cell specific lamin B3 from mouse spermatocytes and analysis of its function by ectopic expression in somatic cells. *EMBO J.* **12**, 97–106.

Furukawa, K., Inagaki, H. and Hotta, Y. (1994). Identification and cloning of an mRNA coding for a germ cell-specific A-type lamin in mice. *Exp. Cell Res.* **212**, 426–30.

Gabriel, D., Roedl, D., Gordon, L. B. and Djabali, K. (2015). Sulforaphane enhances progerin clearance in Hutchinson-Gilford progeria fibroblasts. *Aging Cell* **14**, 78–91.

Galiová, G., Bártová, E., Raška, I., Krejčí, J. and Kozubek, S. (2008). Chromatin changes induced by lamin A/C deficiency and the histone deacetylase inhibitor trichostatin A. *Eur. J. Cell Biol.* **87**, 291–303.

Gelb, M. H., Brunsveld, L., Hrycyna, C. A., Michaelis, S., Tamanoi, F., Van Voorhis, W. C. and Waldmann, H. (2006). Therapeutic intervention based on protein prenylation and associated modifications. *Nat. Chem. Biol.* **2**, 518–28.

Gerace, L., Blobel, G., Petersen, D. F., Branton, D. and Jost, E. (1980). The nuclear envelope lamina is reversibly depolymerized during mitosis. *Cell* **19**, 277–87.

Goldman, A. E., Moir, R. D., Montag-Lowy, M., Stewart, M. and Goldman, R. D. (1992). Pathway of incorporation of microinjected lamin A into the nuclear envelope. *J. Cell Biol.* **119**, 725–35.

Goldman, R. D., Gruenbaum, Y., Moir, R. D., Shumaker, D. K. and Spann, T. P. (2002). Nuclear lamins: building blocks of nuclear architecture. *Genes Dev.* **16**, 533–47.

Goldman, R. D., Shumaker, D. K., Erdos, M. R., Eriksson, M., Goldman, A. E., Gordon, L. B., Gruenbaum, Y., Khuon, S., Mendez, M., Varga, R., et al. (2004). Accumulation of mutant lamin A causes progressive changes in nuclear architecture in Hutchinson-Gilford progeria syndrome. *Proc. Natl. Acad. Sci. U. S. A.* **101**, 8963–8.

Gordon, L. B., Kleinman, M. E., Miller, D. T., Neuberg, D. S., Giobbie-hurder, A., Correia, A., Quinn, N., Ullrich, N. J., Nazarian, A., Liang, M. G., et al. (2012a). Clinical trial of a farnesyltransferase inhibitor in children with Hutchinson – Gilford progeria syndrome. 2–7.

Gordon, L. B., Kleinman, M. E., Miller, D. T., Neuberg, D. S., Giobbie-Hurder, A., Gerhard-Herman, M., Smoot, L. B., Gordon, C. M., Cleveland, R., Snyder, B. D., et al. (2012b). Clinical trial of a farnesyltransferase inhibitor in children with Hutchinson-Gilford progeria syndrome. *Proc. Natl. Acad. Sci. U. S. A.* **109**, 16666–71.

Gordon, L. B., Rothman, F. G., López-Otín, C. and Misteli, T. (2014a). Progeria: A Paradigm for Translational Medicine. *Cell* **156**, 400–407.

Gordon, L. B., Massaro, J., D'Agostino, R. B., Campbell, S. E., Brazier, J., Brown, W. T., Kleinman, M. E. and Kieran, M. W. (2014b). Impact of farnesylation inhibitors on survival in Hutchinson-Gilford progeria syndrome. *Circulation* **130**, 27–34.

Gordon, L. B., Kleinman, M. E., Massaro, J., D'Agostino, R. B., Shappell, H., Gerhard-Herman, M., Smoot, L. B., Gordon, C. M., Cleveland, R. H., Nazarian, A., et al. (2016). Clinical Trial of the Protein Farnesylation Inhibitors Lonafarnib, Pravastatin, and Zoledronic Acid in Children With Hutchinson-Gilford Progeria SyndromeClinical Perspective. *Circulation* **134**,.

GREENBERG, J. R. (1972). High Stability of Messenger RNA in Growing Cultured Cells. *Nature* **240**, 102–104.

Gruenbaum, Y. and Foisner, R. (2014). Lamins: Nuclear Intermediate Filament Proteins with Fundamental Functions in Nuclear Mechanics and Genome Regulation. *Annu. Rev. Biochem.* **84**, 150306093657004.

Gruenbaum, Y., Lee, K. K., Liu, J., Cohen, M. and Wilson, K. L. (2002). The expression, lamin-dependent localization and RNAi depletion phenotype for emerin in C. elegans. *J. Cell Sci.* **115**,.

Gruenbaum, Y., Goldman, R. D., Meyuhas, R., Mills, E., Margalit, A., Fridkin, A., Dayani, Y., Prokocimer, M. and Enosh, A. (2003). The nuclear lamina and its functions in the nucleus. *Int. Rev. Cytol.* **226**, 1–62.

Gruenbaum, Y., Margalit, A., Goldman, R. D., Shumaker, D. K. and Wilson, K. L. (2005). The nuclear lamina comes of age. *Nat. Rev. Mol. Cell Biol.* **6**, 21–31.

Guelen, L., Pagie, L., Brasset, E., Meuleman, W., Faza, M. B., Talhout, W., Eussen, B. H., de Klein, A., Wessels, L., de Laat, W., et al. (2008). Domain organization of human chromosomes revealed by mapping of nuclear lamina interactions. *Nature* **453**, 948–951.

Hamid, Q. A., Fatima, S., Thanumalayan, S. and Parnaik, V. K. (1996).

Activation of the lamin A gene during rat liver development. *FEBS Lett.* **392**, 137–42.

Haraguchi, T., Holaska, J. M., Yamane, M., Koujin, T., Hashiguchi, N., Mori, C., Wilson, K. L. and Hiraoka, Y. (2004). Emerin binding to Btf, a death-promoting transcriptional repressor, is disrupted by a missense mutation that causes Emery-Dreifuss muscular dystrophy. *Eur. J. Biochem.* **271**, 1035–1045.

Heald, R. and McKeon, F. (1990). Mutations of phosphorylation sites in lamin A that prevent nuclear lamina disassembly in mitosis. *Cell* **61**, 579–89.

Hegele, R. A., Cao, H., Liu, D. M., Costain, G. A., Charlton-Menys, V., Rodger, N. W. and Durrington, P. N. (2006). Sequencing of the reannotated LMNB2 gene reveals novel mutations in patients with acquired partial lipodystrophy. *Am. J. Hum. Genet.* **79**, 383–9.

Hennekes, H. and Nigg, E. A. (1994). The role of isoprenylation in membrane attachment of nuclear lamins. A single point mutation prevents proteolytic cleavage of the lamin A precursor and confers membrane binding properties. *J. Cell Sci.* **107**,.

Herman, J. G. and Baylin, S. B. (2003). Gene Silencing in Cancer in Association with Promoter Hypermethylation. *N. Engl. J. Med.* **349**, 2042–2054.

Hinds, P. W., Mittnacht, S., Dulic, V., Arnold, A., Reed, S. I. and Weinberg, R. A. (1992). Regulation of Retinoblastoma Protein Functions by Ectopic Expression of Human Cyclins. *Cell* **70**, 993–1006.

Ho, C. Y. and Lammerding, J. (2012). Lamins at a glance. *J. Cell Sci.* **125**,.

Ho, C. Y., Jaalouk, D. E., Vartiainen, M. K. and Lammerding, J. (2013). Lamin

A/C and emerin regulate MKL1–SRF activity by modulating actin dynamics. *Nature* **497**, 507–511.

Holaska, J. M. and Wilson, K. L. (2006). Multiple roles for emerin: implications for Emery-Dreifuss muscular dystrophy. *Anat. Rec. A. Discov. Mol. Cell. Evol. Biol.* **288**, 676–80.

Holaska, J. M., Lee, K. K., Kowalski, A. K. and Wilson, K. L. (2002). Transcriptional Repressor Germ Cell-less (GCL) and Barrier to Autointegration Factor (BAF) Compete for Binding to Emerin in Vitro*.

Holtz, D., Tanaka, R. A., Hartwig, J. and McKeon, F. (1989). The CaaX motif of lamin A functions in conjunction with the nuclear localization signal to target assembly to the nuclear envelope. *Cell* **59**, 969–977.

Hutchison, C. J. (2002). Lamins: building blocks or regulators of gene expression? *Nat. Rev. Mol. Cell Biol.* **3**, 848–858.

Janaki Ramaiah, M. and Parnaik, V. K. (2006). An essential GT motif in the lamin A promoter mediates activation by CREB-binding protein. *Biochem. Biophys. Res. Commun.* **348**, 1132–1137.

Jung, H.-J., Coffinier, C., Choe, Y., Beigneux, A. P., Davies, B. S. J., Yang, S. H., Barnes, R. H., Hong, J., Sun, T., Pleasure, S. J., et al. (2012). Regulation of prelamin A but not lamin C by miR-9, a brain-specific microRNA. *Proc. Natl. Acad. Sci. U. S. A.* **109**, E423-31.

Kang, H. T., Park, J. T., Choi, K., Choi, H. J. C., Jung, C. W., Kim, G. R., Lee, Y.-S. and Park, S. C. (2017). Chemical screening identifies ROCK as a target for recovering mitochondrial function in Hutchinson-Gilford progeria syndrome.

Aging Cell **16**, 541–550.

Kaufmann, S. H. (1992). Expression of Nuclear Envelope Lamins A and C in Human Myeloid Leukemias1. *CANCER Res.* **52**, 2847–2853.

Khalifa, M. M. (1989). Hutchinson-Gilford progeria syndrome: report of a Libyan family and evidence of autosomal recessive inheritance. *Clin. Genet.* **35**, 125–32.

Kim, J. H., Lee, S. R., Li, L. H., Park, H. J., Park, J. H., Lee, K. Y., Kim, M. K., Shin, B. A. and Choi, S. Y. (2011a). High cleavage efficiency of a 2A peptide derived from porcine teschovirus-1 in human cell lines, zebrafish and mice. *PLoS One* **6**, 1–8.

Kim, W., Bennett, E. J., Huttlin, E. L., Guo, A., Li, J., Possemato, A., Sowa, M. E., Rad, R., Rush, J., Comb, M. J., et al. (2011b). Systematic and Quantitative Assessment of the Ubiquitin-Modified Proteome. *Mol. Cell* **44**, 325–340.

Kim, Y. C., Guan, K.-L., Yuan, J., Pollak, M., Sonenberg, N. and Ohsumi, Y. (2015). mTOR: a pharmacologic target for autophagy regulation. *J. Clin. Invest.* **125**, 25–32.

Kreienkamp, R., Croke, M., Neumann, M. A., Bedia-Diaz, G., Graziano, S., Dusso, A., Dorsett, D., Carlberg, C. and Gonzalo, S. (2014). Vitamin D receptor signaling improves Hutchinson-Gilford progeria syndrome cellular phenotypes. *Oncotarget* **7**, 30018–31.

Krimm, I., Ostlund, C., Gilquin, B., Couprie, J., Hossenlopp, P., Mornon, J.-P., Bonne, G., Courvalin, J.-C., Worman, H. J. and Zinn-Justin, S. (2002). The Ig-like structure of the C-terminal domain of lamin A/C, mutated in muscular

dystrophies, cardiomyopathy, and partial lipodystrophy. *Structure* **10**, 811–23.

Krohne, G., Benavente, R., Scheer, U. and Dabauvalle, M. C. (2005). The nuclear lamina in Heidelberg and W??rzburg: A personal view. *Eur. J. Cell Biol.* **84**, 163–179.

Kubben, N., Voncken, J. W., Demmers, J., Calis, C., van Almen, G., Pinto, Y. and Misteli, T. (2010). Identification of differential protein interactors of lamin A and progerin. *Nucleus* **1**, 513–25.

Kubben, N., Brimacombe, K. R., Donegan, M., Li, Z. and Misteli, T. (2016). A high-content imaging-based screening pipeline for the systematic identification of anti-progeroid compounds. *Methods* **96**, 46–58.

Kudlow, B. A., Kennedy, B. K. and Monnat, R. J. (2007). Werner and Hutchinson-Gilford progeria syndromes: mechanistic basis of human progeroid diseases. *Nat. Rev. Mol. Cell Biol.* **8**, 394–404.

Kumaran, R. I. and Spector, D. L. (2008). A genetic locus targeted to the nuclear periphery in living cells maintains its transcriptional competence. *J. Cell Biol.* **180**, 51–65.

Lammerding, J., Schulze, P. C., Takahashi, T., Kozlov, S., Sullivan, T., Kamm, R. D., Stewart, C. L. and Lee, R. T. (2004). Lamin A/C deficiency causes defective nuclear mechanics and mechanotransduction. *J. Clin. Invest.* **113**, 370–8.

Lanoix, J., Skup, D., Collard, J. F. and Raymond, Y. (1992). Regulation of the expression of lamins A and C is post-transcriptional in P19 embryonal carcinoma cells. *Biochem. Biophys. Res. Commun.* **189**, 1639–44.

Lattanzi, G., Marmiroli, S., Facchini, A. and Maraldi, N. M. (2012). Nuclear damages and oxidative stress: new perspectives for laminopathies. *Eur. J. Histochem.* **56**, e45.

Lazebnik, Y. A., Takahashi, A., Moir, R. D., Goldman, R. D., Poirier, G. G., Kaufmann, S. H. and Earnshaw, W. C. (1995). Studies of the lamin proteinase reveal multiple parallel biochemical pathways during apoptotic execution. *Proc. Natl. Acad. Sci. U. S. A.* **92**, 9042–6.

Lebel, S., Lampron, C., Royal, A. and Raymond, Y. (1987). Lamins A and C appear during retinoic acid-induced differentiation of mouse embryonal carcinoma cells. *J. Cell Biol.* **105**, 1099–104.

Lee, K. K., Haraguchi, T., Lee, R. S., Koujin, T., Hiraoka, Y. and Wilson, K. L. (2001). Distinct functional domains in emerin bind lamin A and DNA-bridging protein BAF. *J. Cell Sci.* **114**, 4567–73.

Lehner, C. F., Fürstenberger, G., Eppenberger, H. M. and Nigg, E. A. (1986). Biogenesis of the nuclear lamina: in vivo synthesis and processing of nuclear protein precursors. *Proc. Natl. Acad. Sci. U. S. A.* **83**, 2096–9.

Lehner, C. F., Stick, R., Eppenberger, H. M. and Nigg, E. A. (1987). Differential expression of nuclear lamin proteins during chicken development. *J. Cell Biol.* **105**, 577–87.

Li, L. and Davie, J. R. (2010). The role of Sp1 and Sp3 in normal and cancer cell biology. *Ann. Anat. - Anat. Anzeiger* **192**, 275–283.

Lin, F. and Worman, H. J. (1993). Structural organization of the human gene encoding nuclear lamin A and nuclear lamin C. *J. Biol. Chem.* **268**, 16321–6.

Lin, F. and Worman, H. J. (1997). Expression of nuclear lamins in human tissues and cancer cell lines and transcription from the promoters of the lamin A/C and B1 genes. *Exp. Cell Res.* **236**, 378–84.

Lin, S. Y., Black, A. R., Kostic, D., Pajovic, S., Hoover, C. N. and Azizkhan, J. C. (1996). Cell cycle-regulated association of E2F1 and Sp1 is related to their functional interaction. *Mol. Cell. Biol.* **16**, 1668–75.

Lin, F., Blake, D. L., Callebaut, I., Skerjanc, I. S., Holmer, L., McBurney, M. W., Paulin-Levasseur, M. and Worman, H. J. (2000). MAN1, an inner nuclear membrane protein that shares the LEM domain with lamina-associated polypeptide 2 and emerin. *J. Biol. Chem.* **275**, 4840–7.

Lloyd, D. J., Trembath, R. C. and Shackleton, S. (2002). A novel interaction between lamin A and SREBP1: implications for partial lipodystrophy and other laminopathies. *Hum. Mol. Genet.* **11**,.

Lo Cicero, A. and Nissan, X. (2015). Pluripotent stem cells to model Hutchinson-Gilford progeria syndrome (HGPS): Current trends and future perspectives for drug discovery. *Ageing Res. Rev.* **24**, 343–348.

Lourim, D., Kempf, A. and Krohne, G. (1996). Characterization and quantitation of three B-type lamins in Xenopus oocytes and eggs: increase of lamin LI protein synthesis during meiotic maturation. *J. Cell Sci.* **109**,.

Lutz, R. J., Trujillo, M. A., Denham, K. S., Wenger, L. and Sinensky, M. (1992). Nucleoplasmic localization of prelamin A: implications for prenylation-dependent lamin A assembly into the nuclear lamina. *Proc. Natl. Acad. Sci. U. S. A.* **89**, 3000–4.

Machiels, B. M., Zorenc, A. H., Endert, J. M., Kuijpers, H. J., van Eys, G. J., Ramaekers, F. C. and Broers, J. L. (1996). An alternative splicing product of the lamin A/C gene lacks exon 10. *J. Biol. Chem.* **271**, 9249–53.

Maciel, A. T., Opitz, J. M. and Reynolds, J. F. (1988). Evidence for autosomal recessive inheritance of progeria (Hutchinson Gilford). *Am. J. Med. Genet.* **31**, 483–7.

Markiewicz, E., Dechat, T., Foisner, R., Quinlan, R. A. and Hutchison, C. J. (2002). Lamin A/C binding protein LAP2alpha is required for nuclear anchorage of retinoblastoma protein. *Mol. Biol. Cell* **13**, 4401–13.

Maske, C. P., Hollinshead, M. S., Higbee, N. C., Bergo, M. O., Young, S. G. and Vaux, D. J. (2003). A carboxyl-terminal interaction of lamin B1 is dependent on the CAAX endoprotease Rce1 and carboxymethylation. *J. Cell Biol.* **162**, 1223–32.

Mattia, E., Hoff, W. D., Blaauwen, J. den, Meijne, A. M. L., Stuurman, N. and Renswoude, J. van (1992). Induction of nuclear lamins A/C during in vitro-induced differentiation of F9 and P19 embryonal carcinoma cells. *Exp. Cell Res.* **203**, 449–455.

McCord, R. P., Nazario-Toole, A., Zhang, H., Chines, P. S., Zhan, Y., Erdos, M. R., Collins, F. S., Dekker, J. and Cao, K. (2013a). Correlated alterations in genome organization, histone methylation, and DNA-lamin A/C interactions in Hutchinson-Gilford progeria syndrome. *Genome Res.* **23**, 260–9.

McCord, R. P., Nazario-Toole, A., Zhang, H., Chines, P. S., Zhan, Y., Erdos, M. R., Collins, F. S., Dekker, J. and Cao, K. (2013b). Correlated alterations in

genome organization, histone methylation, and DNA-lamin A/C interactions in Hutchinson-Gilford progeria syndrome. *Genome Res.* **23**, 260–9.

McKeon, F. D., Kirschner, M. W. and Caput, D. (1986). Homologies in both primary and secondary structure between nuclear envelope and intermediate filament proteins. *Nature* **319**, 463–8.

Meier, J., Campbell, K. H., Ford, C. C., Stick, R. and Hutchison, C. J. (1991). The role of lamin LIII in nuclear assembly and DNA replication, in cell-free extracts of Xenopus eggs. *J. Cell Sci.* **98**,.

Merideth, M. A., Gordon, L. B., Clauss, S., Sachdev, V., Smith, A. C. M., Perry, M. B., Brewer, C. C., Zalewski, C., Kim, H. J., Solomon, B., et al. (2008). Phenotype and Course of Hutchinson–Gilford Progeria Syndrome. *N. Engl. J. Med.* **358**, 592–604.

Miller, R. G., Layzer, R. B., Mellenthin, M. A., Golabi, M., Francoz, R. A. and Mall, J. C. (1985). Emery-Dreifuss muscular dystrophy with autosomal dominant transmission. *Neurology* **35**, 1230–3.

Mislow, J. M. K., Holaska, J. M., Kim, M. S., Lee, K. K., Segura-Totten, M., Wilson, K. L. and McNally, E. M. (2002). Nesprin-1alpha self-associates and binds directly to emerin and lamin A in vitro. *FEBS Lett.* **525**, 135–40.

Moir, R. D., Spann, T. P., Lopez-Soler, R. I., Yoon, M., Goldman, A. E., Khuon, S. and Goldman, R. D. (2000). Review: the dynamics of the nuclear lamins during the cell cycle-- relationship between structure and function. *J. Struct. Biol.* **129**, 324–34.

Moulson, C. L., Fong, L. G., Gardner, J. M., Farber, E. A., Go, G., Passariello,

A., Grange, D. K., Young, S. G. and Miner, J. H. (2007). Increased progerin expression associated with unusual LMNA mutations causes severe progeroid syndromes. *Hum. Mutat.* **28**, 882–889.

Munro, S. and Pelham, H. R. (1987). A C-terminal signal prevents secretion of luminal ER proteins. *Cell* **48**, 899–907.

Muralikrishna, B. and Parnaik, V. K. (2001). SP3 and AP-1 mediate transcriptional activation of the lamin A proximal promoter. *Eur. J. Biochem.* **268**, 3736–43.

Nakajima, N. and Abe, K. (1995). Genomic structure of the mouse A-type lamin gene locus encoding somatic and germ cell-specific lamins. *FEBS Lett.* **365**, 108–114.

Nakamachi, K. and Nakajima, N. (2000a). Dnase I hypersensitive sites and transcriptional activation of the lamin A/C gene. *Eur. J. Biochem.* **267**, 1416–1422.

Nakamachi, K. and Nakajima, N. (2000b). DNase I hypersensitive sites and transcriptional activation of the lamin A/C gene. *Eur. J. Biochem.* **267**, 1416–1422.

Nakamura, N., Rabouille, C., Watson, R., Nilsson, T., Hui, N., Slusarewicz, P., Kreis, T. E. and Warren, G. (1995). Characterization of a cis-Golgi matrix protein, GM130. *J. Cell Biol.* **131**, 1715–26.

Newport, J. W., Wilson, K. L. and Dunphy, W. G. (1990). A lamin-independent pathway for nuclear envelope assembly. *J. Cell Biol.* **111**, 2247–59.

Nikolova, V., Leimena, C., McMahon, A. C., Tan, J. C., Chandar, S., Jogia, D.,

Kesteven, S. H., Michalicek, J., Otway, R., Verheyen, F., et al. (2004). Defects in nuclear structure and function promote dilated cardiomyopathy in lamin A/C–deficient mice. *J. Clin. Invest.* **113**, 357–369.

Nili, E., Cojocaru, G. S., Kalma, Y., Ginsberg, D., Copeland, N. G., Gilbert, D. J., Jenkins, N. A., Berger, R., Shaklai, S., Amariglio, N., et al. (2001). Nuclear membrane protein LAP2β mediates transcriptional repression alone and together with its binding partner GCL (germ cell-less). *J. Cell Sci.* **114**,.

Okumura, K., Hosoe, Y. and Nakajima, N. (2004). c-Jun and Sp1 family are critical for retinoic acid induction of the lamin A/C retinoic acid-responsive element. *Biochem. Biophys. Res. Commun.* **320**, 487–492.

Olins, A. L., Herrmann, H., Lichter, P., Kratzmeier, M., Doenecke, D. and Olins, D. E. (2001). Nuclear Envelope and Chromatin Compositional Differences Comparing Undifferentiated and Retinoic Acid- and Phorbol Ester-Treated HL-60 Cells. *Exp. Cell Res.* **268**, 115–127.

Osorio, F. G., Navarro, C. L., Cadiñanos, J., López-Mejía, I. C., Quirós, P. M., Bartoli, C., Rivera, J., Tazi, J., Guzmán, G., Varela, I., et al. (2011). Splicing-Directed Therapy in a New Mouse Model of Human Accelerated Aging. *Sci. Transl. Med.* **3**,.

Osouda, S., Nakamura, Y., de Saint Phalle, B., McConnell, M., Horigome, T., Sugiyama, S., Fisher, P. A. and Furukawa, K. (2005). Null mutants of Drosophila B-type lamin Dm0 show aberrant tissue differentiation rather than obvious nuclear shape distortion or specific defects during cell proliferation. *Dev. Biol.* **284**, 219–232.

Ostlund, C., Ellenberg, J., Hallberg, E., Lippincott-Schwartz, J. and Worman, H. J. (1999). Intracellular trafficking of emerin, the Emery-Dreifuss muscular dystrophy protein. *J. Cell Sci.* **112**,.

Padiath, Q. S., Saigoh, K., Schiffmann, R., Asahara, H., Yamada, T., Koeppen, A., Hogan, K., Ptáček, L. J. and Fu, Y.-H. (2006). Lamin B1 duplications cause autosomal dominant leukodystrophy. *Nat. Genet.* **38**, 1114–1123.

Pajerowski, J. D., Dahl, K. N., Zhong, F. L., Sammak, P. J. and Discher, D. E. (2007). Physical plasticity of the nucleus in stem cell differentiation. *Proc. Natl. Acad. Sci.* **104**, 15619–15624.

Pankov, R., Neznanov, N., Umezawa, A. and Oshima, R. G. (1994). AP-1, ETS, and transcriptional silencers regulate retinoic acid-dependent induction of keratin 18 in embryonic cells. *Mol. Cell. Biol.* **14**, 7744–57.

Paradisi, M., McClintock, D., Boguslavsky, R. L., Pedicelli, C., Worman, H. J. and Djabali, K. (2005). Dermal fibroblasts in Hutchinson-Gilford progeria syndrome with the lamin A G608G mutation have dysmorphic nuclei and are hypersensitive to heat stress. *BMC Cell Biol.* **6**, 27.

Parra, M. K., Gee, S., Mohandas, N. and Conboy, J. G. (2011). Efficient in Vivo Manipulation of Alternative Pre-mRNA Splicing Events Using Antisense Morpholinos in Mice. *J. Biol. Chem.* **286**, 6033–6039.

Peter, M., Nakagawa, J., Dotie, M., Labbc, J. C. and Nigg, E. A. (1990). In Vitro Disassembly of the Nuclear Lamina and M Phase-Specific Phosphorylation of Lamins by cdc2 Kinase. *Cell* **61**, 591–602.

Pollard, K. M., Chan, E. K., Grant, B. J., Sullivan, K. F., Tan, E. M. and Glass,

C. A. (1990). In vitro posttranslational modification of lamin B cloned from a human T-cell line. *Mol. Cell. Biol.* **10**, 2164–75.

Pollex, R. and Hegele, R. (2004). Hutchinson-Gilford progeria syndrome. *Clin. Genet.* **66**, 375–381.

Pugh, B. F. and Tjian, R. (1990). Mechanism of transcriptional activation by Sp1: Evidence for coactivators. *Cell* **61**, 1187–1197.

Rao, L., Perez, D. and White, E. (1996). Lamin proteolysis facilitates nuclear events during apoptosis. *J. Cell Biol.* **135**, 1441–55.

Rauner, M., Sipos, W., Goettsch, C., Wutzl, A., Foisner, R., Pietschmann, P. and Hofbauer, L. C. (2009). Inhibition of Lamin A/C Attenuates Osteoblast Differentiation and Enhances RANKL-Dependent Osteoclastogenesis. *J. Bone Miner. Res.* **24**, 78–86.

Reunert, J., Wentzell, R., Walter, M., Jakubiczka, S., Zenker, M., Brune, T., Rust, S. and Marquardt, T. (2012). Neonatal progeria: increased ratio of progerin to lamin A leads to progeria of the newborn. *Eur. J. Hum. Genet.* **20**, 933.

Richards, S. A., Muter, J., Ritchie, P., Lattanzi, G. and Hutchison, C. J. (2011). The accumulation of un-repairable DNA damage in laminopathy progeria fibroblasts is caused by ROS generation and is prevented by treatment with N-acetyl cysteine. *Hum. Mol. Genet.* **20**, 3997–4004.

Riemer, D., Stuurman, N., Berrios, M., Hunter, C., Fisher, P. A. and Weber, K. (1995). Expression of Drosophila lamin C is developmentally regulated: analogies with vertebrate A-type lamins. *J. Cell Sci.* **108**,.

Röber, R. A., Weber, K. and Osborn, M. (1989). Differential timing of nuclear lamin A/C expression in the various organs of the mouse embryo and the young animal: a developmental study. *Development* **105**, 365–78.

Rodgers, H. F., Lavranos, T. C., Vella, C. A. and Rodgers, R. J. (1995). Basal lamina and other extracellular matrix produced by bovine granulosa cells in anchorage-independent culture. *Cell Tissue Res.* **282**, 463–71.

Rodriguez-Contreras, D., Aslan, H., Feng, X., Tran, K., Yates, P. A., Kamhawi, S. and Landfear, S. M. (2015). Regulation and biological function of a flagellar glucose transporter in Leishmania mexicana: a potential glucose sensor. *FASEB J.* **29**, 11–24.

Rubinsztein, D. C. (2006). The roles of intracellular protein-degradation pathways in neurodegeneration. *Nature* **443**, 780–786.

Rusiñol, A. E. and Sinensky, M. S. (2006). Farnesylated lamins, progeroid syndromes and farnesyl transferase inhibitors. *J. Cell Sci.* **119**,.

Ryan, M. D., King, A. M. and Thomas, G. P. (1991). Cleavage of foot-and-mouth disease virus polyprotein is mediated by residues located within a 19 amino acid sequence. *J. Gen. Virol.* **72 (Pt 11**, 2727–32.

Sarkar, P. K. and Shinton, R. A. (2001). Hutchinson-Guilford progeria syndrome. *Postgrad. Med. J.* **77**, 312–7.

Sasseville, A. M. and Raymond, Y. (1995). Lamin A precursor is localized to intranuclear foci. *J. Cell Sci.* 273–85.

Schneider, U., Mini, T., Jenö, P., Fisher, P. A. and Stuurman, N. (1999). Phosphorylation of the Major Drosophila Lamin In Vivo: Site Identification

during Both M-Phase (Meiosis) and Interphase by Electrospray Ionization Tandem Mass Spectrometry. *Biochemistry* **38**, 4620–4632.

Shumaker, D. K., Lopez-Soler, R. I., Adam, S. A., Herrmann, H., Moir, R. D., Spann, T. P. and Goldman, R. D. (2005). Functions and dysfunctions of the nuclear lamin Ig-fold domain in nuclear assembly, growth, and Emery-Dreifuss muscular dystrophy. *Proc. Natl. Acad. Sci. U. S. A.* **102**, 15494–9.

Shumaker, D. K., Dechat, T., Kohlmaier, A., Adam, S. A., Bozovsky, M. R., Erdos, M. R., Eriksson, M., Goldman, A. E., Khuon, S., Collins, F. S., et al. (2006). Mutant nuclear lamin A leads to progressive alterations of epigenetic control in premature aging. *Proc. Natl. Acad. Sci. U. S. A.* **103**, 8703–8.

Simon, D. N. and Wilson, K. L. (2013). Partners and post-translational modifications of nuclear lamins. *Chromosoma* **122**, 13–31.

Sinensky, M., Fantle, K., Trujillo, M., McLain, T., Kupfer, A. and Dalton, M. (1994). The processing pathway of prelamin A. *J. Cell Sci.* **107 (Pt 1**, 61–7.

Spann, T. P., Moir, R. D., Goldman, A. E., Stick, R. and Goldman, R. D. (1997). Disruption of Nuclear Lamin Organization Alters the Distribution of Replication Factors and Inhibits DNA Synthesis. *J. Cell Biol.* **136**,.

Spann, T. P., Goldman, A. E., Wang, C., Huang, S. and Goldman, R. D. (2002). Alteration of nuclear lamin organization inhibits RNA polymerase II-dependent transcription. *J. Cell Biol.* **156**, 603–8.

Stadelmann, B., Khandjian, E., Hirt, A., Lüthy, A., Weil, R. and Wagner, H. P. (1990). Repression of nuclear lamin A and C gene expression in human acute lymphoblastic leukemia and non-Hodgkin's lymphoma cells. *Leuk. Res.* **14**,

815–821.

Stewart, C. and Burke, B. (1987). Teratocarcinoma stem cells and early mouse embryos contain only a single major lamin polypeptide closely resembling lamin B. *Cell* **51**, 383–92.

Stick, R. and Hausen, P. (1985). Changes in the nuclear lamina composition during early development of Xenopus laevis. *Cell* **41**, 191–200.

Stuurman, N., Heins, S. and Aebi, U. (1998). Nuclear Lamins: Their Structure, Assembly, and Interactions. *J. Struct. Biol.* **122**, 42–66.

Sullivan, T., Escalante-Alcalde, D., Bhatt, H., Anver, M., Bhat, N., Nagashima, K., Stewart, C. L. and Burke, B. (1999). Loss of A-type lamin expression compromises nuclear envelope integrity leading to muscular dystrophy. *J. Cell Biol.* **147**, 913–20.

Suske, G. (1999). The Sp-family of transcription factors. *Gene* **238**, 291–300.

Takahashi, A., Alnemri, E. S., Lazebnik, Y. A., Fernandes-Alnemri, T., Litwack, G., Moir, R. D., Goldman, R. D., Poirier, G. G., Kaufmann, S. H. and Earnshaw, W. C. (1996). Cleavage of lamin A by Mch2 alpha but not CPP32: multiple interleukin 1 beta-converting enzyme-related proteases with distinct substrate recognition properties are active in apoptosis. *Proc. Natl. Acad. Sci. U. S. A.* **93**, 8395–400.

Tan, N. Y. and Khachigian, L. M. (2009). Sp1 phosphorylation and its regulation of gene transcription. *Mol. Cell. Biol.* **29**, 2483–2488.

Taylor, M. R. G., Slavov, D., Gajewski, A., Vlcek, S., Ku, L., Fain, P. R., Carniel, E., Di Lenarda, A., Sinagra, G., Boucek, M. M., et al. (2005). Thymopoietin

(lamina-associated polypeptide 2) gene mutation associated with dilated cardiomyopathy. *Hum. Mutat.* **26**, 566–574.

Thompson, L. J. and Fields, A. P. (1996). betaII protein kinase C is required for the G2/M phase transition of cell cycle. *J. Biol. Chem.* **271**, 15045–53.

Thompson, L. J., Bollen, M. and Fields, A. P. (1997). Identification of protein phosphatase 1 as a mitotic lamin phosphatase. *J. Biol. Chem.* **272**, 29693–7.

Tilgner, K., Wojciechowicz, K., Jahoda, C., Hutchison, C. and Markiewicz, E. (2009). Dynamic complexes of A-type lamins and emerin influence adipogenic capacity of the cell via nucleocytoplasmic distribution of -catenin. *J. Cell Sci.* **122**, 401–413.

Toth, J. I., Yang, S. H., Qiao, X., Beigneux, A. P., Gelb, M. H., Moulson, C. L., Miner, J. H., Young, S. G. and Fong, L. G. (2005). Blocking protein farnesyltransferase improves nuclear shape in fibroblasts from humans with progeroid syndromes. *Proc. Natl. Acad. Sci. U. S. A.* **102**, 12873–8.

Toyama, B. H., Savas, J. N., Park, S. K., Harris, M. S., Ingolia, N. T., Yates, J. R. and Hetzer, M. W. (2013). Identification of long-lived proteins reveals exceptional stability of essential cellular structures. *Cell* **154**, 971–82.

Varela, I., Pereira, S., Ugalde, A. P., Navarro, C. L., Suárez, M. F., Cau, P., Cadiñanos, J., Osorio, F. G., Foray, N., Cobo, J., et al. (2008). Combined treatment with statins and aminobisphosphonates extends longevity in a mouse model of human premature aging. *Nat. Med.* **14**, 767–772.

Vaughan, A., Alvarez-Reyes, M., Bridger, J. M., Broers, J. L., Ramaekers, F. C., Wehnert, M., Morris, G. E., Whitfield WGF and Hutchison, C. J. (2001).

Both emerin and lamin C depend on lamin A for localization at the nuclear envelope. *J. Cell Sci.* **114**, 2577–90.

Vergnes, L., Peterfy, M., Bergo, M. O., Young, S. G. and Reue, K. (2004). Lamin B1 is required for mouse development and nuclear integrity. *Proc. Natl. Acad. Sci.* **101**, 10428–10433.

Verstraeten, V. L. R. M., Peckham, L. A., Olive, M., Capell, B. C., Collins, F. S., Nabel, E. G., Young, S. G., Fong, L. G. and Lammerding, J. (2011). Protein farnesylation inhibitors cause donut-shaped cell nuclei attributable to a centrosome separation defect. *Proc. Natl. Acad. Sci.* **108**, 4997–5002.

Vidak, S. and Foisner, R. (2016). Molecular insights into the premature aging disease progeria. *Histochem. Cell Biol.* **145**, 401–17.

Vigouroux, C. and Bonne, G. (2013). Laminopathies: One Gene, Two Proteins, Five Diseases..

Viteri, G., Chung, Y. W. and Stadtman, E. R. (2010). Effect of progerin on the accumulation of oxidized proteins in fibroblasts from Hutchinson Gilford progeria patients. *Mech. Ageing Dev.* **131**, 2–8.

Vizcaíno, C., Mansilla, S. and Portugal, J. (2015). Sp1 transcription factor: A long-standing target in cancer chemotherapy. *Pharmacol. Ther.* **152**, 111–124.

Vlcek, S. and Foisner, R. (2007). A-type lamin networks in light of laminopathic diseases. *Biochim. Biophys. Acta* **1773**, 661–74.

Wagner, S. A., Beli, P., Weinert, B. T., Nielsen, M. L., Cox, J., Mann, M. and Choudhary, C. (2011). A Proteome-wide, Quantitative Survey of In Vivo Ubiquitylation Sites Reveals Widespread Regulatory Roles. *Mol. Cell.*

Proteomics **10**, M111.013284-M111.013284.

Ward, G. E., Kirschner, M. W., McIntosh, J. R., Burnett, J. P., Hermodson, M. A., Roach, P. J., Malviya, A. N., Sclafani, R. A., Benton, B. M. and Fisher, P. A. (1990). Identification of cell cycle-regulated phosphorylation sites on nuclear lamin C. *Cell* **61**, 561–77.

Wehnert, M. and Muntoni, F. (1999). 60th ENMC International Workshop: non X-linked Emery-Dreifuss Muscular Dystrophy 5-7 June 1998, Naarden, The Netherlands. *Neuromuscul. Disord.* **9**, 115–21.

Wilson, K. L. and Foisner, R. (2010). Lamin-binding Proteins. *Cold Spring Harb. Perspect. Biol.* **2**, a000554.

Winter-Vann, A. M. and Casey, P. J. (2005). Opinion: Post-prenylation-processing enzymes as new targets in oncogenesis. *Nat. Rev. Cancer* **5**, 405–412.

Wolin, S. L., Krohne, G. and Kirschner, M. W. (1987). A new lamin in Xenopus somatic tissues displays strong homology to human lamin A. *EMBO J.* **6**, 3809–18.

Won, J., Yim, J. and Kim, T. K. (2002). Sp1 and Sp3 recruit histone deacetylase to repress transcription of human telomerase reverse transcriptase (hTERT) promoter in normal human somatic cells. *J. Biol. Chem.* **277**, 38230–8.

Worman, H. J. and Bonne, G. (2007). "Laminopathies": a wide spectrum of human diseases. *Exp. Cell Res.* **313**, 2121–33.

Wright, L. P. and Philips, M. R. (2006). Thematic review series: lipid posttranslational modifications. CAAX modification and membrane targeting of Ras. *J. Lipid Res.* **47**, 883–91.

Wu, D., Flannery, A. R., Cai, H., Ko, E. and Cao, K. (2014). Nuclear localization signal deletion mutants of lamin A and progerin reveal insights into lamin A processing and emerin targeting. *Nucleus* **5**, 66–74.

Wu, D., Yates, P. A., Zhang, H. and Cao, K. (2016). Comparing lamin proteins post-translational relative stability using a 2A peptide-based system reveals elevated resistance of progerin to cellular degradation. *Nucleus* **7**, 585–596.

Xiong, Z.-M., Choi, J. Y., Wang, K., Zhang, H., Tariq, Z., Wu, D., Ko, E., LaDana, C., Sesaki, H. and Cao, K. (2016). Methylene blue alleviates nuclear and mitochondrial abnormalities in progeria. *Aging Cell* **15**, 279–90.

Yang, S. H., Bergo, M. O., Toth, J. I., Qiao, X., Hu, Y., Sandoval, S., Meta, M., Bendale, P., Gelb, M. H., Young, S. G., et al. (2005). Blocking protein farnesyltransferase improves nuclear blebbing in mouse fibroblasts with a targeted Hutchinson-Gilford progeria syndrome mutation. *Proc. Natl. Acad. Sci. U. S. A.* **102**, 10291–6.

Yang, S. H., Meta, M., Qiao, X., Frost, D., Bauch, J., Coffinier, C., Majumdar, S., Bergo, M. O., Young, S. G. and Fong, L. G. (2006). A farnesyltransferase inhibitor improves disease phenotypes in mice with a Hutchinson-Gilford progeria syndrome mutation. *J. Clin. Invest.* **116**, 2115–21.

Yang, S. H., Andres, D. A., Spielmann, H. P., Young, S. G. and Fong, L. G. (2008). Progerin elicits disease phenotypes of progeria in mice whether or not it is farnesylated. *J. Clin. Invest.* **118**, 3291–300.

Yang, S. H., Chang, S. Y., Ren, S., Wang, Y., Andres, D. A., Spielmann, H. P., Fong, L. G. and Young, S. G. (2011). Absence of progeria-like disease

phenotypes in knock-in mice expressing a non-farnesylated version of progerin. *Hum. Mol. Genet.* **20**, 436–44.

Zhang, D., Beresford, P. J., Greenberg, A. H. and Lieberman, J. (2001). Granzymes A and B directly cleave lamins and disrupt the nuclear lamina during granule-mediated cytolysis. *Proc. Natl. Acad. Sci.* **98**, 5746–5751.

Zhang, H., Xiong, Z.-M. and Cao, K. (2014). Mechanisms controlling the smooth muscle cell death in progeria via down-regulation of poly(ADP-ribose) polymerase 1. *Proc. Natl. Acad. Sci. U. S. A.* **111**, E2261-70.

Zhou, P. (2004). Determining protein half-lives. *Methods Mol. Biol.* **284**, 67–77.